

Quantum feedback: theory, experiments, and applications

Jing Zhang^{a,b,c}, Yu-xi Liu^{d,b,c}, Re-Bing Wu^{a,b,c}, Kurt Jacobs^{e,c}, Franco Nori^{c,f}

^aDepartment of Automation, Tsinghua University, Beijing 100084, P. R. China

^bCenter for Quantum Information Science and Technology, TNLIST, Beijing 100084, P. R. China

^cCEMS, RIKEN, Saitama 351-0198, Japan

^dInstitute of Microelectronics, Tsinghua University, Beijing 100084, P. R. China

^eDepartment of Physics, University of Massachusetts at Boston, Boston, MA 02125, USA

^fPhysics Department, The University of Michigan, Ann Arbor, MI 48109-1040, USA

Abstract

The control of individual quantum systems is now a reality in a variety of physical settings. Feedback control is an important class of control methods because of its ability to reduce the effects of noise. In this review we give an introductory overview of the various ways in which feedback may be implemented in quantum systems, the theoretical methods that are currently used to treat it, the experiments in which it has been demonstrated to-date, and its applications. In the last few years there has been rapid experimental progress in the ability to realize quantum measurement and control of mesoscopic systems. We expect that the next few years will see further rapid advances in the precision and sophistication of feedback control protocols realized in the laboratory.

Keywords: quantum control, quantum feedback, linear optics, cavity QED, circuit QED, quantum information processing

Contents

1	Introduction	2
1.1	History and background	2
1.2	A glance at classical feedback control	5
1.2.1	Classical model of a control system	6
1.2.2	System analysis and design	7
1.2.3	Optimal control	7
1.2.4	Fighting disturbances and uncertainties	8
2	Quantum Measurement-Based Feedback	9
2.1	Continuous quantum measurements	9
2.1.1	Quantum filtering	9
2.1.2	Another point of view: quantum trajectories	12
2.2	Markovian quantum feedback	15
2.3	Feedback via time-averaging	16
2.4	Bayesian quantum feedback	17
2.5	Applications	19
2.5.1	Noise reduction and quantum error correction	19
2.5.2	State reduction and stabilization	21
2.5.3	Squeezing via feedback	23
2.5.4	Controlling mechanical resonators	24

Email address: jing-zhang@mail.tsinghua.edu.cn (Jing Zhang)

2.5.5	Controlling transport in nano-structures	24
2.5.6	Entanglement creation and control	24
2.5.7	Quantum state discrimination	25
2.5.8	Quantum parameter estimation	26
2.5.9	Rapid state-purification and measurement	27
2.5.10	Control-free control	28
3	Coherent Quantum Feedback	28
3.1	Direct coherent feedback	30
3.2	Field-mediated coherent feedback	31
3.2.1	Networks of quantum systems	32
3.2.2	Quantum transfer function model	34
3.3	Applications	35
3.3.1	Noise-reduction in linear systems	35
3.3.2	Optical squeezing	35
3.3.3	Quantum error correction	36
3.3.4	Controlling mechanical resonators	36
3.3.5	Quantum nonlinear optics	38
3.3.6	Controlling entanglement	39
4	Other Kinds of Quantum Feedback	39
4.1	Adaptive feedback	39
4.2	Quantum self-feedback	40
5	Experiments Realizing Quantum Feedback	42
5.1	Linear optics	42
5.2	Trapped particles and Cavity-QED	51
5.3	Superconducting circuits	57
5.4	Optomechanics and electromechanics	61
5.5	Quantum dots	65
6	Summary and Outlook	66
	Acknowledgements	67
	References	68

1. Introduction

1.1. History and background

The subject of *control* is concerned with methods to manipulate the evolution of dynamical systems. As such it is relevant to many fields both inside and outside physics [1–39]. Control has a long history, but it emerged as a modern scientific discipline only after the pioneering work of Norbert Wiener in the 1940’s [40]. Up until the 1960’s, control was largely studied by analyzing dynamical systems in the frequency domain (that is, the Fourier transform of the evolution). This was a reasonable approach because people were mainly interested in steady-state behavior. So long as the fluctuations about the steady-state are sufficiently small, even nonlinear systems can be well-approximated by linear dynamics, and are thus amenable to frequency-domain methods. For networks of linear systems in which the outputs of some systems are connected to the inputs of others, frequency-space methods are also extremely useful, because complex exponentials are the eigenfunctions of all linear systems.

Frequency-domain methods were less helpful in understanding how control systems should make use of real-time information, and for this reason control theorists turned to the time domain. The techniques that were developed

include the Kalman-Bucy filter [41] and the Hamilton-Jacobi-Bellman equation [42]. These are referred to as state-space methods, and are often referred to as “modern” control theory. Much of modern control theory is concerned with feedback control, in which a control system, or “controller” obtains a stream of information about the trajectory of the system, or “plant”, and uses this information in real time to control it. The term “feedback” comes from the notion that the controller is “feeding” the information it obtains “back” to the system. Feedback control is also referred to as “closed-loop” control, because the flow of information to the controller, together with the action taken by the controller to affect the system is thought of as a loop that starts and ends at the system [43, 44].

One usually speaks of a controller as trying to achieve some *objective*. This objective may be to have the system reach a given state at a given time, or to have it evolve in a precise way, despite the presence of noise in its inputs or slight errors in its construction. Given an objective, the central problem in feedback control is to obtain a rule (or mapping) that the controller can use to select the action it should take based on the data it has received. Traditionally such a rule was referred to as a “feedback algorithm”, but in quantum control theory the term “feedback protocol” is usually used instead, so as to avoid confusion with the algorithms of quantum computing [45].

The idea of controlling systems using feedback has been around for a long time; the first device on record employing feedback appears to have been the water clock of Ktesibios in the first half of the third century B.C. [46–48] Another successful example of a feedback mechanism is the Watt governor developed in the 1780’s. This centrifugal governor was a core component of the Watt steam engine which fueled the industrial revolution. Incidentally it was Maxwell that first performed a mathematical analysis of this control mechanism [49]. By introducing feedback control one can speed up transient processes, tune the stationary output of a system, and most importantly, reduce the effects of disturbances. The importance of using feedback in controlling a system is that it is the only way to reduce the effects of noise. Noise introduces uncertainty into the system dynamics, and the only way to reduce this uncertainty is to transfer it to another system. To understand this better, consider what happens if we make a measurement on a system. This reduces our uncertainty and allows us to correct the motion. In doing so, we reduce the spread in the state of the system, and thus the randomness in the system. But note that the measuring device must record the result of the measurement, and this result is necessarily as random as the quantity being measured. Thus the measurement and feedback transfers randomness from the system to the memory of the measuring device. More fundamentally, randomness is entropy, and because all physical laws are reversible, the only way to reduce entropy in any system is to transfer it to another system, which might be a thermal bath. In the study of quantum feedback control, it is natural to refer to any process that transfers entropy from the system to the controller as a feedback process.

Feedback control was introduced into quantum dynamics in the early 1980’s [50–55], but it was not until the 1990’s that it began to be studied and applied in earnest. The first person to present a mathematical theory of feedback control in quantum systems was Belavkin [56, 57] who obtained a quantum version of the Stratonovich equation, which is the classical equation to describe the continuous measurement of a system [58]. The Kalman-Bucy filter is the special case of the Stratonovich equation for linear systems, in which the measurement is restricted to linear functions of the dynamical variables. The highly mathematical nature of Belavkin’s work prevented it from having an impact in the physics community, and the quantum version of the Stratonovich equation, referred to as the Stochastic Master Equation (SME), was obtained independently by Wiseman and Milburn [59, 60] building on the work by Carmichael [61, 62]. Srinivas and Davies [63], Gisin [64], and Diosi [65] also presented stochastic equations for measured systems in this time period. In 1994, Wiseman and Milburn showed that a Markovian master equation could be derived to describe continuous feedback in quantum systems, called Markovian feedback, if the feedback was given by a particularly simple function of the stream of measurement results [66]. In 1998, Yanigasawa and Kimura [67] and Doherty and Jacobs [68] introduced the notion of performing feedback using estimates obtained from the SME, in the control literature and physics literature, respectively. Both sets of authors showed that for linear systems this class of feedback protocols was equivalent to modern classical feedback control, so that standard results for optimal control could be transferred to quantum systems. This method was in fact that proposed by Belavkin in 1983 in analogy to that used in classical control theory [69, 70]. In quantum control, using estimates obtained from the SME is often referred to as Bayesian feedback to distinguish it from Markovian feedback. In the former the measurement results are processed (“filtered”) to obtain an estimate of properties of the current state, whereas in the latter the measurement stream is fed back directly.

In Wiseman’s seminal work on feedback control, he showed that feedback mediated by continuous measurements can in fact be implemented without measurements [71]. To see how this works, let us consider two parallel mirrors between which a single mode of the electromagnetic field is trapped (the two mirrors are referred to as an “optical

cavity”). The light that leaks out through one of the mirrors can be detected, and the information is used to manipulate the optical mode. Alternatively, the output light can be directed to a mirror of another optical cavity, and thus forms an input for this cavity. If we then connect an output from the second cavity back to the first we have a loop, and light can be made to travel only one way around the loop by the use of optical circulators [72]. For describing this situation the quantum input-output theory developed by Collet and Gardiner is invaluable [73, 74]. The process of connecting quantum systems together via free-space one-way traveling-wave fields was first considered by Gardiner [75] and Carmichael [76], where the former called it a “cascade connection”. Wiseman showed that cascade connections can implement the same feedback control processes as Markovian measurement-based feedback and can perform tasks that the latter cannot [71].

A second notion of feedback control without explicit measurements was introduced by Lloyd in 2000. He suggested that a unitary interaction between two quantum systems could be used to implement feedback control [77, 78]. This can be achieved, for example, by choosing the interaction so as to correlate the two systems, i.e., the controlled system and the controller, whereby the state of the controller is dependent on the state of the system. One then chooses a second interaction in which the evolution of the system depends on the state of the controller. This particular process is equivalent to a measurement followed by a unitary feedback operation that depends upon the measurement result, although coherent feedback processes are not restricted to this form [79, 80]. Both kinds of “measurement-free” feedback, that mediated by cascade connections and that which uses unitary interactions are now referred to as *coherent feedback control* (CFC), and the latter is often called “direct” coherent-feedback. All control involving explicit measurements is usually called *measurement-based* feedback control, or just *measurement feedback control* (MFC).

In the 2000’s James and his collaborators studied “feedback networks” of linear quantum systems connected by one-way fields [81], and Gough and James built on input-output theory to construct a compact and convenient formalism to handle arbitrarily complex networks [82]. More recently a number of authors have considered the use of nonlinear coherent-feedback networks for various control tasks [83–86]. In 2009, Nurdin, James, and Peterson showed that linear coherent feedback networks could out-perform linear measurement-based feedback [87], suggesting that measurement-based feedback was limited by the need to reduce the information about a system to classical numbers. It is also shown quite recently that coherent feedback can achieve more for generating quantum nonlinearity [85, 86] and cooling [88] compared with the measurement-based feedback. The relationship between measurement-based and coherent feedback is a topic of current research [79].

There are not only fundamental differences between measurement-based and coherent feedback, but also important practical differences. Making measurements on quantum systems, often possessing only a few quanta, usually requires a tremendous amplification of the signal. This is because the measurement results, by definition, are well-defined classical numbers. To robustly store and manipulate such numbers requires states with energies much greater than a single quantum. Amplifying signals at the single-quantum scale without swamping them with noise is a great challenge, and is one major practical disadvantage of measurement-based feedback. A second disadvantage is the timescale required to obtain and then process the measurement results (usually on a digital device). On the other hand, measurement-based feedback has the advantage that the processing of the information is essentially noise-free. By contrast, if a quantum system is used as a controller it will likely be subject to noise processes from its environment. It may also be less clear how to use the quantum system to process the information to achieve a control objective.

It is important to note that the method of “adaptive feedback”, in which the term “feedback” is used, is not the feedback control, i.e., measurement-based or coherent feedback, that we are concerned with in this review. Adaptive feedback [4] is a method for obtaining control protocols, not a class of protocols for controlling a system. In this method, one chooses an arbitrary control protocol, tries it out on the system, and based on the result make a modification to the protocol and tries it again. In this way one can use one of many search algorithms to look for a good protocol. People who refer to adaptive feedback as a feedback method distinguish the feedback control we consider here by calling it “real-time feedback control”.

It is also important to note that we do not discuss here all the ways in which feedback can be realized. One could, for example, perform a series of “single-shot” measurements with a discrete set of outcomes, and perform a unitary action on the system for each outcome. While there are certainly a range of interesting and non-trivial questions regarding such feedback, such as controlling thermal dynamics [89–93] and quantum error correction [94–100], the mathematical machinery required to analyze it does not require stochastic differential equations. This is also true of coherent feedback implemented via unitary interactions. This latter topic has only recently begun to be explored in earnest, and there are certainly many open questions [101]. However in this review we focus on continuous-time

feedback control, both measurement-based and coherent. Both of these require the use of stochastic (Ito) calculus, something that is less familiar to many researchers in quantum theory. While measurement-based feedback requires only the usual Ito stochastic calculus, cascaded quantum feedback requires a quantum version of Ito calculus developed by Gardiner and Collett as part of their input-output theory [73, 102]. This quantum stochastic calculus was also developed independently by Hudson and Parthasarathy in a more rigorous measure-theoretic way [103]. A readily accessible introduction to Ito calculus can be found in [104], and the quantum version is described in [73, 74, 105].

To distinguish between experiments that realize quantum feedback control rather than classical control, we apply the criterion that an experiment involves the former if quantum measurement theory is required to correctly explain its results. This is certainly the case if the control process realizes a signature of quantum behavior that is not manifest classically. For linear systems, the only distinction between quantum and classical motion is that the joint-uncertainty of position and momentum is limited by Heisenberg’s uncertainty principle. A measurement introduces noise because a reduction in the uncertainty of one canonical variable tends to increase the uncertainty of the conjugate variable. Feedback control of a quantum harmonic oscillator can thus be considered quantum mechanical if either (i) the “back-action” noise from the measurement must be taken into account in understanding the behavior, or (ii) alternatively one of the canonical variables has its uncertainty reduced below that of the vacuum state (so-called “squeezed states”).

Experiments implementing measurement-based feedback in the quantum regime were realized initially in quantum optics, where it first became possible to measure individual microscopic degrees of freedom with sufficient fidelity. These were followed by experiments involving trapped atoms and ions, and very recently it has become possible to realize measurement-based feedback control in mesoscopic superconducting circuits. We review experiments in these various physical settings in Section 5. Experiments involving continuous coherent feedback were performed prior to those realizing continuous measurement-based feedback, although at the time these experiments were not thought of as involving feedback. An example is the cooling of trapped ions using the “resolved sideband” cooling method [106, 107]. In Section 5.4 we summarize recent experiments implementing coherent feedback cooling of mechanical resonators (using the resolved-sideband technique) and in Sections 5.1 and 5.3 we summarize recent experiments whose primary purpose is the demonstration of coherent feedback.

In the remainder of this section we give a brief introduction to classical feedback control. In Sec. 2 we discuss quantum continuous (weak) measurements and filtering, and their application to quantum measurement-based feedback. In particular we discuss the two ends of the spectrum of measurement-based feedback: the simplest in which the measurement signal is not processed at all before it is fed back to the system (“Markovian” feedback), and that in which the measurement signal is fully processed to obtain the observer’s complete state-of-knowledge of the system as it evolves (“Bayesian” feedback). We complete Sec. 2 by giving an overview of most of the applications of measurement-based feedback that have been considered in the literature to-date. In Sec. 3 we turn to coherent feedback. We discuss the two primary ways in which it can be implemented, and the formalism used to describe them. As with measurement-based feedback, we then review the majority of applications of coherent feedback that have been considered to-date. In Sec. 4 we review two further topics that involve feedback, but not in the way envisioned in the traditional notion of feedback control. In Sec. 5 we turn to experiments, and give an overview of all experiments to-date that have realized continuous feedback control in the quantum regime. These experiments cover a range of physical settings from quantum optics to superconducting circuits. We also review all experiments realized to-date whose purpose is to demonstrate coherent feedback, as well as recent experiments that use coherent feedback to cool mechanical resonators. In Section 6 we give a perspective on the current state of quantum feedback control and discuss some open questions.

1.2. A glance at classical feedback control

In the engineering discipline called *control theory*, a control system is always broken into three parts [108]:

- The system (or “plant”): the device we want to control, having inputs and outputs;
- The input(s) to the system (or “control”): the entity that we have freedom to choose to affect the system;
- The output(s) of the system (or “yield”): this includes the quantity we want to control, and any quantities we can measure to obtain information about the plant.

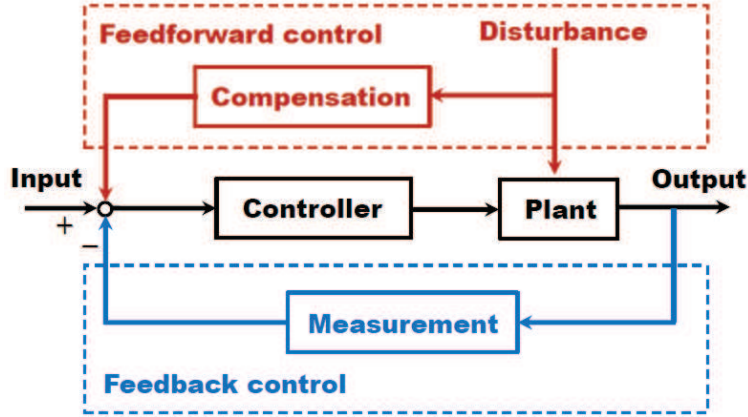


Figure 1: (Color online) Basic components in a control system with feedback (bottom loop, in blue) and feedforward (top branch, in red) controllers.

As explained above, the explicitly causal structure, in which the control system first obtains information from a measurement and uses this to determine the input to the system, is a way of thinking about the interaction between two systems that is conceptually useful for feedback control. One can think about the interaction in this way even if this structure is not explicit in the mathematical description of the interaction. An example in which it is not explicit is in the Hamiltonian description of an interaction.

The usual objective of control is to steer one or more outputs of the plant toward a prescribed behavior against unknown disturbances or noises. As shown in Fig. 1, when the disturbance is known (or can be precisely measured), a feedforward controller can be used to cancel the effects of disturbances at the input side. Otherwise, if the disturbance is unknown (or cannot be precisely measured), a feedback controller must be introduced to adjust the input according to the outputs of the prescribed measurements imposed on the controlled system.

1.2.1. Classical model of a control system

We are concerned with dynamical systems that change continuously in time, and are therefore modeled by differential equations. The standard model of a control system can be written as

$$\dot{x}(t) = F[x(t), u(t)], \quad x(0) = x_0, \quad (1.1)$$

$$y(t) = G[x(t), u(t)], \quad (1.2)$$

where F and G are arbitrary vector-valued functions, the vector $x(t)$ is the state of the system, $u(t)$ is the control (set of inputs) that drives the system, and $y(t)$ is the set of outputs, which is allowed to be some algebraic function of both the state and the input.

In practice, the following linear control system model is favored by control engineers:

$$\dot{x}(t) = Ax(t) + Bu(t), \quad x(0) = x_0, \quad (1.3)$$

$$y(t) = Cx(t), \quad (1.4)$$

in which A , B , and C are constant matrices. This model can be solved analytically, which makes it convenient for design purposes. Many nonlinear systems can be transformed to a linear system under a proper nonlinear coordinate transformation. Such a procedure is called linearization, which is broadly used in the literature. For those systems that cannot be precisely linearized, one can still often approximately linearize them in a small neighborhood of the “working point”, using a perturbative technique.

The relation between the input and output of a linear control system can be alternatively characterized in the frequency domain by a transfer function obtained by taking the Laplace transform of Eq. (1.1):

$$Y(s) = G(s)U(s), \quad G(s) = C(sI - A)^{-1}B, \quad (1.5)$$

where $U(s)$ and $Y(s)$ are the Laplace transforms of the input $u(t)$ and the output $y(t)$, respectively, and $G(s)$ is the transfer function of the system. Transfer function models are popular in control engineering because they can be constructed directly from the input-output data without having to know the internal structure of the system. The corresponding analysis and design are conceptually simple and can be visualized using Nyquist or Bode plots, which require few computational resources [7].

1.2.2. System analysis and design

Consider the linear control system given by Eqs. (1.3) and (1.4). To implement feedback control, we make the control, $u(t)$, a function of the state $x(t)$, assuming that $x(t)$ can be determined from the measured outputs. To keep the system dynamics linear, we set $u(t) = Kx(t) + r(t)$, where K is a constant matrix and $r(t)$ is the external input signal. The matrix K is called the feedback *gain*, and the function $r(t)$ is called the *reference signal* or *command signal*, which is sometimes chosen as the reference signal to be tracked by the system output under control. With this choice for $u(t)$, the dynamics of the resulting *closed-loop* system becomes

$$\dot{x}(t) = (A - BK)x(t) + Br(t), \quad y(t) = Cx(t). \quad (1.6)$$

Correspondingly, the closed-loop transfer function from the reference signal, $r(t)$, to the output we wish to control, $y(t)$, becomes

$$G_{CL}(s) = C(sI - A - BK)^{-1}B. \quad (1.7)$$

The gain matrix and reference signal are together called the *control law*.

Two common control tasks are:

- Regulation: to find a control law that keeps $y(t)$ close to some predetermined function of time.
- Tracking: to find a control law that keeps $y(t)$ close to a time-varying signal that is not known beforehand.

A prerequisite for accomplishing these tasks is that the controlled system is *stable*, and the systems stability considered here is usually quantified by using the concept of *Lyapunov stability*. For linear systems, stability is ensured by choosing the gain matrix K so that the poles of the transfer function lie in the left half of the complex plane, and sufficiently far from the imaginary axis. A central result of control theory for linear systems, referred to as the *pole assignment theorem*, states that one can choose K to place the poles at arbitrary locations in the complex plane if and only if the system is fully controllable, meaning that it is possible to choose K and $r(t)$ to steer the system from any state to the origin.

1.2.3. Optimal control

In applications, one is often interested in obtaining a given output while using minimal resources [43]. We can formulate this goal as a typical constrained optimization problem. If we define a function that measures how far the output is to the desired output (the error incurred by the control law), and another function that quantifies the resource cost of the inputs, we can attempt to minimize the latter under a constraint on the former. The dynamics of the system is essentially another constraint in this optimization problem. We can alternatively define a single “cost” function that combines the error and resource cost, and attempt to minimize it. A well-motivated form for the cost function J is

$$J[u(t)] = \Phi[x(T)] + \int_0^T L[x(t), u(t)] dt, \quad (1.8)$$

where the differential equation given by Eq. (1.1) is the dynamical constraint.

The theory of optimal control is a beautiful part of modern control theory that can be analyzed with variational methods. In fact, with the above form for J , this theory has the same structure as that of Lagrangian and Hamiltonian mechanics. The reason for this is that the Lagrange equations give the conditions for the minimization of an action, which has the same form as J .

Subject to the restriction given by Eq.(1.1), one can introduce a Lagrangian multiplier $\lambda(t)$, and this turns out to be the “momentum coordinate” conjugate to $x(t)$ in the sense of Hamiltonian mechanics. The (pseudo) Hamiltonian to which this conjugate coordinate corresponds is

$$\mathbf{H}[x(t), u(t)] = L[x(t), u(t)] + \lambda(t)^T F[x(t), u(t)]. \quad (1.9)$$

One can prove that the necessary condition for a control $u(t)$ to be optimal is

$$\left. \frac{\partial \mathbf{H}[x(t), u(t)]}{\partial u(t)} \right|_{u(t)=u_{\text{opt}}(t)} = 0, \quad (1.10)$$

and $x(t)$ and $\lambda(t)$ can be obtained by solving the following conjugate equations

$$\dot{x}(t) = \frac{\partial \mathbf{H}[x(t), u(t)]}{\partial \lambda(t)}, \quad (1.11)$$

$$\dot{\lambda}(t) = -\frac{\partial \mathbf{H}[x(t), u(t)]}{\partial x(t)}. \quad (1.12)$$

From the viewpoint of Lagrangian mechanics, the evolution of the system under the control $u(t)$ minimizes the “action” J .

If the set of admissible controls $u(t)$ is not an open set, the condition (1.10) must be replaced by a more general condition, due to the fact that $u(t)$ can no longer be taken at any point in this set. In this case, the necessary condition under which $u(t)$ is optimal is that $u(t)$ minimizes $\mathbf{H}[x(t), u(t)]$. We can write this condition as

$$u_{\text{opt}}(t) = \arg \left[\min_{u(t)} \mathbf{H}[x(t), u(t)] \right], \quad (1.13)$$

which is referred to as the “Maximum Principle”. An alternative technique called dynamical programming can be used to locate the global optimal solutions for $u(t)$ by solving the so-called Hamiltonian-Jacobi-Bellman equation [105], but requires much higher computation resources than solving Eq. (1.10) or (1.13). All these approaches merely provide necessary conditions for optimality.

1.2.4. Fighting disturbances and uncertainties

So far we have not included the effects of uncertainty or noise in the system control model, but we have to do so if the controller is to combat them. If the system is driven by a noise of which the spectrum is known, we can include this noise in the model of the system, and explicitly calculate the observer’s estimate of the system state derived from a measurement process in real-time. Feedback control can then be implemented based on this estimate. Sometimes it is possible to minimize the noise in a subset of system variables at the expense of others, which is analogous to the squeezing of an optical beam or a quantum oscillator.

Alternatively, there may be uncertainties in the parameters that determine the dynamics of the system. If we consider a linear system whose equation of motion has the form of $\dot{x} = Ax + f(t)$, there are two distinct ways to show the uncertainty in the system parameters. First, the driving term $f(t)$ may contain unknown or partially known parameters, such as the phase or amplitude of a sinusoidal drive. This is very similar to a time-variant noise driving the system, except that in this case a continuous measurement imposed on the system will provide sufficient information to estimate the values of the unknown parameters, and thus reduce the parametric uncertainty. Second, there may exist uncertainty in the system dynamical matrix A , due to which the oscillation frequencies of the system are partially unknown. Such parametric uncertainty is often referred to as *model uncertainty*. Once again a measurement can be used to extract information about A , and then one can implement a feedback control with a gain matrix K and reference signal $r(t)$ to minimize the effects induced by the model uncertainty. A control law that maintains a specific performance under (bounded) variations in the system parameters is referred to as being *robust*. Such robust control problems have stimulated a rich body of studies in the literature [109].

2. Quantum Measurement-Based Feedback

As a first example we consider feedback based on the results of a von Neumann measurement. Each outcome of a von Neumann measurement projects a system into one of a set of basis states. For each of these states we are then able to perform a different unitary operation on the system. This form of measurement-based feedback does have important applications, an example of which is quantum error correction [94–100]. The simplest example of error-correction is the three-qubit “bit-flip” code, in which the state of a single logical qubit is encoded in three physical qubits by using the mapping $|0\rangle \rightarrow |\bar{0}\rangle = |000\rangle$ and $|1\rangle \rightarrow |\bar{1}\rangle = |111\rangle$. If any one of the physical qubits suffers from an error that flips the states $|0\rangle$ and $|1\rangle$, then this error can be corrected without otherwise disturbing the joint state of the three qubits. This correction is achieved by making a measurement that tells us about the total parity of each pair of adjacent qubits. To do this we make two measurements, one of which projects the state onto one of the eigenstates of $M_0 = \sigma_z \otimes \sigma_z \otimes I$ and the other onto the eigenstates of $M_1 = I \otimes \sigma_z \otimes \sigma_z$. From the two measurement outcomes we can determine which bit has flipped, and thus apply a σ_x operator to that qubit to correct the error. For example, if the two measurements return even and odd parity, respectively, then it is the third qubit that has flipped, and the feedback operation that corrects the error is the unitary operator $I \otimes I \otimes \sigma_x$ [94, 110, 111]. Since this error-correction code can correct a flip error on any single qubit, it is only if an error occurs on two or more of the physical qubits that the logical qubit will be corrupted. If the errors on each of the physical qubits are independent, and occur with a probability $p \ll 1$, then the probability of an error on two or more qubits is proportional to p^2 , which is much less than p .

Maxwell’s famous demon is another simple example of quantum feedback, and one that can be usefully analyzed in terms of von Neumann measurements. The “demon” is a device that makes measurements on a system and uses the information obtained to extract work [89–93].

2.1. Continuous quantum measurements

2.1.1. Quantum filtering

When we make a continuous measurement on a quantum system, if we know the dynamics of the system, then we can derive an equation of motion for our full state-of-knowledge of the system determined by the continuous stream of measurement results. For a classical system, an observer’s state-of-knowledge is given by a probability distribution over the state-space. For a quantum system, it is the density matrix that captures all the information that an observer has about a system. Control theorists refer to the process by which an observer calculates his or her state of knowledge of a system from a series of measurement results *filtering*, and the quantum version of this *quantum filtering* [56, 57, 112]. In classical control theory, when we can only obtain partial information of the system state from the measurement output (e.g., we can measure the position but not the momentum of a mechanical system), we can introduce a dynamical system called a filter, using the measurement results as inputs to recover the whole system dynamics. However, quantum filtering is not just a trivial extension of classical filtering. In quantum filtering, we feed the measurement output (which is a classical signal) into a classical system to generate an estimated state of the measured quantum system. Thus, we use a classical system to mimic a quantum system, and some particular quantum effects, such as quantum coherence, may be lost during this process by the action of the measurement on the system. Quantum filtering is a bridge between a quantum system and a classical controller, since the classical controller can use the resulting state-of-knowledge to decide how to apply control forces to the system. For certain systems, results for optimal control from classical control theory can be directly applied to obtain optimal protocols for quantum system [68, 113].

We now present the theory of quantum measurement and filtering by first extending classical probability theory to quantum mechanics. A different approach to deriving the quantum filtering equation, which uses the Schrödinger picture and avoids the use of measure-theoretic probability theory, can be found in [114]. The main difference between classical and quantum mechanics is that quantum mechanics is *noncommutative*, by which we mean that the operators that represent different physical variables do not always commute with each other. Heisenberg’s uncertainty principle, for example, is a direct result of the commutation relation $[x, p] = i\hbar$, between the position x and the momentum p of a quantum degree of freedom. Because of this, quantum probability theory is a noncommutative version of classical probability theory. Recall that classical probability theory consists of the triple, $(\Omega, \mathcal{F}, \mathbb{P})$, referred to as a probability space. Here Ω is the sample space which is the set of all elementary, mutually exclusive outcomes. For example, for probability experiment of throwing a coin, the sample space is the set $\Omega = \{\text{head, tail}\}$. The second item in the triple, \mathcal{F} , is the set of “events”, where each event is some subset of the possible outcomes (a subset of the set Ω). This makes

\mathcal{F} a so-called σ -algebra, which satisfies the following conditions: (i) the empty set \emptyset belongs to \mathcal{F} ; (ii) \mathcal{F} is closed under complement: $\Omega \setminus A \in \mathcal{F}$ if $A \in \mathcal{F}$; and (iii) \mathcal{F} is closed under countable unions: $\bigcup_{n=1}^{\infty} A_n \in \mathcal{F}$ if all $A_n \in \mathcal{F}$. The elements of \mathcal{F} can also be equivalently expressed as a function defined on Ω (that is, something that associates a value with every outcome), which is called a random variable. In fact, for any $A \in \mathcal{F}$, we can define a random variable $\chi_A : \Omega \rightarrow \mathcal{R}$ such that $\chi_A(\omega) = 1$ if $\omega \in A$, and $\chi_A(\omega) = 0$ if it is not. The final item in the triple is the probability measure \mathbb{P} , which is a function that associates a probability with every subset of \mathcal{F} : ($\mathbb{P} : \mathcal{F} \rightarrow [0, 1]$) such that: (i) \mathbb{P} is countably additive, i.e., $\mathbb{P}(\bigcup_{n=1}^{\infty} A_n) = \sum_{n=1}^{\infty} \mathbb{P}(A_n)$ for any sequence A_1, A_2, \dots, A_n of disjoint sets in \mathcal{F} , and (ii) the measure of the whole sample space Ω is normalized so that $\mathbb{P}(\Omega) = 1$.

Quantum probability theory, developed in the 1980s [56, 57, 68, 103, 112, 113] is a non-commutative analog of classical probability theory. In quantum probability theory, there is no longer an underlying sample space, and so the quantum probability model can be described by a pair $(\mathcal{N}, \mathbb{P})$. The first item, \mathcal{N} , is an algebra, and is defined as the set of all Hermitian operators in the Hilbert space of the system. An element $A \in \mathcal{N}$ is an observable of the quantum system which can be looked as the quantum version of the random variable. The ‘‘events’’ of quantum probability are defined as all the projection operators $P \in \mathcal{N}$. These project onto the subspaces of the Hilbert space. Thus each possible set of outcomes is given by a subspace of the Hilbert space. This is simply the projection postulate of quantum measurement theory. The function $\mathbb{P} : \mathcal{N} \rightarrow \mathbb{C}$, where \mathbb{C} is the complex space, is called a state on \mathcal{N} . In fact, we can always find a system density operator ρ such that $\mathbb{P}(A) = \text{tr}(A\rho)$ for any $A \in \mathcal{N}$.

By comparing the classical probability model $(\Omega, \mathcal{F}, \mathbb{P})$ and the quantum probability model $(\mathcal{N}, \mathbb{P})$, the main difference is that the algebra \mathcal{N} , called the von Neumann algebra, is noncommutative (the Hermitian operators may not commute with each other) while the σ -algebra \mathcal{F} in classical probability is a commutative algebra. As an example, let us consider a quantum measurement of the observable A . Before this measurement, the quantum system can be described by the quantum probability model $(\mathcal{N}, \mathbb{P})$. After this measurement, the quantum state collapse occurs. The measurement output corresponds to a classical probability model $(\mathcal{A}, \mathbb{P})$, where

$$\mathcal{A} = \{X : X = f(A), f : \mathcal{R} \rightarrow \mathbb{C}\} \quad (2.1)$$

forms a commutative algebra. Thus, the quantum measurement of the observable A converts a quantum probability model into a classical probability model. More generally, in the following discussions, we will show that the quantum filtering process, which is based on quantum measurement, is merely a bridge between a quantum probability model and a classical probability model.

To better understand quantum filtering, let us consider an indirect quantum measurement, which is achieved by interacting the measured system with a bath via a system operator L , and then making a measurement on the bath. The bath is a continuum of harmonic oscillators of different frequencies. The bath also describes a field, such as the electromagnetic field, in which the oscillators are the modes of the field. The Hamiltonian of the total system composed of the measured system and the bath is given by

$$\begin{aligned} H &= H_s + H_b + H_{\text{int}}, \\ H_b &= \int_{-\infty}^{+\infty} d\omega \omega b^\dagger(\omega) b(\omega), \\ H_{\text{int}} &= i \int_{-\infty}^{+\infty} d\omega [\kappa(\omega) b^\dagger(\omega) L - \text{h.c.}], \end{aligned} \quad (2.2)$$

where H_s is the free Hamiltonian of the measured system, $b^\dagger(\omega)$ and $b(\omega)$ are the creation and annihilation operators of the bath mode with frequency ω , and satisfy

$$[b(\omega), b^\dagger(\tilde{\omega})] = \delta(\omega - \tilde{\omega}). \quad (2.3)$$

The bath mode with frequency ω interacts with the system via the system operator L , where $\kappa(\omega)$ is the corresponding coupling strength. Hereafter we set $\hbar = 1$. The total Hamiltonian H can be re-expressed in the interaction picture as

$$H_{\text{eff}} = \exp(iH_b t) (H_s + H_{\text{int}}) \exp(-iH_b t) = H_s + i \int_{-\infty}^{+\infty} d\omega [\kappa(\omega) e^{i\omega t} b^\dagger(\omega) L - \text{h.c.}]. \quad (2.4)$$

We now introduce the Markovian assumption

$$\kappa(\omega) = \sqrt{\frac{\gamma}{2\pi}}, \quad (2.5)$$

which allows the Hamiltonian H_{eff} to be expressed as

$$H_{\text{eff}} = H_s + i\sqrt{\gamma} [b_{\text{in}}^\dagger(t)L - L^\dagger b_{\text{in}}(t)], \quad (2.6)$$

where

$$b_{\text{in}}(t) = \frac{1}{\sqrt{2\pi}} \int_{-\infty}^{+\infty} d\omega e^{-i\omega t} b(\omega) \quad (2.7)$$

is the Fourier transform of the bath modes. The operator $b_{\text{in}}(t)$ is, in fact, the time-varying field that is incident on, and thus the input to, the system, and satisfies [73, 74, 105]

$$[b_{\text{in}}(t), b_{\text{in}}^\dagger(\tilde{t})] = \delta(t - \tilde{t}). \quad (2.8)$$

We now define a new bath operator

$$B_{\text{in}}(t) = \int_0^t b_{\text{in}}(\tau) d\tau \quad (2.9)$$

which is called a *quantum Wiener process*. If we assume that the bath is initially in a vacuum state, the increment of the quantum Wiener process dB_{in} and its conjugate dB_{in}^\dagger satisfy the following algebraic conditions:

$$dB_{\text{in}} dB_{\text{in}}^\dagger = dt, \quad dB_{\text{in}}^\dagger dB_{\text{in}} = dB_{\text{in}}^\dagger dB_{\text{in}}^\dagger = dB_{\text{in}} dB_{\text{in}} = 0. \quad (2.10)$$

These are the quantum version of *Itô rule* [103]. With the above notation, in the Heisenberg picture, an arbitrary system operator $X(t)$ satisfies the following quantum stochastic differential equation [73, 74]

$$dX = -i[X, H_s] dt + \frac{\gamma}{2} \{L^\dagger [X, L] + [L^\dagger, X] L\} dt + \sqrt{\gamma} \{dB_{\text{in}} [L^\dagger, X] + [X, L] dB_{\text{in}}^\dagger\}. \quad (2.11)$$

It is then possible to define an output field $b_{\text{out}}(t)$ which describes the field leaving the system after it has interacted with it, and we can similarly define its Ito increment

$$B_{\text{out}}(t) = \int_0^t d\tau b_{\text{out}}(\tau).$$

The celebrated input-output relation for the system can then be written as [73, 74]

$$dB_{\text{out}} = dB_{\text{in}} + \sqrt{\gamma} L. \quad (2.12)$$

If homodyne detection is performed on the output field $B_{\text{out}}(t)$, then the operator corresponding to the measured output is

$$dY_{\text{out}} = \frac{1}{\sqrt{\gamma}} (dB_{\text{out}} + dB_{\text{out}}^\dagger),$$

and satisfies the following equation

$$dY_{\text{out}} = (L + L^\dagger) dt + \frac{1}{\sqrt{\gamma}} (dB_{\text{in}} + dB_{\text{in}}^\dagger). \quad (2.13)$$

With the above preparation, we can now present the main results of quantum filtering theory [112]. The purpose of quantum filtering is to provide an estimate $\pi(X)$ of the value of the system observable X , at time t , given the stream of measurement results up until that time. We will define this estimate as the expectation value of X given the measurement results. To obtain $\pi(X)$ we first define

$$\mathcal{Y}_{\text{out}} = \{X : X = f(Y_{\text{out}}), f : \mathcal{R} \rightarrow \mathcal{C}\}, \quad (2.14)$$

which is the smallest commutative algebra generated by the observation process Y_{out} , and denote \mathbb{P} as the probability measure on \mathcal{Y}_{out} . The estimate $\pi(X)$ is then the conditional expectation of X on \mathcal{Y}_{out}

$$\pi(X) = \mathbb{P}(X|\mathcal{Y}_{\text{out}}). \quad (2.15)$$

From the definition of $\pi(X)$ given in Eq. (2.15), it can be proved (see, e.g., the derivations in Ref. [112]) that we can obtain the following dynamical equation for $\pi(X)$ and the corresponding output equation from Eqs. (2.11) and (2.13)

$$d\pi(X) = \pi[\mathcal{L}(X)]dt + \sqrt{\gamma}[\pi(L^\dagger X + XL) - \pi(L + L^\dagger)\pi(X)]dW, \quad (2.16)$$

$$dY_{\text{out}} = \pi(L + L^\dagger)dt + \frac{1}{\sqrt{\gamma}}dW, \quad (2.17)$$

where $\mathcal{L}(X)$ is the Liouville superoperator of the system defined as

$$\mathcal{L}(X) = -i[X, H_s] + \gamma\left(L^\dagger XL - \frac{1}{2}L^\dagger LX + \frac{1}{2}XL^\dagger L\right).$$

The process $W(t)$ in Eqs. (2.16) and (2.17) is called the innovation process of quantum filtering, and has been shown to be a classical Wiener process [112]. The increment of $W(t)$ satisfies the following classical Itô relations

$$E(dW) = 0, \quad (dW)^2 = dt, \quad (2.18)$$

where $E(\cdot)$ is the ensemble of the stochastic process induced by dW . The dynamical equation (2.16) of $\pi(X)$ is called the *quantum filtering equation*. The filtering equation (2.16) and the output equation (2.17) are the main results of quantum filtering theory.

Additionally, we can convert the filtering equation (2.16) from the Heisenberg picture to the Schrödinger picture, and thus obtain a stochastic equation for the evolution of the density matrix. To show this, we use the fact that the density operator ρ_c satisfies $\text{tr}[\pi(X)\rho_0] = \text{tr}(X_0\rho_c)$, where ρ_0 is the initial density operator of the system and X_0 is the corresponding system observable in the Schrödinger picture. Substituting Eq. (2.16) into the above relation, the system density operator ρ_c evolves according to the following stochastic master equation:

$$d\rho_c = -i[H_s, \rho_c]dt + \frac{1}{2}(2L\rho_c L^\dagger - L^\dagger L\rho_c - \rho_c L^\dagger L)dt + \{L\rho_c + \rho_c L^\dagger - \text{tr}[(L + L^\dagger)\rho_c]\rho_c\}dW. \quad (2.19)$$

From Eq. (2.15), we have

$$\rho_c = \mathbb{P}(\rho|\mathcal{Y}_{\text{out}}). \quad (2.20)$$

That is, ρ_c is the conditional expectation of the density operator ρ which is defined by $\text{tr}[X\rho_0] = \text{tr}(X_0\rho)$. The stochastic master equation (2.19) is also often referred to as *quantum filtering equation*.

To summarize, the quantum stochastic differential equation (2.11) and the output equation (2.13) give the dynamics of the operators that describe the measured quantum system. These equations are driven by the quantum Wiener noise dB_{in} , and are thus defined on a quantum probability space. As a comparison, the quantum filtering equation (2.16) (or the stochastic master equation (2.19)) and the output equation (2.17) give the observers state-of-knowledge of the measured quantum system based on the information extracted by the quantum measurement. These equations are driven by the classical Wiener noise dW and thus defined on a classical probability space. Thus in quantum filtering theory we use a classical stochastic system to mimic the dynamics of a quantum stochastic model, which is why we refer to quantum filtering as a bridge between a quantum probability model and a classical probability model.

2.1.2. Another point of view: quantum trajectories

An alternative, albeit less rigorous way to obtain the quantum filtering equation (2.19) and output equation (2.17), is to work in the Schrödinger picture [61, 114, 115]. In this approach the evolution of the density matrix conditioned on the stream of measurement results (the “measurement record”), is often referred to as a *quantum trajectory*, a term coined by *Camichael* [61]. Before the development of the quantum trajectory approach, most of the initial studies involving quantum systems interacting with a bath considered only the ensemble description, in which one discards

the measurement record, and thus calculates only the evolution of the system averaged over all possible records. This was all that was required before experimental techniques made it possible to observe single quantum systems in real-time. However, with the experimental progress, especially in optical systems and ion traps in the 1990s, it became necessary to describe the evolution of a system for an individual measurement record.

One of the early approaches to obtaining a quantum trajectory for a given measurement record was to express the quantum master equation as an average over a stochastic equation for the evolution of a pure quantum state. This is equivalent to the use of a ‘‘Monte Carlo’’ method to simulate the master equation [116]. Carmichael referred to the process of expressing a master equation as the average of a stochastic equation as *unravelling* it. For a single master equation there is more than one stochastic equation that will unravel it, and it can be unravelled by stochastic equations driven either by Gaussian white noise (Wiener noise) [114, 117, 118] or by a ‘‘point process’’ [63, 115, 119, 120]. A point process consists of intervals of smooth (deterministic) motion, punctuated by instantaneous events in which the state of the system changes discontinuously. The Poisson process is an example of a point process. The different stochastic equations correspond to different ways in which the system can be continuously monitored.

1. *Quantum jumps:*

Consider the master equation

$$\dot{\rho} = -i[H, \rho] + \frac{1}{2} \sum_{\mu} (2c_{\mu}\rho c_{\mu}^{\dagger} - c_{\mu}^{\dagger}c_{\mu}\rho - \rho c_{\mu}^{\dagger}c_{\mu}). \quad (2.21)$$

A stochastic equation that unravels this master equation, and that is driven by a point process, is

$$d|\psi_c\rangle = \left[-iH + \frac{1}{2} \sum_{\mu} (\langle c_{\mu}^{\dagger}c_{\mu} \rangle(t) - c_{\mu}^{\dagger}c_{\mu}) \right] |\psi_c\rangle dt + \sum_{\mu} \left[\frac{c_{\mu}}{\sqrt{\langle c_{\mu}^{\dagger}c_{\mu} \rangle(t)}} - 1 \right] |\psi_c\rangle dN_{\mu}. \quad (2.22)$$

Here, for each μ , the increment dN_{μ} is an increment of a point process, and takes only two values, either 0 or 1. The value 1 corresponds to an instantaneous event, and thus dN_{μ} is equal to 1 only at a set of discrete points. The rest of the time $dN_{\mu} = 0$. The events occur randomly and independently, and the probability per unit time that an event occurs for the process labelled by μ is $\langle c_{\mu}^{\dagger}c_{\mu} \rangle(t)$. This means that the probability for an event in the time interval $[t, t + dt]$ is $\langle c_{\mu}^{\dagger}c_{\mu} \rangle dt$. The point-process increments satisfy the relations

$$E[dN_{\mu}(t)] = \langle c_{\mu}^{\dagger}c_{\mu} \rangle dt, \quad dN_{\mu}dN_{\nu} = dN_{\mu}\delta_{\mu\nu}. \quad (2.23)$$

Since Eq. (2.22) is a stochastic equation for the state vector, it is usually called a *stochastic Schrödinger equation*. We can alternatively write down a *stochastic master equation* for the density matrix $\rho_c = |\psi_c\rangle\langle\psi_c|$, which is

$$d\rho_c = \sum_{\mu} \mathcal{G}[c_{\mu}]\rho_c dN_{\mu}(t) + \mathcal{H}\left[-iH - \frac{1}{2} \sum_{\mu} c_{\mu}^{\dagger}c_{\mu}\right]\rho_c dt. \quad (2.24)$$

The superoperators $\mathcal{G}[c]\rho_c$ and $\mathcal{H}[c]\rho_c$ are defined as

$$\begin{aligned} \mathcal{G}[c]\rho_c &= \frac{c\rho_c c^{\dagger}}{\text{tr}[c\rho_c c^{\dagger}]} - \rho_c, \\ \mathcal{H}[c]\rho_c &= c\rho_c + \rho_c c - \langle c + c^{\dagger} \rangle \rho_c. \end{aligned} \quad (2.25)$$

The point process (quantum jump) stochastic Schrödinger equation (SSE) describes, for example, an optical cavity in which the light that leaks out of the cavity is measured with a photon-counter [121]. In this case there is a single Lindblad operator $c = \sqrt{\gamma}a$, where γ and a are the damping rate and annihilation operator for the cavity, respectively. The events at which $dN = 1$ correspond to the detection of a photon by the photo-detector.

If the photon-detector is ideal, meaning that it never misses a photon, and never clicks when there is no photon, then an initially pure state remains pure, and the SSE is sufficient to describe the observer’s state-of-knowledge as the measurement proceeds. But if the photon-detector is not perfect, the observer no longer has full information about

the quantum state as the measurement proceeds. The observer's state-of-knowledge is then necessarily given by a density matrix, and we must use a stochastic master equation (SME), rather than a Schrödinger equation. We must also modify the master equation to include imperfect detection. If the photon-detector is inefficient, so that it records only a fraction η of the photons emitted by the cavity, and does not record any non-existent photons, then the SME in Eq.(2.24) becomes

$$d\rho_c = \left\{ dN\mathcal{G}[\sqrt{\gamma\eta}a] + dt\mathcal{H}\left[-iH - \frac{\eta\gamma}{2}a^\dagger a\right] + dt(1-\eta)\mathcal{D}[\sqrt{\gamma}a] \right\} \rho_c, \quad (2.26)$$

where

$$\mathcal{D}[c]\rho = c\rho c^\dagger - \frac{1}{2}c^\dagger c\rho - \frac{1}{2}\rho c^\dagger c. \quad (2.27)$$

2. Quantum diffusion:

The master equation given by Eq. (2.21) is also unravelled by the SSE [59, 114, 117, 118]

$$d|\psi\rangle = -iH|\psi\rangle dt + \sum_{\mu} \left(\langle c_{\mu}^{\dagger} \rangle c_{\mu} - \frac{1}{2}c_{\mu}^{\dagger}c_{\mu} - \frac{1}{2}\langle c_{\mu}^{\dagger} \rangle \langle c_{\mu} \rangle \right) |\psi\rangle dt + \sum_{\mu} (c_{\mu} - \langle c_{\mu} \rangle) |\psi\rangle dW_{\mu}, \quad (2.28)$$

where the dW_{μ} are a set of mutually independent Wiener noises satisfying

$$E(dW_{\mu}) = 0, \quad dW_{\mu}dW_{\nu} = \delta_{\mu\nu}dt. \quad (2.29)$$

The equivalent stochastic master equation is

$$d\rho_c = -i[H, \rho_c] dt + \sum_{\mu} \left(\mathcal{D}[c_{\mu}] \rho_c dt + \mathcal{H}[c_{\mu}] \rho_c dW_{\mu} \right). \quad (2.30)$$

Stochastic SSE's and SME's driven by Wiener noise correspond to measurement techniques that are quite different from photon-counting. If, instead of detecting the light from a cavity with a photo-detector directly, one first interferes the light with a laser whose intensity is much greater than the cavity output, the result is a measurement containing Wiener noise. This measurement technique is sensitive to the phase of the cavity output, whereas direct photo-detection is not, and is called *homodyne detection* [59].

In the limit that the power of the laser is infinite, the dynamics of a single mode of an optical cavity measured by homodyne detection is given by Eq.(2.30) with a single Lindblad operator $c = \sqrt{\gamma}a$. The measured output is

$$dy = \langle x \rangle dt + \frac{1}{\sqrt{2\gamma}} dW, \quad (2.31)$$

where $x = (a + a^\dagger) / \sqrt{2}$ is the normalized position operator of the cavity mode, and dW is the same Wiener noise increment that appears in the SME. If the photo-detector is inefficient, then the SME becomes

$$d\rho_c = -i[H, \rho_c] dt + \gamma\mathcal{D}[a]\rho_c + \mathcal{H}[\sqrt{\eta\gamma}a]\rho_c dW, \quad (2.32)$$

and the measurement output is

$$dy = \langle x \rangle dt + \frac{1}{\sqrt{2\eta\gamma}} dW, \quad (2.33)$$

where η is the detection efficiency. Continuous measurements containing Wiener noise are also sometimes referred to as weak measurements. We prefer to call them continuous measurements because (i) weak measurements are not necessarily continuous, and (ii) it can lead to confusion with the "weak values" of Aharonov, Albert and Vaidman [122, 123].

More generally, a continuous measurement of the quantum variables A_l ($l = 1, \dots, m$) can be expressed as the stochastic master equation [114]

$$d\rho_c = -i[H, \rho] dt + \sum_{l=1}^m \left(\Gamma_l \mathcal{D}[A_l] \rho_c dt + \sqrt{\eta_l \Gamma_l} \mathcal{H}[A_l] dW_l \right), \quad (2.34)$$

and output equation

$$dy_l = \langle A_l \rangle dt + \frac{1}{\sqrt{2\eta_l\Gamma_l}} dW_l, \quad (2.35)$$

where Γ_l and η_l represent the measurement strengths and measurement efficiencies.

The stochastic master equation (2.34) and the equation for the stream of measurement results, Eq. (2.35), can be derived from the quantum filtering equations (Eqs. (2.19) and (2.17)). The quantum filtering equations give the evolution of the system and the output field before any measurement is made on the output field. Making a measurement on the output field turns the quantum filtering equations into a stochastic master equation.

As mentioned above, we can simultaneously make more than one continuous measurement on a system, and we can simultaneously measure observables that do not commute. Since the respective dynamics induced by the continuous measurements of two different observables commute to first order in dt , we can think of the measurements of the two observables as being interleaved — the process alternates between infinitesimal measurements of each observable. Note that a von Neumann measurement cannot simultaneously project a system onto the eigenstates of two non-commuting observables, but continuous measurements do not perform instantaneous projections. The effect of simultaneously measuring the position and momentum of a single particle, for example [124, 125], is to feed noise into both observables. Measuring noncommuting observables therefore in general introduces more noise into a system than is necessary to obtain a given amount of information. The optical measurement techniques of heterodyne detection [50] and eight-port homodyne detection [126] are very similar to simultaneous measurements of momentum and position.

2.2. Markovian quantum feedback

The continuous collapse of the quantum state in continuous quantum measurement means that we can execute real-time quantum feedback control before the quantum state collapses to a completely classical state. That is the starting point of continuous measurement-based feedback control. The key questions in feedback control are usually (i) what observable should we measure? and (ii) how should we choose the feedback forces as a function(al) of the stream of measurement results? Optimal feedback strategies can always be obtained by using the SME to determine the observer's full state of knowledge (the density matrix) given the stream of measurement results up to the present time, and using this to determine the choice of Hamiltonian at each time. But solving the SME can take significant numerical resources, and it may not be possible to do so in real-time. In that, one can attempt to approximate the SME with a simpler differential equation, which may be possible depending on the dynamics of the system [127–129]. Alternatively we can take the opposite approach, and see what can be achieved with quantum feedback when we perform no processing of the measurement results, and merely engineer a term in the Hamiltonian of the system that, at each time, is proportional to the measurement result at that time. This is the kind of feedback protocols that were introduced by Wiseman and Milburn [59, 60, 66], and are now referred to as Markovian feedback. The reason for this name is that for this kind of feedback, if we average the evolution over all trajectories, the result is a Markovian master equation. This is not usually true for feedback protocols.

Let us consider a quantum continuous measurement of the operator A with efficiency η . From Eqs. (2.34) and (2.35), the measurement and output equations of this measurement can be expressed as

$$d\rho_c = -i[H, \rho_c] dt + \Gamma_A \mathcal{D}[A] \rho_c dt + \sqrt{\eta\Gamma_A} \mathcal{H}[A] \rho_c dW, \quad (2.36)$$

and

$$dy = \langle A \rangle dt + \frac{1}{\sqrt{2\eta\Gamma_A}} dW. \quad (2.37)$$

These two equations can also be expressed equivalently by

$$\dot{\rho}_c = -i[H, \rho_c] + \Gamma_A \mathcal{D}[A] \rho_c + \sqrt{\eta\Gamma_A} \mathcal{H}[A] \rho_c \xi(t), \quad (2.38)$$

and

$$I_A(t) = \langle A \rangle + \frac{1}{\sqrt{2\eta\Gamma_A}} \xi(t), \quad (2.39)$$

where $\xi(t)$ is the white noise satisfying

$$E(\xi(t)) = 0, \quad E(\xi(t)\xi(t')) = \delta(t-t'). \quad (2.40)$$

Formally, we can convert Eqs. (2.36) and (2.37) into Eqs. (2.38) and (2.39) by setting $\xi(t) = dW/dt$.

The main object of measurement-based quantum feedback is to use the output signal $I_A(t)$ to engineer the system dynamics given by Eq. (2.36). The most general form of the system dynamics, modified based on the output signal $I_A(t)$, can be expressed as [50]

$$\dot{\rho}_f = \mathcal{F}[t, \{I_A(\tau) | \tau \in [0, t]\}] \rho_f, \quad (2.41)$$

where $\mathcal{F}[t, \{I_A(\tau) | \tau \in [0, t]\}]$ is the superoperator depending on the output signal $I_A(t)$ for all past times. In this general form of the response of the feedback control loop, the control induces both unitary dynamics and dissipation effects on the controlled system. However, for most of the existing studies, quantum feedback control is introduced coherently by varying the parameters in the system Hamiltonian, which leads to the following modified closed-loop stochastic master equation

$$\dot{\rho}_f = -i[H + H_f(t, \{I_A(\tau) | \tau \in [0, t]\}), \rho_f] + \Gamma_A \mathcal{D}[A] \rho_f + \sqrt{\eta \Gamma_A} \mathcal{H}[A] \rho_f \xi(t). \quad (2.42)$$

As discussed above, in Markovian quantum feedback a term in the Hamiltonian is made proportional to the output signal. Denoting this term by H_f , we set $H_f = I_A(t)F$ for some Hermitian operator F . Then, by averaging over the noise term and using the Ito rule of the white noise $\xi(t)$, we can derive the following Wiseman-Milburn master equation [50] from Eq. (2.42):

$$\dot{\rho} = -i[H, \rho] + \Gamma_A \mathcal{D}[A] \rho - i[F, A\rho + \rho A] + \frac{1}{\eta} \mathcal{D}[F] \rho. \quad (2.43)$$

The effects induced by the feedback loop are clearer in this form: (i) the first feedback term $-i[F, A\rho + \rho A]$ plays a positive role to steer the system dynamics to achieve the desired effects; and (ii) the second feedback term $\mathcal{D}[F] \rho / \eta$ represents the decoherence effects induced by feedback, which tends to play a negative role for purposes of control. The master equation (2.43) can be reexpressed as the traditional Lindblad form [50, 66]

$$\dot{\rho} = -i \left[H + \frac{(AF + FA)}{2}, \rho \right] + \mathcal{D}[A - iF] \rho + \frac{1 - \eta}{\eta} \mathcal{D}[F] \rho. \quad (2.44)$$

Although the Markovian quantum feedback given by Eq. (2.43) is the simplest measurement-based quantum feedback approach, it can be used to solve various problems by choosing A and F appropriately. Markovian quantum feedback has been used to stabilize arbitrary one-qubit quantum states [130–132], manipulate quantum entanglement [133–146], generate and protect Schrödinger cat states [147–151], and induce optical, mechanical, and spin squeezing [152–160].

2.3. Feedback via time-averaging

Markovian quantum feedback is simple to describe analytically, but is also rather limited. Further, feeding back the measurement signal at each instant of time does not make optimal use of the information extracted by the measurement. To do that we must process the measurement results using the SME. It is worth pausing at this point to understand a little more how the measurement results, given by Eq. (2.35), provide information about the measured operator and the state of the system. If we process the measurement results so that we know ρ_c at each time, then we also know the expectation value of the measured operator, $\langle A \rangle$, at each time. The first term in Eq. (2.35) is therefore already known, and provides no new information about the system. It is the noise term dW that carries the new information, and that modifies our state-of-knowledge. In fact, by definition we always know the expectation value $\langle A \rangle = \text{Tr}[A\rho_c]$ at the start of the continuous measurement, because ρ_c is our state-of-knowledge. But the system might really be in some pure state $|\psi\rangle$, so that the true mean value of A is $\bar{A} = \langle \psi | A | \psi \rangle$. As the measurement proceeds, the conditional expectation value $\langle A \rangle$ tends to \bar{A} and ρ_c tends to $|\psi\rangle$.

Now consider what happens if A is a Hermitian observable, and $|\psi\rangle$ is an eigenstate of both the system Hamiltonian and A . In this case, assuming that the system is not driven by other noise sources, it remains in the state $|\psi\rangle$ as the

measurement proceeds, and \bar{A} is constant. In that case we can obtain an estimate of \bar{A} of ever increasing accuracy without solving the SME. All we need to do is to average the measurement results obtained so far, and divide by the total time [161]. If we define

$$Y_A(t) = \frac{1}{t} \int_0^t dy = \frac{1}{t} \int_0^t \langle A \rangle dt + \frac{1}{t \sqrt{2\eta\Gamma_A}} \int_0^t dW, \quad (2.45)$$

then as $t \rightarrow \infty$ the second term tends to zero and $Y_A(t) \rightarrow \bar{A}$. The reason that the second term, being the average of the noise, tends to zero is that it has equally positive and negative fluctuations and these average to zero over time.

The mean value of the measured observable, \bar{A} , is usually not constant for a system that we are trying to control. Nevertheless we can still use an averaging procedure to obtain an estimate of \bar{A} and use this to choose our feedback forces. This method is not as complex as processing the measurements using the SME, but more complex than Markovian feedback [162–165]. To do this we average the signal over a time T that is long enough to reduce the noise but not so long that \bar{A} changes too much during T . We can also include a weighting function, $f(t)$, to smoothly reduce the dependence on our estimate of \bar{A} on measurement results that are too far in the past. For example, if we use an exponential weighting function, our estimate of \bar{A} at time t is

$$\tilde{Y}_A(t) = \frac{1}{T} \int_{t-T}^t e^{-\gamma_f t} \left(\langle A \rangle dt + \frac{1}{\sqrt{2\eta\Gamma_A}} dW \right). \quad (2.46)$$

When $T \ll 1/\gamma_f$, the estimate converges as

$$\tilde{Y}_A(t) - \bar{A}(t) = \exp(-\gamma_f t) [\tilde{Y}_A(0) - \bar{A}(0)]. \quad (2.47)$$

Such an exponentially-convergent filter has been introduced in the literature to stabilize two-qubit entanglement [166, 167] and a three-qubit GHZ state [168] both in optical systems and in superconducting circuits. It has also been applied experimentally to the adaptive estimation of the optical phase [169].

2.4. Bayesian quantum feedback

To make full use of the information provided by the measurement, we must process the measurement results using the SME (Eq. (2.34)) to obtain the conditional density matrix. Since this density matrix, along with the knowledge of the dynamics of the system, determines the probabilities of the results of any measurement on the system at any time in the future, any optimal strategy for controlling the system can ultimately be specified as a rule for choosing the Hamiltonian at time t as a function of the density matrix at that time and possibly the time itself: $H(t) = f(\rho_c(t), t)$. Feedback control in which the feedback protocol is specified in this way is sometimes referred to as “Bayesian feedback” because the SME is the quantum equivalent of processing the measurement record using Bayes’ theorem [170].

As we have mentioned above, the SME, since it requires simulating the full dynamics of the system, may be impractical to solve in real-time. Sometimes it is possible to approximately, or even exactly, reduce the computational overhead by choosing an ansatz for ρ_c that contains only a small number of parameters. The SME then reduces to a stochastic differential equation for these parameters. Two examples in which an approximate ansatz provides an effective control protocol can be found in [127–129]. There is one class of systems in which an ansatz with a small number of parameters provides an *exact* solution to the SME, that of linear systems. A quantum system is referred to as linear if its Hamiltonian is no more than quadratic in the position and momentum operators, any Lindblad operators that describe the noise driving the system are linear in the position and momentum operators, and any measurements are (i) driven by Wiener noise, and (ii) of operators that are linear in the position and momentum.

The noise that drives linear systems reduces all initial states to Gaussian states (states that are Gaussian in the position and momentum bases, and thus have Gaussian Wigner functions), and Gaussian states remain Gaussian under the evolution. No proof of the first of these statements exists, but experience leads us to believe it. The second statement is not difficult to show, and implies immediately that if the state of a linear system is Gaussian, the SME reduces to a stochastic differential equation for the means and (co-)variances of the position and momentum [68]. What is more, the dynamics of these variables are exactly reproduced by those of a classical linear system driven by Gaussian noise, and subjected to continuous measurements of the same observables. To correctly reproduce the quantum dynamics, for each continuous measurement made on the system a noise source must be added to the classical system to mimic Heisenberg’s uncertainty principle.

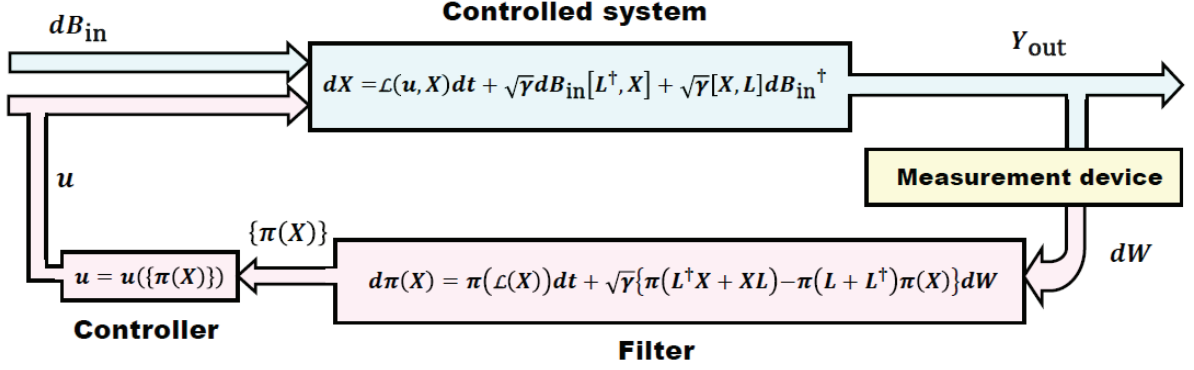


Figure 2: (Color online) Diagram for state-based quantum feedback. The controlled system (top branch, in blue) is described by a quantum stochastic differential equation driven by the quantum Wiener noise dB_{in} . Part of the quantum output field Y_{out} from the controlled system is converted into a classical signal dW by a measurement device (shown in yellow) and then fed into the filter. The dynamics of the filter is determined by the quantum filtering equation driven by the classical Wiener noise, i.e., the innovation process dW . The estimated quantum state $\{\pi(X)\}$ is fed into a classical controller to obtain a control signal u , which is then fed back to steer the dynamics of the controlled system. The filter and controller which form the classical control loop (in pink) can be realized by a classical Digital Signal Processor (DSP).

Consider a linear quantum system with N degrees of freedom [171–175], and write the N position and momentum operators, denoted respectively by q_n and p_n , in the vector

$$\mathbf{x} = (q_1, p_1, \dots, q_N, p_N)^T. \quad (2.48)$$

We scale these operators so that $[q_n, p_n] = i$. If x_m is the m^{th} element of the vector \mathbf{x} , then we have $[x_n, x_m] = i\Sigma_{nm}$, where

$$\Sigma = \bigotimes_{n=1}^N \begin{pmatrix} 0 & 1 \\ -1 & 0 \end{pmatrix}.$$

For linear quantum systems, the system Hamiltonian H_s and the dissipation operator L in Eq. (2.11) can be written as [171–173]

$$H_s = \frac{1}{2}\mathbf{x}^T G \mathbf{x} - \mathbf{x}^T \Sigma \mathbf{b} u, \quad L = \mathbf{l}^T \mathbf{x}, \quad (2.49)$$

where G is a real and symmetric matrix, and \mathbf{b}, \mathbf{l} are real and complex vectors, respectively. The second term in H_s , including the time-dependent function $u(t)$, describes the force applied by the feedback controller (see Fig. 2). This feedback Hamiltonian must be linear in the conditional mean values of the position and momentum operators, in order to ensure that the system remains linear. This also means that there is a linear map from the measurement output Y_{out} to $u(t)$, and thus a linear input-output relation for the controlled system. From Eq. (2.11), the dynamics of the controlled system can be expressed as the following linear quantum stochastic differential equation:

$$d\mathbf{x} = A \mathbf{x} dt + \mathbf{b} u dt + i\sqrt{\gamma}\Sigma [\mathbf{l} dB_{\text{in}}^\dagger - \mathbf{l}^* dB_{\text{in}}], \quad (2.50)$$

where the matrix $A = \Sigma [G + \text{Im}(\mathbf{l}^* \mathbf{l}^T)]$. The output equation (2.13) can be written as

$$dY_{\text{out}} = F \mathbf{x} dt + \frac{1}{\sqrt{\gamma}} (dB_{\text{in}} + dB_{\text{in}}^\dagger), \quad F = \mathbf{l}^T + \mathbf{l}^\dagger. \quad (2.51)$$

After quantum measurement, the dynamics of this linear quantum system can be fully described by the conditional means $\pi(\mathbf{x})$ and variances $V_t = \mathbb{P}(P_t | \mathcal{Y})$, where P_t is the covariance matrix of the position and momentum variables with the (i, j) -element being $P_{ij} = (\Delta x_i \Delta x_j + \Delta x_j \Delta x_i)/2$, and $\Delta x_i = x_i - \pi(x_i)$. The conditional mean values $\pi(\mathbf{x})$ obey the filtering equation

$$d\pi(\mathbf{x}) = A \pi(\mathbf{x}) dt + B u dt + [V_t F^T + \Sigma^T \text{Im}(l)] \times [dY - F \pi(\mathbf{x}) dt], \quad (2.52)$$

and the conditional covariance matrix satisfies the deterministic Riccati differential equation

$$\dot{V}_t = A V_t + V_t A^T + D - [V_t F^T + \Sigma^T \text{Im}(l)] \times [F V_t + \text{Im}(l^T) \Sigma], \quad (2.53)$$

where $D = \Sigma \text{Re}(l^* l^T) \Sigma^T$. Thus, the filtering equation (2.16) or (2.19) is equivalent to the closed set of filtering equations (2.52) for the first-order quadrature and the Riccati differential equation (2.53), which is finite-dimensional and thus simulated with relative ease. The quantum filter given by Eqs. (2.52) and (2.53) is called a quantum Kalman filter [68, 113, 171–173].

For linear quantum feedback control systems, many objectives, such as cooling and squeezing, can be reduced to the optimization of the following quadratic cost function of the system state \mathbf{x}

$$J_q = \frac{1}{2} \mathbf{x}_T^T S \mathbf{x}_T + \frac{1}{2} \int_0^T [\mathbf{x}_\tau^T Q \mathbf{x}_\tau + u_\tau^T R u_\tau] d\tau. \quad (2.54)$$

To obtain a closed-form control problem, we should first take the expectation value over the conditioned state and then average over all the stochastic trajectories to define a new quadratic cost function $J = \langle \mathbb{P}(J_q | \mathcal{Y}_{\text{out}}) \rangle_c$, where $\langle \cdot \rangle_c$ is the average taken over the classical Wiener noise dW . From Eq.(2.54) we have

$$J = \left\langle \frac{1}{2} \int_0^T [\pi(\mathbf{x}_\tau)^T Q \pi(\mathbf{x}_\tau) + \text{tr}(Q V_\tau) + u_\tau^T R u_\tau] d\tau \right\rangle_c + \left\langle \frac{1}{2} \pi(\mathbf{x}_T)^T S \pi(\mathbf{x}_T) + \frac{1}{2} \text{tr}(S V_T) \right\rangle_c. \quad (2.55)$$

Here the control $u_t = u(\pi(\mathbf{x}_t), V_t)$ is a function of the conditional means and variances $\pi(\mathbf{x}_t)$ and V_t . The optimization of the quadratic cost function (2.55) subject to the quantum filtering equations (2.52) and (2.53) is a standard classical Linear-Quadratic-Gaussian (LQG) control problem which can be solved by the Kalman filtering theory well developed in the field of classical control.

2.5. Applications

2.5.1. Noise reduction and quantum error correction

Similar to classical feedback, one of the most important applications of quantum feedback is to suppress the effects of noise, which in quantum systems causes decoherence. Markovian quantum feedback can be used to suppress the decoherence of macroscopic-superposition states (so-called ‘‘Schrödinger cat’’ states) [147–151] if we measure the output channel that is causing the decoherence. As an example, if we prepare the following superposition of two coherent states,

$$|\psi\rangle = \frac{|\alpha_0\rangle + |-\alpha_0\rangle}{\sqrt{2}}, \quad (2.56)$$

in an optical cavity, then by making a Homodyne measurement of the light that leaks out of the cavity we can use Markovian feedback to extend the time over which the coherence survives. Without quantum feedback, the timescale over which the coherence between the two coherent states survives is $\tau = 1/(2\gamma|\alpha_0|^2)$, where γ is the decay rate of the cavity [176]. If the signal from the Homodyne measurement is used to control the transmissivity of an electro-optic modulator (EOM), as depicted in Fig. 3, then the timescale over which the coherence survives is [148]

$$\tau_{\text{fb}} = \frac{\tau}{(1 - g \sin \theta)^2}, \quad (2.57)$$

where ϕ and g are the phase shift and gain of the feedback, respectively.

Another example of the use of Markovian quantum feedback is to reduce the phase noise in an atom laser [177, 178]. The primary source of this phase noise is collisions between atoms. A single-mode atom laser can be described by the master equation

$$\dot{\rho} = -i[C(a^\dagger)^2 a^2, \rho] + \kappa \mu \mathcal{D}[a^\dagger] \mathcal{A}[a^\dagger]^{-1} \rho + \kappa \mathcal{D}[a] \rho, \quad (2.58)$$

where as usual a is the annihilation operator for the mode, $\kappa, \mu \gg 1$ are respectively the damping rate and the stationary mean number of atoms in the laser mode, and the superoperator $\mathcal{A}[\cdot]$ is defined by

$$\mathcal{A}[r] \rho = \frac{1}{2} \{r^\dagger r, \rho\},$$

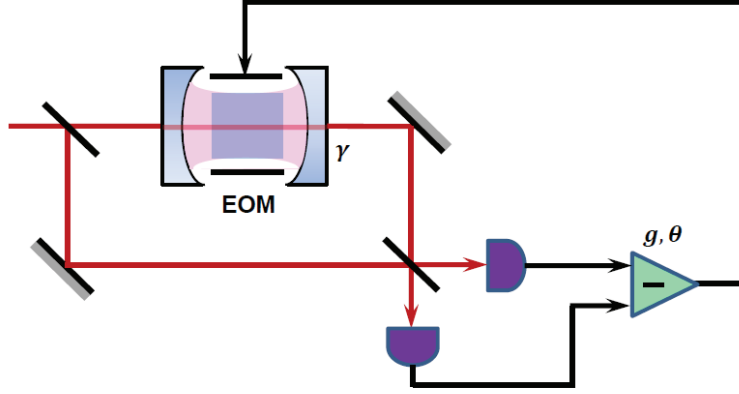


Figure 3: (Color online) Schematic diagram of a scheme proposal [148] to extend the lifetime of superpositions of macroscopically distinguishable coherent states. Such a “Schrödinger-cat” state is initially prepared inside an optical or superconducting cavity. The output field from the cavity is measured by homodyne detection and then the homodyne photocurrent is fed back to control the transmissivity of an electro-optic modulator. The feedback gain and phase are denoted by g and θ , respectively. The negative sign in the triangle indicates that the two signals are subtracted.

The nonlinear Hamiltonian

$$H_{\text{coll}} = \hbar C (a^\dagger)^2 a^2$$

describes the collisions between atoms at a rate C . From Eq. (2.58) the linewidth of the atom laser without feedback can be shown to be

$$l = \begin{cases} \frac{\kappa}{2\mu} (1 + \chi^2), & \chi \ll \sqrt{\mu}, \\ \frac{\kappa\chi}{\sqrt{\pi\mu/2}}, & \chi \gg \sqrt{\mu}, \end{cases} \quad (2.59)$$

where $\chi = 4\mu C/\kappa$ is a dimensionless atomic interaction strength. We now make a quantum nondemolition measurement of the atomic number, and use the photocurrent (the stream of measurement results) from this measurement to modulate the external field applied to the condensate of atoms to generate the output of the laser. With this feedback the linewidth of the atom laser becomes

$$l = \frac{\kappa}{2\mu} \left(1 + \frac{\chi}{\sqrt{\eta}} \right). \quad (2.60)$$

The feedback is thus capable of eliminating the effect of atomic collisions on the linewidth of the laser [177, 178].

Continuous-time feedback has also been applied to quantum error correction, a technique that is able to slow the decoherence of unknown quantum states [110, 111, 179–182]. By “unknown”, we mean that the controller is able to preserve the initial state without knowing what the state is. This requires that the state is initially encoded in a larger Hilbert space before the error-correction can be applied. As an example, we return to the three-qubit bit-flip code given in the beginning of this section. The idea is to replace the projective measurements that extract the error syndrome with continuous measurements [110]. Recall that the state of a single logical-qubit is encoded (stored) in three physical qubits. To extract the information about the error, we make a continuous measurement of the three operators ZZI , IZZ , and ZIZ , all with the same measurement strength, κ . We also apply three control Hamiltonians, $H_1 = \hbar\lambda_1 XII$, $H_2 = \hbar\lambda_2 IXI$, and $H_3 = \hbar\lambda_3 IIX$. These three Hamiltonians apply the corrections for the three possible errors, and thus the rates λ_1 , λ_2 , and λ_3 are to be determined by the measurement results. Recall that Bayesian feedback involves integrating the stochastic master equation, which in this case is

$$d\rho_c = -i[\lambda_1 XII + \lambda_2 IXI + \lambda_3 IIX, \rho_c]dt + \gamma(\mathcal{D}[XII] + \mathcal{D}[IXI] + \mathcal{D}[IIX])\rho_c dt + \kappa(\mathcal{D}[ZZI] + \mathcal{D}[IZZ] + \mathcal{D}[ZIZ])\rho_c dt + \sqrt{\kappa}(\mathcal{H}[ZZI]dW_1 + \mathcal{H}[IZZ]dW_2 + \mathcal{H}[ZIZ]dW_3)\rho_c. \quad (2.61)$$

The feedback control parameters $\{\lambda_j\}$ are then determined from the conditional density matrix $d\rho_c$. By minimizing a cost function, which is defined as the distance between the conditional density matrix and the space in which the

logical qubit should reside (the codespace), the optimal feedback is determined to be

$$\begin{aligned}
\lambda_1 &= \lambda \operatorname{sgn}\langle YZI + YIZ \rangle_c, \\
\lambda_2 &= \lambda \operatorname{sgn}\langle ZYI + IYZ \rangle_c, \\
\lambda_3 &= \lambda \operatorname{sgn}\langle ZIY + IZY \rangle_c,
\end{aligned}
\tag{2.62}$$

where λ is the maximum available feedback strength. Here, $\operatorname{sgn}(x) = +1$ if $x > 0$, $\operatorname{sgn}(0) = 0$, and $\operatorname{sgn}(x) = -1$ if $x < 0$. It is shown in Ref. [110] that this quantum error correction protocol can efficiently increase the fidelity of the encoded quantum states beyond that achieved by traditional projective-measurement-based error-correction, so long as the time delay induced by the feedback loop is small enough.

It was shown in [179] that averaging the stream of measurement results is sufficient to perform quantum error-correction, thus replacing the highly complex Bayesian feedback with time-averaged feedback. Further efficient methods for continuous-time quantum error-correction are presented in [180].

A simpler situation occurs if the environment that is causing the errors can itself be measured. An example of this is when the light that leaks out of an optical cavity is detected. In this case the measurement provides direct information about what error has occurred, reducing the resources required for quantum error correction. It is shown in [111] that when the bath that causes the errors is detected, Markovian feedback is all that is required to perform error-correction, and only $n + 1$ physical qubits are required to encode n logical qubits.

Quantum feedback has been combined with open-loop control protocols to reduce errors in quantum systems. The open-loop technique of dynamical decoupling allows errors to be reduced if they are due to noise that has a sufficiently long correlation time [183–185]. In [186] feedback and dynamical decoupling are combined by feeding the output of a dynamical decoupling protocol to a feedback controller. It is shown that for a single qubit the combination of quantum feedback and dynamical decoupling outperforms either method when used alone.

2.5.2. State reduction and stabilization

In the previous section we discussed the use of feedback to protect quantum state temporarily. We refer to the indefinite protection of a quantum state as stabilization. Unknown states cannot be stabilized, but known states certainly can be. Sometimes open-loop control can be used to stabilize states, but only in certain circumstances, for example when an effectively zero-temperature environment is available [130]. Markovian quantum feedback can be used to stabilize the states of a single two-level atom when the source of decoherence is detected [130–132]. In Ref. [130] it is shown that for a two-level atom, states in an ellipse in the lower half part of the Bloch ball can be stabilized by open-loop control under the damping process. However, when we introduce Markovian quantum feedback and carefully choose the feedback gain and the strength of the driving field, it is only states on the equator of the Bloch sphere that cannot be stabilized.

More generally, Bayesian feedback has been applied to the stabilization of quantum states in a variety of mesoscopic systems [187–207]. These include nano-mechanical resonators [189–191], quantum-dots [192–203], and superconducting qubits [204–207].

Immediately before a stabilization feedback process starts, the system to be controlled will likely be in some steady-state determined by the noise processes that drive it, and this state is often significantly mixed. When we first apply measurement-based feedback, the measurement will reduce the entropy of the system, a process often called *purification*. If the state towards which the measurement projects the system is not one of the eigenstates of the initial density matrix, then the measurement necessarily also induces a “collapse” of the wave-function, a process often called “state-reduction”. Thus purification may or may not involve state-reduction, although often these terms are used interchangeably.

If we make a continuous measurement of an observable, and perform no feedback, then the measurement will continually try to project the system onto one of the eigenstates of the observable, where the choice of eigenstate is random. In the absence of noise that interferes with the reduction process, the final state of the system will be one of these eigenstates. As shown in [208–212], if we perform feedback control during the state-reduction process, we can control which eigenstate that the measurement projects onto.

To examine this process further, we consider the single-qubit state-reduction protocol presented in Ref. [208]. As shown in Fig. 4, a single two-level system, such as atom, is inserted into an optical cavity, and the output of the cavity

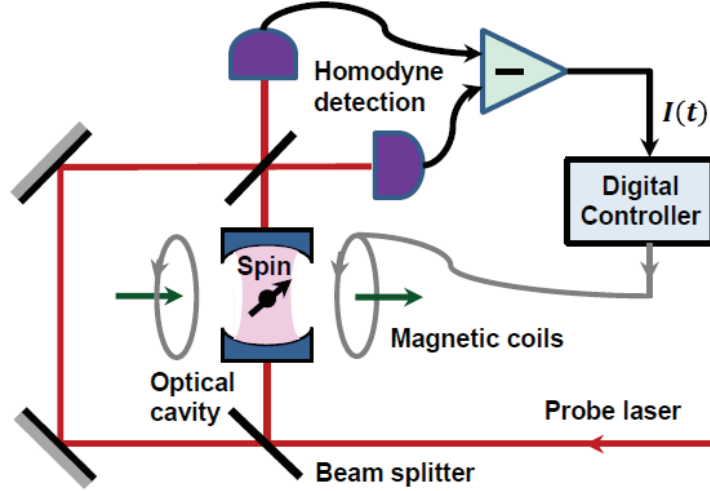


Figure 4: (Color online) Schematic diagram of a proposed theoretical setup [208] for qubit state stabilization. The information of the spin inside the cavity is continuously extracted by an optical probe field and then detected by homodyne measurement. The electric output signal $I(t)$ of the homodyne measurement is fed into a digital controller and then fed back to control the magnetic field (shown in green) imposed on the spin.

is measured by a homodyne detection. When the cavity damping rate is much faster than the dynamics of the qubit, this measurement procedure realizes a continuous measurement of the σ_z operator of the two-level system.

The stream of measurement results is fed into a digital controller and then back to control a classical field that allows us to rotate the two-level system around the y -axis. The control Hamiltonian is thus $H = B(t) \sigma_y$, where $B(t)$ is the control parameter that we can vary. Writing the state of the two-level system using the Bloch vector $\mathbf{v} = (v_x, v_y, v_z)^T = (\langle \sigma_x \rangle, \langle \sigma_y \rangle, \langle \sigma_z \rangle)^T$, the dynamics under the feedback process is

$$\begin{aligned}
 dv_x &= \left[B(t) v_z - \frac{\Gamma_z}{2} v_x \right] dt - \sqrt{\Gamma_z} v_x v_z dW, \\
 dv_y &= -\frac{\Gamma_z}{2} v_y dt - \sqrt{\Gamma_z} v_y v_z dW, \\
 dv_z &= -B(t) v_x dt + \sqrt{\Gamma_z} (1 - v_z^2) dW.
 \end{aligned} \tag{2.63}$$

If we assume that $v_y = 0$, the control field $B(t) = G v_x$ with $G > 0$ can steer the system to the spin-up state with unit probability. This method is extended in [209] to systems with any fixed total angular momentum J , such as a dilute gas of two-level atoms. In this work a piecewise-continuous control protocol is designed to stabilize any selected eigenstate of the J_z operator, and can also be used to stabilize the symmetric and antisymmetric states in a system with two qubits.

As our final example of stabilization, we now present the approaches introduced in [213–215] in which feedback is used to stabilize a particular dressed state in a strongly-coupled cavity-QED system. For a weakly-driven single-cavity mode strongly coupled to N atoms with coupling strength g , the steady state is

$$|\psi_{ss}\rangle = |0, g\rangle + \lambda \left(|1, g\rangle - \frac{2g\sqrt{N}}{\gamma} |0, e\rangle \right) + O(\lambda^2). \tag{2.64}$$

Here γ is the damping rate of the atom, and $\lambda \ll 1$ is proportional to the ratio ε_d/κ , where ε_d and κ are the driving strength and damping rate of the cavity, respectively. The state $|j, g\rangle$ denotes j photons in the cavity mode, and all the atoms in their ground states, while $|j, e\rangle$ denotes j photons in the cavity mode and all but one of the atoms are in their ground states.

Since the steady-state has almost no photons, photon detections are relatively rare. When a photon is detected, the

conditional state changes abruptly, and evolves as

$$|\psi_c(\tau)\rangle = |0, g\rangle + \lambda[\xi(\tau)|1, g\rangle + \theta(\tau)|0, e\rangle], \quad (2.65)$$

where $\xi(\tau)$ and $\theta(\tau)$ are oscillatory functions of time. It turns out that by adjusting the driving field at a specific time after the detection, the state of the system can be frozen indefinitely. Once the driving field is returned to its original value, the evolution of the conditioned state continues as if it had never been interrupted, and returns to the steady-state. This feedback scheme was realized experimentally in Ref. [215].

It has also been shown that the same atom-cavity system can be stabilized in the opposite regime of strong-driving [213]. In this case one of the dressed states is stabilized by flipping the atomic state using a π -pulse when a measurement-induced quantum jump is observed. The signature of this stabilization process appears in the atomic fluorescence spectrum as the enhancement of one sideband.

Not all feedback involves changing the Hamiltonian of a system conditional upon the measurement stream. If the purpose is to engineer a specific kind of measurement, for example, one may change the *measurement* conditional on the stream of measurement results. The result of this feedback-modified measurement is referred to as an *adaptive* measurement. We will give examples of adaptive measurements below. In Refs. [216, 217], the authors consider how to design an adaptive measurement to minimize the classical memory required to track the state of the measured system. They show that for a d -dimensional system it is possible to modify the measurement with time so that the system is restricted to jumping between a discrete set of just $k \geq (d - 1)^2 + 1$. This means that a d -dimensional system can be tracked by a classical k -state machine, and a special case shows that a qubit can be tracked by a classical bit.

2.5.3. Squeezing via feedback

A quantum harmonic oscillator obeys Heisenberg's uncertainty principle, meaning that the momentum variance can only be reduced below $\hbar m\omega/2$ at the expense of increasing the position variance above $\hbar/(2m\omega)$. Here m and ω are respectively the mass and frequency of the oscillator. For an optical mode, the equivalent conjugate variables are referred to as the amplitude quadrature X and phase quadrature Y . A state in which the variance of one conjugate variable is decreased at the necessary expense of the other is called a *squeezed* state. For a single mode of an optical or electrical cavity it is not only the state of the mode that is of interest, but the state of the travelling-wave light or electrical signal that is emitted from the cavity. We may want to squeeze either the oscillator or this output. Methods for squeezing both have been investigated quite extensively.

Assuming that the thermal noise on an oscillator is negligible, its state can be squeezed merely by modulating its frequency ω at 2ω . This is called *parametric amplification* because it amplifies one quadrature, and because ω is a "parameter" in the Hamiltonian. If we want to squeeze the oscillator in the presence of thermal noise, then we need to reduce this noise, for which measurement-based feedback is one option. Neither measuring a single quadrature, nor making a homodyne measurement are sufficient for this purpose [152]. There are two methods presently known to do this. One is to make a measurement of a single quadrature, but do so in the rotating frame of the oscillator. Braginsky *et al.* [218] were the first to devise a method to do this, which effectively involves making a measurement of an oscillator's position, and turning the measurement off and on at the frequency 2ω (see also [158, 190, 219]). This "strobing" of the measurement can be achieved merely by modulating the interaction with the measuring device sinusoidally at this frequency. In the interaction picture the quadrature variables are unchanging, so that Braginsky's measurement is a *quantum non-demolition* (QND) measurement. Other methods for making QND measurements of the quadratures have been devised [152–156], but Braginsky's is probably still the most practical. A QND measurement produces a squeezed conditional state — a squeezed state from the point of view of someone who is able to have processed the measurement record to determine the means of the quadratures. Since the means fluctuate, without this information the state is not squeezed. But since a linear feedback force can be used to stabilize the means, we can use feedback from the QND measurement to produce an unconditional squeezed steady-state [190, 219].

The second method to produce squeezed states in the presence of significant thermal or other noise is to combine a parametric drive with a standard (unmodulated) measurement of position. Here the parametric drive creates the squeezing and the measurement is much weaker, and extracts the entropy injected by the thermal noise [220, 221]. This method of producing squeezing has been realized, although not in the quantum regime, in [159, 222].

We note that QND measurements have also been used to generate squeezing in the collective spin state of a gas of two-level atoms, both theoretically [160] and experimentally [223–225].

2.5.4. *Controlling mechanical resonators*

In the previous section we discussed the use of feedback to squeeze oscillators, mechanical or otherwise. We now focus on mechanical oscillators, and consider the creation of other states. The first task in bringing a mechanical resonator into the quantum regime is to suck out all the thermal noise so as to put the resonator in its ground state. From there we can use purely open-loop control protocols to place it in a more interesting nonclassical state. To make it possible to cool a mechanical resonator to the ground state (see, e.g., [226, 227]), it must have a very high frequency so as to reduce the thermal noise, even when placed in a dilution refrigerator. To attain the required frequencies the resonators must have a very small mass, and there are a number of ways to realize such microscopic and mesoscopic resonators. One can merely make them small [228–240], in which case their frequencies are still a little low to enter the quantum regime. One can go even smaller by fabricating resonators on layered structures using lithography, and these are usually referred to as nano-resonators [241–245]. One can also use microscopic systems such as trapped ions [246], electrons [247], laser-trapped nano-particles [248], a gas of neutral atoms trapped in an optical lattice [249–254].

State-of-the-art cooling schemes for nano- and micro-mechanical resonators currently use coherent feedback, to be discussed in Section 3. Nevertheless measurement-based cooling methods for mechanical resonators have been investigated quite extensively. When the resonator is far from the classical regime, feedback cooling of resonators can be considered classical [255–257]. The primary obstacle to cooling resonators to the ground state using measurement-based feedback is the requirement that the measurement has an efficiency near unity. At the time of writing, measurements on nano-resonators do not have the required efficiency, but we expect this to change in the near future. Cooling via measurement has been investigated both for Markovian feedback [258–260] and Bayesian feedback [128, 129, 189, 190, 261]. Feedback can also be used to create and control highly non-classical states of resonators [127].

2.5.5. *Controlling transport in nano-structures*

Measurement-based quantum feedback can be used to control the quantum transport process in nanostructures [262–265]. This can be thought of as stabilizing the quantum state of the transport device. The proposal in Ref. [264] shows that a classical feedback control can freeze the fluctuations of quantum transport by changing parameters in the Hamiltonian conditional to the number of tunneled particles. This feedback method can be further used to reconstruct the full counting statistics of the transport device from on the frozen distribution. In [265], this proposal was applied to nonequilibrium-electron-transport through a double-quantum-dot, which for this purpose can be treated as a two-level system. The feedback is able to purify the transport state, represented by the full counting statistics of the electron flow through the device, and it is shown that half of the quantum states on the Bloch sphere of the double-quantum-dot can be stabilized. The feedback is also able to stabilize the coherent delocalized states of the electrons.

2.5.6. *Entanglement creation and control*

It is shown in [266] that when a cavity containing two two-level atoms is resonantly driven, the steady-state of the atoms can be entangled. More specifically, if (i) the cavity damping rate κ is much faster than all other timescales, so that the cavity can be adiabatically eliminated, and (ii) the collective damping rate of the atoms induced by the cavity is much larger than the atoms' spontaneous emission rates, then one can recover a Dicke model for the atoms. The steady state of this Dicke model can be written in the angular momentum basis and analyzed in terms of the symmetric and antisymmetric subspaces. When the initial state of the atoms is symmetric, the stationary state is entangled, although this entanglement, measured by the Wootters' concurrence [267], is only about 0.11 [266].

It turns out that Markovian quantum feedback can be used to increase the steady-state entanglement of the atoms [133–146]. It has been shown that this is possible using both feedback based on photon detections (quantum jumps) [140–146], and feedback using homodyne detection (trajectories driven by Gaussian noise) [133–137].

In Ref. [133] the authors show that for homodyne detection the stationary entanglement can be increased from 0.31 under feedback that is symmetric for the two atoms (see Fig. 5). This stationary entanglement can be increased further to 0.82 if local asymmetric feedback is introduced [134]. Feedback based on photon detections is even better at maintaining entangled states, and for symmetric feedback is able to achieve a concurrence of 0.49 [141]. This stationary entanglement is reduced by spontaneous emission, but can be increased further by the use of local asymmetric feedback. Feedback based on photon-detections is also robust against fluctuations in various parameters, such as the

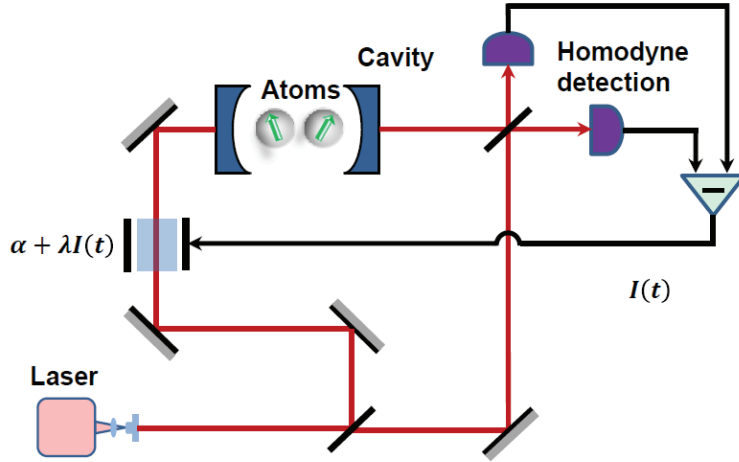


Figure 5: (Color online) Schematic diagram of a theoretical proposal [133] for two-atom entanglement creation by homodyne-mediated feedback. The homodyne current $I(t)$ from the damped cavity is directly fed back to generate a control signal $\alpha + \lambda I(t)$, which is converted into an optical signal by an electro-optic modulator and then used to resonantly drive the cavity coupled to the two atoms. These two atoms are entangled in the steady state.

detection efficiency, especially in the adiabatic regime [141]. Bayesian feedback has also been used to generate and protect entanglement in the above system [161, 268]. Although the computational complexity for this kind of control is higher, it can also potentially produce higher entanglement.

As an extension of the above feedback schemes, the stabilization of multipartite entanglement via feedback has also been considered [269, 270]. Due to the lack of a measure for multipartite entanglement, these studies have focussed on stabilizing particular multipartite entangled states, such as Dicke states [161] or GHZ states [168]. More recently, the control of entanglement via feedback has been discussed for solid-state systems, especially superconducting circuits [166–168], and has been demonstrated experimentally both in superconducting circuits [271] and cavity QED systems [272].

Continuous-variable entanglement of optical beams, which is closely related to multi-mode optical squeezing, can, and usually is, produced by using nondegenerate parametric oscillator in an optical cavity. This method is limited by the strength of the optical nonlinearity employed, which is usually very weak, and is further reduced by the cavity damping. It has been shown that feedback can be used to increase the continuous-variable entanglement [273–277, 279–282] generated in this way.

Consider two optical modes with quadrature operators X_1, Y_1 and X_2, Y_2 , respectively. In Ref. [273] it is shown that a single-loop Markovian feedback scheme can be used to reduce the variance of the operator $X_1 - X_2$ while preserving the variance of the operator $Y_1 + Y_2$, thus improving the steady-state entanglement of the two modes. However, the entangled state in this case is a mixed state. A modified proposal in Refs. [274, 275] is able to produce a pure steady-state two-mode entangled state by using two independent feedback loops to control the variances of $X_1 - X_2$ and $Y_1 + Y_2$ simultaneously.

It has been shown that the problem of finding the optimal homodyne measurement and Markovian feedback to produce two-mode intracavity Einstein-Podolsky-Rosen correlations for both a vacuum environment [276] and a thermal bath [277] is a semidefinite programming problem [278]. This means that a global optimum can be found numerically in a systematic way. A general upper bound for the generation of steady-state entanglement for multi-mode bosonic fields via feedback has also been obtained [279]. Quantum feedback has been applied to the problem of generating deterministic entanglement at the single-photon level [280], to avoid entanglement sudden death [281], and to enhance entanglement distributed between cavities including propagation delays and photon loss [282].

2.5.7. Quantum state discrimination

The efficient discrimination of nonorthogonal quantum states has various applications in quantum and classical communications and quantum-enhanced metrology. For discrete-variable quantum systems, such as qubits, it has

been shown theoretically [283] and experimentally [284] that continuous measurement and feedback can efficiently discriminate two nonorthogonal states of a single qubit, as well as correct these states against dephasing noise. It has also been demonstrated experimentally that adaptive local measurement and feedback performs much better than non-adaptive measurements for discriminating non-orthogonal states of qubits, given multiple copies, and can efficiently suppress noise [285].

Quantum feedback has also been used for the discrimination of coherent states of oscillators or traveling-wave fields. Such discrimination is useful for communication, because coherent states are easy to be prepared and manipulated. Adaptive measurement schemes can maximize the information rate so as to achieve Holevo's bound [286], and allow for long-distance communication. It has been shown both theoretically [287] and experimentally [288–290] that joint-detection and adaptive feedback with pulse-position-modulation codewords reduces the error probability for both conditioned and unconditioned coherent-state discrimination, compared with traditional direct detection methods (e.g., homodyne detection). This method can also beat the standard quantum limit to approach the Helstrom limit [291], being the minimum achievable average probability of error for discriminating quantum states.

2.5.8. Quantum parameter estimation

High-precision phase measurements of optical beams, especially those in the quantum regime, have various important applications, such as interferometric gravity-wave detection or quantum communication. However, the phase of the electromagnetic field mode is not a directly-measurable quantity, and phase measurement protocols always measure some other quantity that introduces excess uncertainty and noise into the estimation process.

The traditional method for measuring phase was to use heterodyne detection, in which the field mode to be measured is combined with a far-detuned strong local oscillator field. It is well-known that phase measurements based on heterodyne detection can reach the standard quantum limit, in which the phase sensitivity, being the variance of the measured phase $(\delta\phi)^2$, scales as N^{-1} when a state with an average of N photons is fed into the input port to be measured. But this is not the fundamental limit to phase estimation. The latter is the Heisenberg limit, which gives a scaling of N^{-2} . The Heisenberg limit could be achieved with a perfect measurement of canonical phase [303, 304], but this appears to be essentially impossible.

Wiseman and collaborators [292–300] have shown that by using an adaptive measurement it is possible to realize a measurement of phase that is very close to the Heisenberg limit [301–304]. There are primarily two approaches. One can use an adaptive homodyne measurement [292–297] or an adaptive interferometric measurement [298–300] (see Fig. 6). As shown in Fig. 6(a), the key element of an adaptive homodyne phase measurement is to feed back the output of the homodyne detection to control the phase of a local oscillator, and thus track the phase quadrature to be estimated. It is shown in Ref. [293] for a semiclassical model and in Ref. [294] for a full quantum analysis that an excess phase uncertainty scaling as $N^{-3/2}$ can be reached. A modified approach in Ref. [296] shows that a more sophisticated feedback protocol can reach a better theoretical limit, scaling as $\ln N/N^2$.

The adaptive interferometric phase measurement can perform even better than the adaptive homodyne method. In an adaptive interferometry phase measurement, a Mach-Zehnder interferometer is introduced with the unknown phase to be estimated in one arm and the controllable phase used to track the unknown phase in the other arm. This achieves a phase sensitivity very close to the Heisenberg limit [298, 299]. It has also been shown that both the adaptive homodyne method [297] and the interferometric method [300] can be used to estimate a stochastically-varying phase. More complex feedback designs, such as those based on time-symmetric smoothing [305–307], can also be used in adaptive phase measurement. A number of adaptive phase-measurement schemes have been demonstrated in experiments [169, 308–313].

More generally, we may wish to estimate one or more numbers that parameterize the state, Hamiltonian, or overall evolution of a system. Such parameters can be estimated by making a continuous measurement on an evolving system and processing the measurement results [314–319]. Such a procedure has applications to metrology, such as the detection of weak force by monitoring a harmonic oscillator [318], or estimating the Rabi frequency of a two-level atom [315]. Feedback control can be used to make the estimation process more robust to the uncertainty in the system parameters [319]. The basic method involved in parameter estimation and metrology via continuous measurements to use a “hybrid” master equation that evolves the observer's knowledge of the system as well as their knowledge of the parameters [318], or an equivalent quantum particle filtering equation [317].

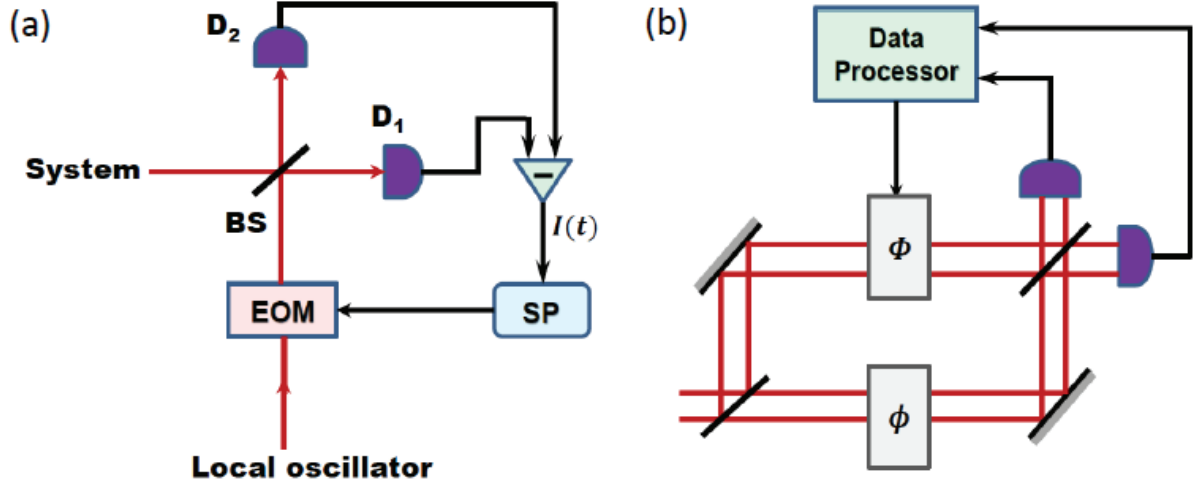


Figure 6: (Color online) (a) Theoretical proposal [292] for adaptive homodyne phase measurement. The output $I(t)$ of the homodyne detection is processed by a Signal Processor (SP) which then controls the phase of the local oscillator by an electro-optic modulator (EOM). (b) Theoretical proposal [299] for adaptive interferometry phase measurements. The figure shows a Mach-Zehnder interferometer with the unknown phase ϕ to be estimated in one arm and the controllable phase Φ (used to track the unknown phase ϕ) in another arm.

2.5.9. Rapid state-purification and measurement

It is possible to use quantum feedback to speed up the rate at which a continuous measurement purifies, or provides information about a quantum system [196, 320–332]. To understand this further, let us consider a continuous measurement of a qubit which provides information about the basis $\{|0\rangle, |1\rangle\}$. The dynamics of this measurement is given by the SME

$$d\rho = \mathcal{D}[\sigma_z]\rho dt + \mathcal{H}[\sigma_z]\rho dW. \quad (2.66)$$

In order to study how one can reduce the observer’s uncertainty of the measured quantum system, an algebraically simple measure of the observer’s uncertainty, called “linear entropy”, $s = 1 - \text{tr}[\rho^2]$, is useful. If we assume without loss of generality that $y = 0$, we can obtain from Eq. (2.66) that [322]

$$ds = -(8s^2 + 4x^2s) dt - 4zs dW, \quad (2.67)$$

where $\alpha = \text{tr}[\sigma_\alpha \rho]$, $\alpha = x, y, z$. It can be seen that s will decrease more rapidly when x is maximized. If we introduce an ideal Hamiltonian feedback that rotates the qubit at each time step to maintain $z = 0$, then ds is maximized and given by $ds = -4s dt$. As shown in Ref. [320], if we start from a maximally mixed state, then under this feedback, and in the long time limit, the time required to achieve a purity of $1 - \epsilon$ is $\tau_q = \ln(\epsilon^{-1})/4$, which is half the time taken for the average purity to reach this level without feedback. Here $\epsilon \ll 1$ denotes the error threshold value. Such an increase in the rate of purification is a purely quantum effect, and cannot be realized for an equivalent measurement on a classical bit.

Although the above analysis shows that using feedback to continually rotate the quantum state onto the plane orthogonal to the measurement axis will speed up purification, Ref. [322] shows that keeping the quantum states parallel to the measurement axis can reduce the average time for the measured quantum system to reach a given purity.

As an extension of the results in Ref. [320], a more general study in Ref. [321] shows that Hamiltonian feedback can speed up the rate of purification, or state reduction, by at least a factor of $2(d+1)/3$ for an observable with d equispaced eigenvalues. However, the quantum feedback methods in these studies concentrate only on maximizing the purity of the measured quantum states, and do not care about how to obtain information about the initial state of the system. That is why they are referred to as rapid purification protocols rather than rapid measurement protocols.

In contrast to quantum rapid purification, in Ref. [327] the authors show that quantum feedback can increase the rate of information gain about the initial preparation. It is found that the information-extraction rate for a d -dimensional system can be increased by a factor that scales as d^2 . More exact bounds for rapid measurement protocols are given in [329], in which it is shown that feedback can increase the rate of information extraction by a factor R by

$$\frac{2}{3}(d+1) \leq R \leq \frac{d^2}{2} \quad (2.68)$$

for an observable with d equispaced eigenvalues. Further results on quantum rapid purification and measurement can be found in Ref. [330].

2.5.10. Control-free control

The term “control-free control” refers to measurement-based feedback control in which the state of the system is controlled without modifying the Hamiltonian of the system, but merely by changing the measurement with time. This is an adaptive measurement process designed to control the system. Control-free control exploits the fact that, in general, quantum measurements affect the dynamics of a system in ways that classical measurements do not. Several approaches for control-free control have been discussed to-date. In one of these, the quantum anti-Zeno effect is used to drag the system in the direction of one of the states onto which the measurement projects [333, 334]. However, this requires rather strong measurements. In another approach, a small set of measurements [335–337] is able to prepare a state by alternating between the measurements [338, 339]. This process is able to stochastically drive the system towards a final pure state with unit probability. A third method involves making a continuous measurement, and exploiting the fact that when the measurement-basis is chosen in the right way, the measurement generates diffusion of the state in Hilbert space. By changing the measurement basis with time, a diffusion gradient can be created in Hilbert space. This diffusion gradient will then stochastically drive the system towards a single pure state [340]. The control-free control protocols [338] have been realized in recent experiments. For example, in Ref. [341], measurement-only state manipulations are realized on a nuclear spin qubit in diamond by adaptive partial measurements (see Fig. 7). By combining a quantum non-demolition readout on the electron ancilla qubit with real-time adaptation of the measurement strength, the nuclear spin can be steered to a target state by measurements alone. This interesting work [341] shows that it is possible to implement measurement-based quantum computing by quantum feedback.

3. Coherent Quantum Feedback

As explained above, measurement-based feedback involves using the results of measurements on a quantum system to direct its motion. When we make a measurement on a quantum system, we obtain classical information. But we necessarily obtain only partial information about the dynamical variables, and in general we disturb the state at the same time. It is therefore interesting to consider a feedback loop in which classical information is not extracted. This concept, now referred to as *coherent feedback*, was first introduced by Lloyd in 2000 [77], and it can be seen as the more general case of the all-optical feedback proposed earlier, in 1994, in quantum optical systems by Wiseman and Milburn [71]. The idea is that instead of having a classical controller that makes a measurement on the system, the controller is a quantum system, and the control is achieved simply by having the two systems interact. To understand this better, it is worth examining the Watt governor, which has a very simple feedback mechanism. The purpose of the Watt governor is to control the speed of an engine. To do this, the engine is connected to a simple mechanical device so that it spins the device. The device is designed so that the centrifugal force from the spinning causes it to expand, so that the faster the engine spins, the more it expands. This expansion is then used to reduce the fuel supply to the engine, thus stabilizing the engine at some chosen speed. The nice thing about this simple feedback system is that we can think of it as a loop in which the control device obtains information from the engine, and uses this to control it. It is also clear that the engine and controller are merely two coupled mechanical systems. In the Hamiltonian description of the joint system, there is therefore no loop, but merely an interaction between the two systems. A quantum controller can therefore act in the same way, performing feedback control even though the description of the system may not involve an explicit loop.

In fact, there is a way to make the loop explicit for a quantum controller in which there are no measurements. This is done by coupling the system to a travelling-wave electrical (optical) field that propagates in one direction

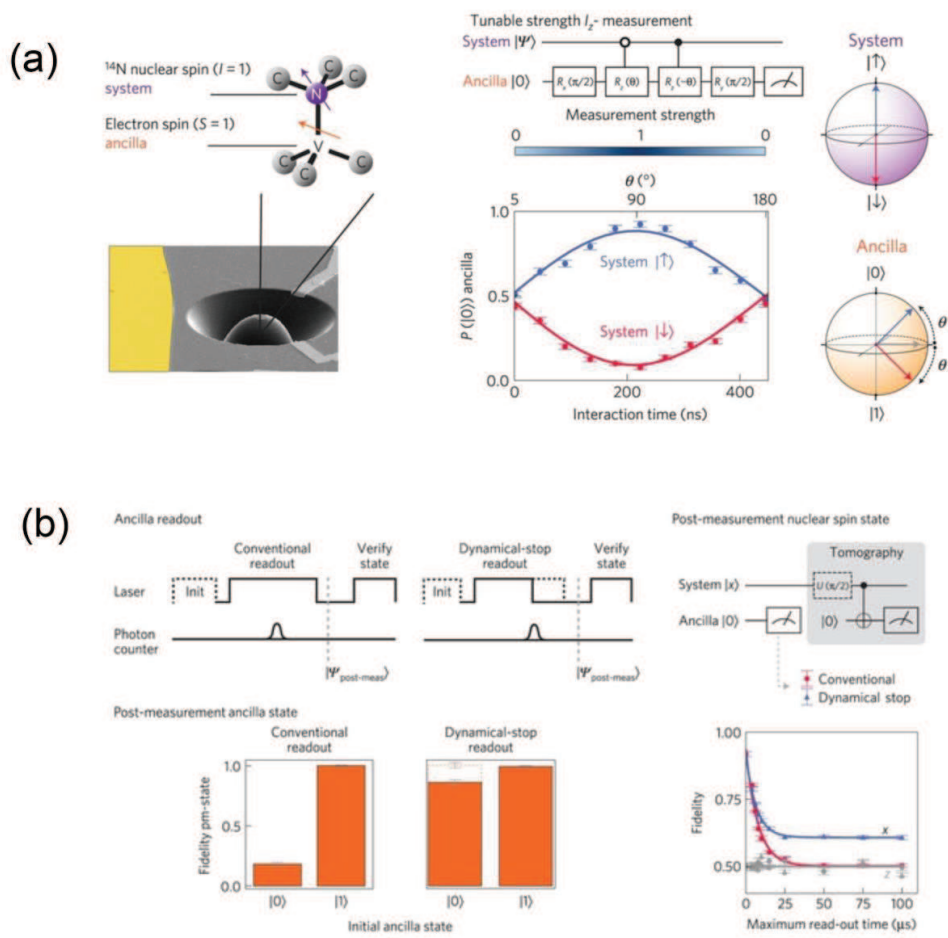


Figure 7: (Color online) Control-free control [338] experiment [341] on nuclear spin qubits in diamond. (a) Partial measurement of a spin qubit in diamond. (b) Quantum non-demolition measurement of the ancilla and system qubit coherence during readout. The figure is from Ref. [341].

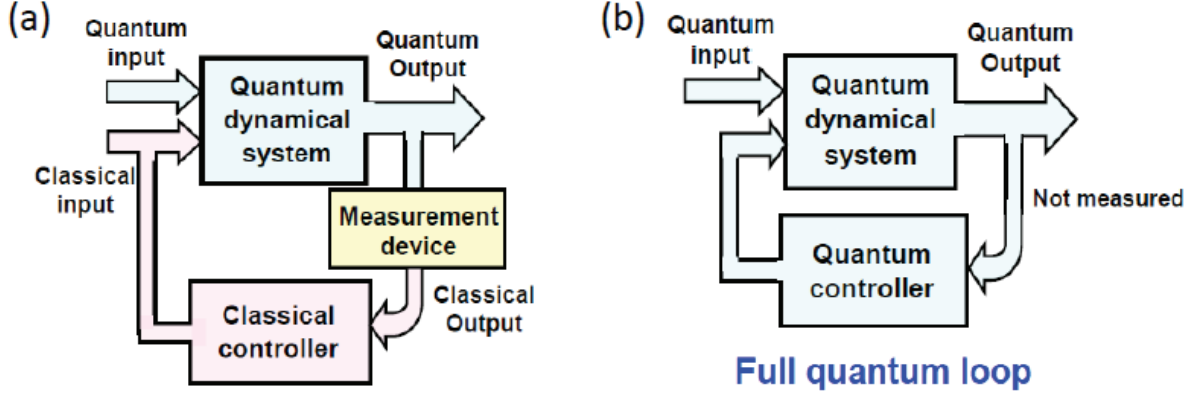


Figure 8: (Color online) Comparison of (a) measurement-based feedback and (b) coherent feedback. In measurement-based feedback in (a), the system (in blue) is controlled by a classical feedback loop (in pink); while in coherent feedback (b) the system is coherently controlled by a fully quantum feedback loop.

from the system to the controller. We then use a second travelling-wave field that propagates from the controller to the system, thus closing the loop. To do this, the two travelling fields must continue propagating after they interact with the systems, and this introduces an irreversible element to the dynamics. However, since control systems are usually intended to introduce some kind of damping to the system, this irreversibility need not be detrimental. In what follows, we discuss feedback control that employs a unitary (Hamiltonian) interaction between the system and controller, often referred to as *direct coherent feedback*, where the interaction is mediated by travelling-wave fields, often referred to as *field-mediated* feedback.

3.1. Direct coherent feedback

In general, the action of a controller that is coupled to a system via a unitary interaction may not break down into clearly defined processes which involve the extraction of information and use of this information to apply forces to the system. Nevertheless, it is interesting to construct an interaction that does perform these individual processes. As an example, let us consider the control of a single qubit by a controller that is also a qubit. The qubit to be controlled (the primary) is initially in some unknown state $|\phi\rangle = \alpha|0\rangle + \beta|1\rangle$, and we want to place it in the state $|0\rangle$. If the state of the primary is completely unknown, then from the point of view of any observer, and the controller, the state of the qubit is the density matrix $\rho = (1/2)|0\rangle\langle 0| + (1/2)|1\rangle\langle 1|$. We cannot do this by executing a unitary operation on the system, because to choose the right unitary we would need to know the initial state. If we were using measurement-based feedback, then we could perform a projective measurement on the primary, at which point we would know what unitary to apply and execute a unitary operation according to the measurement output. Note, however, that if we did this we would have destroyed the initial state, so that no other information can be extracted from it.

To use a unitary interaction to prepare the primary in the state $|1\rangle$, we need the controller to be in a pure state. Starting the controller in the state $|0\rangle$, we turn on an interaction that will transform the controller to the state $|1\rangle$ only if the primary is in state $|1\rangle$. If we write the states of the primary on the left of the tensor product, and those of the controller on the right, then the unitary operator required is

$$U = |0\rangle\langle 0| \otimes I + |1\rangle\langle 1| \otimes (|0\rangle\langle 1| + |1\rangle\langle 0|), \quad (3.1)$$

where “ \otimes ” is the tensor product. This unitary transforms the state of the two systems as

$$U|\psi\rangle \otimes |0\rangle = U(\alpha|0\rangle + \beta|1\rangle) \otimes |0\rangle = \alpha|0\rangle \otimes |0\rangle + \beta|1\rangle \otimes |1\rangle. \quad (3.2)$$

The two qubits are now correlated, since the controller is in state $|1\rangle$ if and only if the primary is in state $|1\rangle$. The controller now “knows” the state of the system, and can act accordingly. To do this, we need an interaction that

performs a different action on the primary for each of the states of the controller. In particular, we need to transform the state of the primary from $|0\rangle$ to $|1\rangle$ only if the state of the controller is $|0\rangle$. The unitary that does this is

$$U_{fb} = (|0\rangle\langle 1| + |1\rangle\langle 0|) \otimes |0\rangle\langle 0| + I \otimes |1\rangle\langle 1|. \quad (3.3)$$

Acting on the joint state in Eq.(3.2) with this unitary produces the final state

$$U_{fb}|0\rangle \otimes |0\rangle + \beta|1\rangle \otimes |1\rangle = |1\rangle \otimes (\alpha|0\rangle + \beta|1\rangle) = |1\rangle \otimes |\psi\rangle. \quad (3.4)$$

This completes the feedback procedure, placing the primary in the state $|1\rangle$ for every value of α and β . Interestingly the initial state of the primary has not been destroyed. This state, and thus the “quantum information” in the primary has been transferred to the controller.

In the above example, the controller in the measurement-free feedback procedure performs essentially the same action as a measurement that projects the primary onto the basis $\{|0\rangle, |1\rangle\}$. The controller becomes correlated with the system in the basis $\{|0\rangle, |1\rangle\}$, and then performs an action depending on whether the system is in state $|0\rangle$ or $|1\rangle$, just as the measurement-based feedback would. But because the projection is not actually performed, and the whole process is “coherent”, the quantum information in the primary is not destroyed. We note that direct coherent feedback was experimentally demonstrated in a nuclear magnetic resonance (NMR) system shortly after it was proposed [78].

If we perform the feedback coherently (without measurement), then the above procedure, in which a “correlation step” is followed by a “feedback” step, is not necessary. The same operation can be performed by a single interaction that follows a different path in state space. The interaction Hamiltonian

$$H = \hbar\lambda (|0\rangle\langle 1| \otimes |1\rangle\langle 0| + |1\rangle\langle 0| \otimes |0\rangle\langle 1|) \quad (3.5)$$

generates the unitary

$$U = |0\rangle\langle 1| \otimes |1\rangle\langle 0| + |1\rangle\langle 0| \otimes |0\rangle\langle 1| \quad (3.6)$$

in a time $\tau = \pi/(2\lambda)$. This unitary transforms the initial joint state $|\psi\rangle \otimes |0\rangle$ to the final state $|1\rangle \otimes |\psi\rangle$, but there is no clear breakdown into information gathering and feedback.

3.2. Field-mediated coherent feedback

To explain how traveling-wave fields can mediate interactions between quantum systems, it may be simplest to begin with an example. As mentioned in the introduction, feedback mediated by fields was first introduced by Wiseman and Milburn in the setting of quantum optics [71]. In Fig. 9, we show the configuration considered in [71]. In this scheme, there are two optical cavities, one of these is horizontal in the figure (cavity 1), and the other is vertical (cavity 2). The two cavities are coupled directly by a nonlinear crystal, but this is not the field-mediated part of the coupling. The output beam from the horizontal cavity is fed through a combination of a polarization beam-splitter and a Faraday rotator, and then into cavity 2. This combination breaks time-reversal symmetry, and acts differently depending on the direction that a beam passes through it. Because of this, it is able to separate the input beam to cavity 2 from the beam that comes back out in the reverse direction, so that this output beam does not go back into cavity 1. The output field from cavity 1 thus travels to cavity 2 but does not travel in the reverse direction, and, because of this, it is referred to as a unidirectional, one-way, or cascade coupling between the cavities. The combination of the polarization beam splitter and Faraday rotator is called a unidirectional coupler, or isolator, and the equivalent exists for electrical (microwave) circuits.

In the feedback scheme in Fig. 9, cavity 1 is the primary system, and cavity 2 is the controller. The controller obtains information about the system from the one-way field, and applies feedback via the direct coupling. Wiseman and Milburn [71] considered three kinds of interaction Hamiltonian V . If we define A to be an arbitrary observable of the mode in cavity 1, B an arbitrary operator of this mode, and c_2 is the annihilation operator for cavity 2, then the three interactions are (i) $V = c_2^\dagger c_2 A$, (ii) $V = (c_2 + c_2^\dagger)A$ and (iii) $V = c_2^\dagger B + c_2 b^\dagger$. The first reproduces feedback via photon counting and the second feedback via homodyne detection. The third has no equivalent measurement-based feedback protocol, and can generate nonclassical states in the primary mode. For example, if we choose $B = i\lambda(c_1 + c_1^\dagger)$, the resulting feedback produces squeezed states of the primary mode when $0 < |\mu| < 1$.

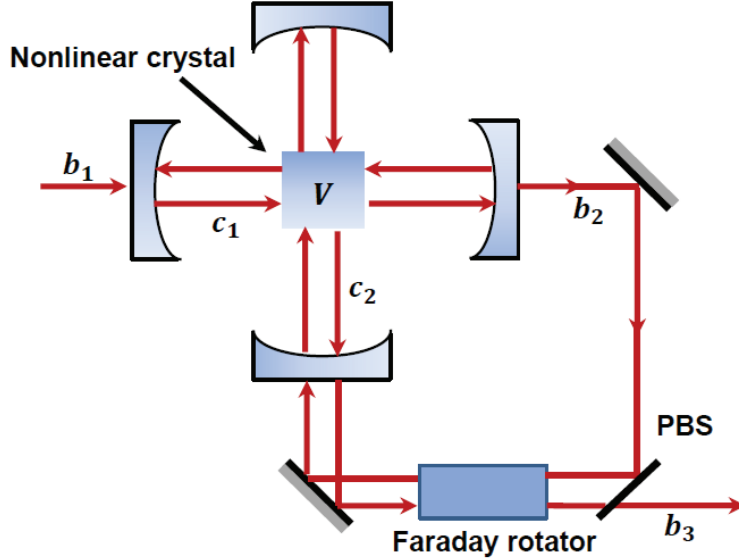


Figure 9: (Color online) Schematic diagram of a theoretical proposal [71] for an all-optical feedback scheme. An external input field b_1 is first fed into the source cavity c_1 , and then the output field b_2 is directed back to be fed into another driven cavity c_2 via an all-optical feedback loop. The source (vertical) cavity and the driven (horizontal) cavity are coupled to each other by a nonlinear crystal which induces a nonlinear coupling, denoted by the interaction Hamiltonian V . The Faraday rotator and the Polarization-sensitive Beam Splitter (PBS) are introduced to generate a unidirectional feedback loop.

3.2.1. Networks of quantum systems

The configuration of the feedback system in Fig. 9 has a unidirectional connection from the system to controller, which replaces the measurement in measurement-based feedback, but does not use a unidirectional coupling for the feedback part of the loop. We can, however, use a cascade connection for both, in which case we have a complete unidirectional loop. What we now need to know is how to describe these cascade connections mathematically. To do this, we use the input-output, or “quantum noise” formalism of Collet and Gardiner (CG) [73, 102], also known as the Hudson-Parthasarathy (HP) model, as the latter independently derived the same formalism in a more rigorous, measure-theoretic way [103]. The formalism uses Heisenberg equations of motion for the operators of the systems, with input operators that drive these equations in a similar way to that in which Wiener noise drives classical stochastic equations. The formalism also contains output operators, and systems are then easily connected together by setting the input of one system equal to the output of another.

In the CG/HP formalism, each system is described by a Hamiltonian, along with the operators through which it is coupled to the input/output fields. Further, the fields can be coupled to each other using beam-splitters, which take two inputs and produce two outputs that are linear combinations of the inputs. By describing a single “unit” as having a Hamiltonian H , a vector of input coupling operators \mathbf{L} , and a linear transformation between inputs and outputs codified by a matrix \mathbf{S} , Gough and James [82] elucidated a set of rules that covered the ways in which these units, or network elements, could be combined into networks. We now describe the CG/HP formalism, and the Gough-James rules [82] for combining circuit elements.

The dynamics of a system coupled to input fields is given by the quantum Langevin equations, i.e., Eq. (2.11), and the output fields that correspond to each input are given by Eq. (2.12). As mentioned above, we describe each unit by a tuple

$$G = (\mathbf{S}, \mathbf{L}, H), \quad (3.7)$$

where H is the internal Hamiltonian of the system; \mathbf{S} is a $n \times n$ unitary matrix with operator entries and is called a scattering matrix; $\mathbf{L} = (L_1, \dots, L_n)^T$ is a vector of operators through which the system couples to the inputs, with one for each input. We denote the inputs to the system by $\mathbf{b}_{\text{in}}(t) = [b_1(t), \dots, b_n(t)]^T$ in which each of the $b_i(t)$, ($i = 1, \dots, n$) are separate input fields, all initially in the vacuum state. The notation given in Eq. (3.7) can

Table 1: Quantum Itô Rule for quantum stochastic calculus

dX/dY	$d\mathbf{B}$	$d\mathbf{\Lambda}$	$d\mathbf{B}^\dagger$	dt
$d\mathbf{B}$	0	$d\mathbf{B}$	dt	0
$d\mathbf{\Lambda}$	0	$d\mathbf{\Lambda}$	$d\mathbf{B}^\dagger$	0
$d\mathbf{B}^\dagger$	0	0	0	0
dt	0	0	0	0

be used to describe a wide range of dynamical and static systems. A single quantum input-output system given by Eqs. (2.11) and (2.12) can be written as $G_{\text{LH}} = (I, \mathbf{L}, H)$, and a quantum beam splitter is given by $G_{\text{BS}} = (\mathbf{S}, 0, 0)$. Many examples of the use of this formalism can be found in Refs. [82, 342–347]. We now present the Langevin equations describing input-output systems in more generality. To begin, we introduce a vector of quantum Wiener processes $\mathbf{B}(t)$ and a matrix of quantum Poisson process $\mathbf{\Lambda}(t)$ as

$$\mathbf{B}(t) = \begin{pmatrix} B_1 \\ \vdots \\ B_n \end{pmatrix}, \quad \mathbf{\Lambda}(t) = \begin{pmatrix} B_{11} & \cdots & B_{1n} \\ \vdots & \ddots & \vdots \\ B_{n1} & \cdots & B_{nn} \end{pmatrix}. \quad (3.8)$$

These noise processes are integrals of the input fields:

$$B_i(t) = \int_0^t b_i(\tau) d\tau, \quad B_{ij}(t) = \int_0^t b_i^\dagger(\tau) b_j(\tau) d\tau. \quad (3.9)$$

The increments of these gauge processes $\mathbf{B}(t)$, $\mathbf{\Lambda}(t)$ satisfy the quantum stochastic calculus relations given in table 1. Let $V(t)$ be the unitary evolution operator of the total system composed of the controlled system and the input field, then the evolution equation of the total system can be written as [82]

$$dV(t) = \left\{ \text{tr}[(\mathbf{S} - I) d\mathbf{\Lambda}^\text{T}] + d\mathbf{B}^\dagger \mathbf{L} - \mathbf{L}^\dagger \mathbf{S} d\mathbf{B} - \frac{1}{2} \mathbf{L}^\dagger \mathbf{L} dt - iH dt \right\} V(t) \quad (3.10)$$

with initial condition $V(0) = I$.

In the Heisenberg picture, the system operator $X(t) = V(t) X V^\dagger(t)$ satisfies the following quantum stochastic differential equation

$$\begin{aligned} dX(t) &= \{ \mathcal{L}_{\mathbf{L}(t)}[X(t)] - i[X(t), H(t)] \} dt + d\mathbf{B}^\dagger(t) \mathbf{S}^\dagger(t) [X(t), \mathbf{L}(t)] + [\mathbf{L}^\dagger(t), X(t)] \mathbf{S}(t) d\mathbf{B}(t) \\ &\quad + \text{tr} \left\{ [\mathbf{S}^\dagger(t) X(t) \mathbf{S}(t) - X(t)] d\mathbf{\Lambda}^\text{T}(t) \right\}, \end{aligned} \quad (3.11)$$

where the Liouville superoperator $\mathcal{L}_{\mathbf{L}}(\cdot)$ is defined by

$$\mathcal{L}_{\mathbf{L}}(X) = \frac{1}{2} \mathbf{L}^\dagger [X, \mathbf{L}] + \frac{1}{2} [\mathbf{L}^\dagger, X] \mathbf{L} = \sum_{j=1}^n \left\{ \frac{1}{2} L_j^\dagger [X, L_j] + \frac{1}{2} [L_j^\dagger, X] L_j \right\}, \quad (3.12)$$

which is of the standard Lindblad form. Similar to Eq. (2.12), the output fields corresponding to the inputs $\mathbf{B}(t)$ and Poisson process $\mathbf{\Lambda}(t)$ are given by

$$\mathbf{B}_{\text{out}}(t) = V^\dagger(t) \mathbf{B}(t) V(t), \quad \mathbf{\Lambda}_{\text{out}}(t) = V^\dagger(t) \mathbf{\Lambda}(t) V(t),$$

from which we obtain the following input-output relation

$$\begin{aligned} d\mathbf{B}_{\text{out}}(t) &= \mathbf{S}(t) d\mathbf{B}(t) + \mathbf{L}(t) dt, \\ d\mathbf{\Lambda}_{\text{out}}(t) &= \mathbf{S}^*(t) d\mathbf{\Lambda}(t) \mathbf{S}^\text{T}(t) + \mathbf{S}^*(t) d\mathbf{B}^*(t) \mathbf{L}^\text{T}(t) + \mathbf{L}^*(t) d\mathbf{B}^\text{T}(t) \mathbf{S}^\text{T}(t) + \mathbf{L}^*(t) \mathbf{L}^\text{T}(t) dt. \end{aligned} \quad (3.13)$$

It can be verified that the increments $d\mathbf{B}_{\text{out}}, d\mathbf{\Lambda}_{\text{out}}$ of the output processes also satisfy the rules of quantum stochastic calculus shown in table 1.

For linear quantum systems, the quantum Langevin equations can be solved directly. In order to perform calculations for nonlinear quantum systems, one must transform the Heisenberg equations of the input-output formalism to master equations. The corresponding master equations are

$$\dot{\rho} = -i[H, \rho] + \sum_j \left(L_j \rho L_j^\dagger - \frac{1}{2} L_j^\dagger L_j \rho - \frac{1}{2} \rho L_j^\dagger L_j \right). \quad (3.14)$$

Although the scattering matrix \mathbf{S} does not appear in the master equation (3.14), it affects the input-output relation of the system as shown in Eq. (3.13) and thus will affect the dynamics of more complex quantum input-output systems, such as the quantum cascade systems which will be specified below.

To connect the outputs of one unit to the inputs of another, so as to form an arbitrary network, we need only two rules. The first is merely a rule that says how to represent a universe that contains more than one separate unit, none of which are connected. If we have the two units $\mathbf{G}_1 = (\mathbf{S}_1, \mathbf{L}_1, H_1)$ and $\mathbf{G}_2 = (\mathbf{S}_2, \mathbf{L}_2, H_2)$, the unit that describes both these units with no connections between them is

$$\mathbf{G}_1 \boxplus \mathbf{G}_2 = \left(\begin{pmatrix} \mathbf{S}_1 & 0 \\ 0 & \mathbf{S}_2 \end{pmatrix}, \begin{pmatrix} \mathbf{L}_1 \\ \mathbf{L}_2 \end{pmatrix}, H_1 + H_2 \right). \quad (3.15)$$

Gough and James [82] refer to this rule as the *concatenation product*.

The second rule for combing circuit elements tells us how to determine the unit that describes a network in which the outputs of a unit \mathbf{G}_1 are connected to the inputs of a unit \mathbf{G}_2 . This rule is

$$\mathbf{G}_2 \triangleleft \mathbf{G}_1 = \left(\mathbf{S}_2 \mathbf{S}_1, \mathbf{L}_2 + \mathbf{S}_2 \mathbf{L}_1, H_1 + H_2 + \frac{1}{2i} (\mathbf{L}_2^\dagger \mathbf{S}_2 \mathbf{L}_1 - \mathbf{L}_1^\dagger \mathbf{S}_2^\dagger \mathbf{L}_2) \right), \quad (3.16)$$

and is called the *series product*. The concatenation and series products can also be used to decompose a given system into subsystems, and are thus fundamental to feedforward and feedback control.

3.2.2. Quantum transfer function model

The Collet-Gardiner/Hudson-Parthasarathy cascade connections can be used to model essentially any network. However, for linear systems, time-delays and quantum amplifiers can be modeled more easily in frequency space. If we specialize the network formalism of Gough and James [82] so that all the systems are linear, and transform the equations of motion to frequency space, then we have the method of quantum transfer functions [342–345].

A general linear quantum network described by the tuple $(\mathbf{S}, \mathbf{L}, H)$ satisfies the following conditions [344]: (i) the entries of the scattering matrix \mathbf{S} are scalars; (ii) the dissipation operators L_j are linear combinations of the a_k and a_k^\dagger ; and (iii) the system Hamiltonian H is a quadratic function of the a_k and a_k^\dagger . To elucidate the transfer function method further, we consider a useful special case, in which each system is a harmonic oscillator, and the field coupling operators are linear combinations of only the annihilation operators. In this case, the Langevin equations for the annihilation operators are not coupled to those for the creation operators. The annihilation operators for the n oscillators, $\{a_j : j = 1, \dots, n\}$, satisfy the commutation relations

$$[a_j, a_k^\dagger] = \delta_{jk}, \quad [a_j, a_k] = [a_j^\dagger, a_k^\dagger] = 0.$$

For our special case, the total Hamiltonian is $H = \sum_{ij} \omega_{ij} a_i^\dagger a_j$ and the coupling operators $L_j = \sum_{jk} c_{jk} a_k$, and so we can simplify the SLH formalism, writing the tuple as

$$G = (\mathbf{S}, C, \Omega), \quad (3.17)$$

where

$$C = \begin{pmatrix} c_{11} & \cdots & c_{1n} \\ \vdots & \ddots & \vdots \\ c_{n1} & \cdots & c_{nn} \end{pmatrix}, \quad \Omega = \begin{pmatrix} \omega_{11} & \cdots & \omega_{1n} \\ \vdots & \ddots & \vdots \\ \omega_{n1} & \cdots & \omega_{nn} \end{pmatrix}.$$

If we now introduce an operator vector, which we will call the state vector of the system, $\mathbf{a} = (a_1, \dots, a_n)^T$, then from Eqs. (3.11) and (3.13), we can obtain the following Langevin equation and input-output relation:

$$\dot{\mathbf{a}}(t) = A \mathbf{a}(t) - C^\dagger \mathbf{S} \mathbf{b}_{\text{in}}(t), \quad (3.18)$$

$$\mathbf{b}_{\text{out}} = \mathbf{S} \mathbf{b}_{\text{in}}(t) + C \mathbf{a}(t), \quad (3.19)$$

where $A = -C^\dagger C/2 - i\Omega$.

We can now transform these equations to frequency space by taking either the Laplace transform or the Fourier transform. Using the Fourier transform, defined as

$$R(\nu) = \int_0^\infty \exp(-i\nu t) R(t) dt, \quad (3.20)$$

the Langevin equations can be rearranged to obtain

$$\mathbf{a}(\nu) = -(i\nu I_n - A)^{-1} C^\dagger \mathbf{S} \mathbf{b}_{\text{in}}(\nu), \quad (3.21)$$

$$\mathbf{b}_{\text{out}}(\nu) = \mathbf{S} \mathbf{b}_{\text{in}}(\nu) + C \mathbf{a}(\nu). \quad (3.22)$$

From Eqs. (3.21) and (3.22), we can obtain the input-output relation of the whole system or network

$$\mathbf{b}_{\text{out}}(\nu) = \Xi(i\nu) \mathbf{b}_{\text{in}}(\nu), \quad (3.23)$$

where $\Xi(\cdot)$ is the transfer function of the linear quantum system which can be calculated by

$$\Xi(i\nu) = \mathbf{S} - C (i\nu I_n - A)^{-1} C^\dagger \mathbf{S}. \quad (3.24)$$

The input-output relation (3.23) show the linear map between the input and output of the linear quantum system given by Eqs. (3.18) and (3.19).

The quantum transfer function approach is useful for a number of reasons. While the time-domain network formalism can describe essentially any network, it cannot be used to incorporate static models of non-conservative elements, such as quantum amplifiers, and such components must be treated as dynamical systems. In frequency space, a static model of a quantum amplifier is simply a Bogoliubov transformation [345]. Time delays are also much simpler to include in frequency space, and of course frequency space has the advantage that the transfer function of two cascaded systems is merely the product of the transfer functions of each.

3.3. Applications

3.3.1. Noise-reduction in linear systems

Like measurement-based quantum feedback, the main merit of quantum coherent feedback is that it can be used to suppress sources of entropy, such as external noise, uncertainty in the parameters that define the system, and even to some extent errors in the modeling of the system. In general, the problem of noise-reduction can be captured by asking how to minimize the effect of a set of inputs on a set of outputs. For linear networks, this problem has been studied by a number of authors. James, Nurdin, and Petersen developed linear-quadratic-Gaussian control [87] and H-infinity (H_∞) control [81]. Control of linear systems with squeezers and phase-shifters has been explored by Zhang *et al.* [347], and Zhang and James [346] have investigated the relationship between direct and field-mediated coupling in networks. The extension of the Collet and Gardiner input-output formalism to non-Markovian field couplings has been developed by Diosi [348] and Zhang *et al.* [349], and noise suppression via non-Markovian coherent feedback has been analyzed by Xue *et al.* [38]. Coherent noise-reduction for a single cavity was demonstrated experimentally by Mabuchi in [350].

3.3.2. Optical squeezing

Squeezing as an application of coherent feedback was considered early on by Wiseman and Milburn [71]. More recently, a coherent protocol for squeezing was devised by Gough and Wildfeuer [351] which is simpler and allows more control of the amount squeezing. This protocol [351] has now been experimentally realized by Furusawa's group in a linear optical system [352]. We schematically depict the protocol in Fig. 10, in which we see that the coherent feedback loop is composed of a squeezing component, such as a degenerate parametric amplifier in the strong-coupling regime, and a beam splitter whose reflectivity can be adjusted. By tuning this reflectivity, the effective damping rate of the cavity is modified, and the squeezing effects are enhanced or suppressed.

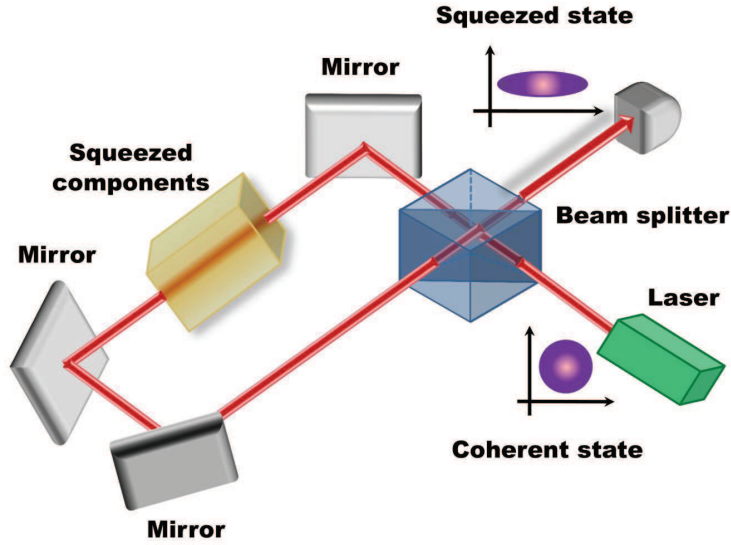


Figure 10: (Color online) Schematic diagram of a theoretical proposal [351] for tunable optical squeezing by coherent feedback. The optical squeezing output produced by a squeezing device can be enhanced and suppressed by tuning the reflectivity of a control beam splitter within the coherent feedback loop.

3.3.3. Quantum error correction

Coherent quantum feedback has been used to implement continuous quantum error-correction (see the start of Section 2 for a brief introduction to quantum error correction) [353, 354]. In Ref. [353], the authors propose a three-qubit error correction method to correct single-qubit bit-flip or phase flip errors using coherent feedback. As shown in Fig. 11, the atoms in cavities Q_1 , Q_2 , and Q_3 are the three physical qubits that code for, and thus allow, the single logical qubit to be corrected. The blue lines are the optical beams for error detection and the red lines are the laser beams that apply the bit flips or phase flips. The central components of this autonomous error correction network are the two relays R_1 and R_2 , which work as controlled quantum switches [355, 356]. When the “Reset” (“Set”) input port of the relay receives a coherent input signal, the input from the “Power in” port will be transferred to the “Out” (“Out”) port. The operating principle of the quantum error correction network can be summarized as follows. If the qubits Q_1 and Q_2 have even (odd) parity, the “Set” (“Reset”) input port of the relay R_1 receives a signal, while the “Reset” (“Set”) input port remains in the vacuum. The same relationship exists between the relay R_2 and the qubits Q_2 and Q_3 . This detected signal controls the power transfer of the relay from the “Power in” port to the “Out” or “Out” port, which is then directed back to the qubits. When a qubit is simultaneously stimulated by two feedback signals from the output ports of the relays, the Raman resonance process will lead to a coherent Rabi oscillation of the qubit and thus correct the errors. Otherwise, the control signal will only introduce an ac Stark shift for the qubit. Such a coherent feedback network can thus automatically correct the bit-flip or phase-flip errors. In Ref. [354], the authors extend this method to perform corrections for Shor’s nine-bit error-correcting code, which concatenates two three-bit codes so as to correct an arbitrary error.

3.3.4. Controlling mechanical resonators

Mechanical resonators can be built with sufficiently high frequencies that they will behave quantum mechanically at a temperature of a few milliKelvin, only an order-of-magnitude from temperatures that can be reached with dilution refrigerators. These mechanical resonators can be coupled to optical modes (“optomechanics”) or cryogenic superconducting circuits (nano-electro-mechanics) for potential use in more complex devices. To prepare highly non-classical states, or for the purpose of using mechanical resonators for quantum technologies, it is useful to prepare them in the ground state. This is usually referred to as cooling.

As far as experiments are concerned, the present state-of-the-art in cooling mechanical resonators is a version of “resolved-sideband” cooling [106, 107]. This method is, in fact, an example of coherent feedback. The mechani-

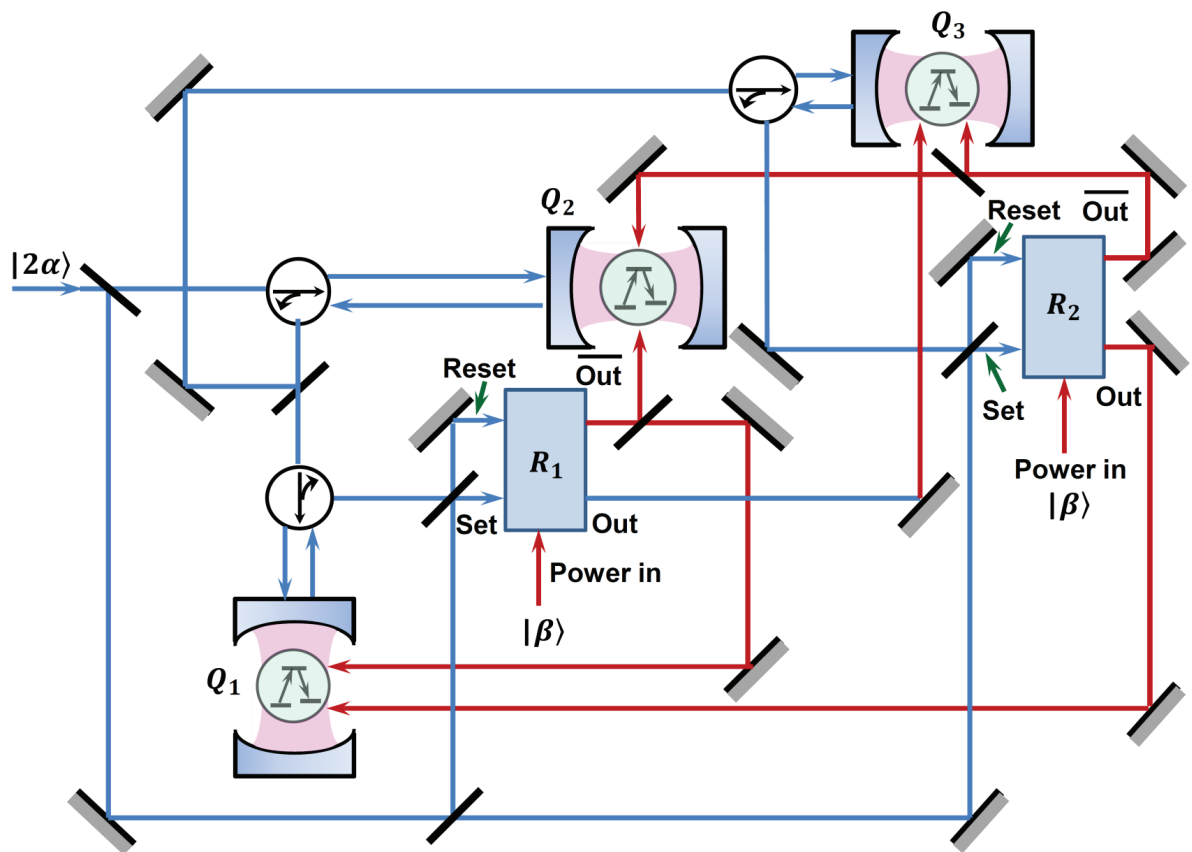


Figure 11: (Color online) Schematic diagram of a theoretical proposal [353] for an autonomous three-qubit quantum error correction network. This scheme has been proposed to correct single-qubit bit-flip or phase-flip errors, which includes register qubits $Q_{1,2,3}$, beam splitters, circulators, and the relays R_1 and R_2 . The blue lines and red lines represent the probe beam and the feedback correction beam, respectively. The relays are quantum switches introduced in Ref. [355]. R_1 and R_2 have two outputs denoted by Out and $\overline{\text{Out}}$.

cal resonator is linearly coupled to another “auxiliary” harmonic oscillator, a mode of an optical or superconducting cavity. These auxiliary resonators have such high frequencies that they sit in their ground states at cryogenic temperatures. The coupling is modulated at the difference frequency of the two resonators, which allows them to exchange excitations as if they were on resonance. The auxiliary oscillator is arranged to have a higher damping rate than the mechanical resonator, and because the former is in its ground state at the ambient temperature, it sucks the energy out of the mechanical resonator [105, 357–359]. The coupling can be direct or field-mediated. Sideband cooling is limited by the linear interaction: to transfer energy without causing heating the strength of the interaction must be much smaller than the frequency of the mechanical resonator, so that the rotating-wave approximation is valid. It has been shown that if the interaction strength is modulated in a more complex way, then this limitation can be overcome, and energy (or quantum information) can be transferred between the resonators within a single period of the mechanical resonator [360].

It has been shown that if one is restricted to a linear interaction with a resonator, then coherent feedback performs much better than measurement-based feedback in the quantum regime, including the regime of ground-state cooling [88, 361]. The superiority of coherent feedback in this case can be traced to the projection noise from the position measurement [362]. This noise is the change in the quantum state induced by the measurement, which is the term proportional to the Wiener noise in the stochastic master equation.

A recent experiment by Kerckhoff *et al.* [361] has shown that coherent feedback can be used as a practical method to tune the coupling strength between a mechanical oscillator and a superconducting circuit.

3.3.5. Quantum nonlinear optics

As is well known, it is not easy to deterministically generate non-classical optical states due to the absence of strong optical nonlinearities. To solve this problem, an interesting study by Yanagisawa in Ref. [363] showed that non-classical optical states can be produced via linear optical components by introducing a multi-feedback structure. It is first shown how a quantum-nondemolition output of x^2 can be constructed by reading out the x quadrature of the optical field and feeding it back to adjust the system-environment coupling strength. In this way one can produce eigenstates of x^2 , which are superpositions of two eigenstates of position with eigenvalues of equal magnitude. A further feedback loop is then introduced in which the Hamiltonian of the controlled system is adjusted by the quantum nondemolition output of x to increase the probability to obtain a desired superposition state. However, in this method the first form of feedback is hard to realize experimentally. To solve this problem, Zhang *et al.* [85, 86] proposed a method which they called “quantum feedback nonlinearization”. This enables strong nonlinear effects in a linear plant by the use of a weak-nonlinear component and a quantum amplifier. With this method it is possible to generate strong Kerr effects that are four or five orders of magnitude stronger than the initial nonlinearity, and can demonstrate nonclassical optical phenomena such as sub-Poisson photon counting statistics and photon anti-bunching effects.

Another potential application of coherent feedback in non-linear optical systems is classical information processing. An optical Kerr-nonlinear resonator in a nanophotonic device can exhibit dispersive bistability effects, and these can be used for all-optical switching in the attojoule regime [364–367]. However, in this regime, the optical logic states are separated by only a few photons and thus suffer from random switching due to quantum noise [368, 369]. In Ref. [370], Mabuchi proposed a coherent feedback method to avoid the quantum noise. In this scheme, a Kerr-nonlinear ring resonator works as an optical switch in which the two states have differing numbers of photons. This switch is connected to a second Kerr-nonlinear ring resonator, which acts as a controller that suppresses the spontaneous switching, in a feedback configuration. Since the effective cavity detuning of a Kerr resonator varies with the driving strength, the controller induces an amplitude-dependent phase shift ϕ on the optical beam. This leads to a ϕ -dependent effective detuning, and a ϕ -dependent effective cavity decay rate for the switch (the controlled resonator). One chooses the control parameter ϕ in an optimal way so that the overall feedback phase is close to π when the switch is in the “low” state and close to zero when it is in the “high” state. In this way, the spontaneous switching between the “low” and “high” states can be efficiently suppressed.

The proposal [370] is extended in Ref. [84] to implement photonic sequential logic by using optical Kerr resonators, in which interference effects enable the binary logic gates. Binary logic elements, such as single-output AND gate and NOT gates with an output fan-out of two, can be generated in this way. These theoretical proposals have been experimentally realized both in superconducting circuits [83], in which the emergent bistable and astable states were used to realize a latch, and in cavity-QED in which optical “NOR” and “OR” gates were realized [371].

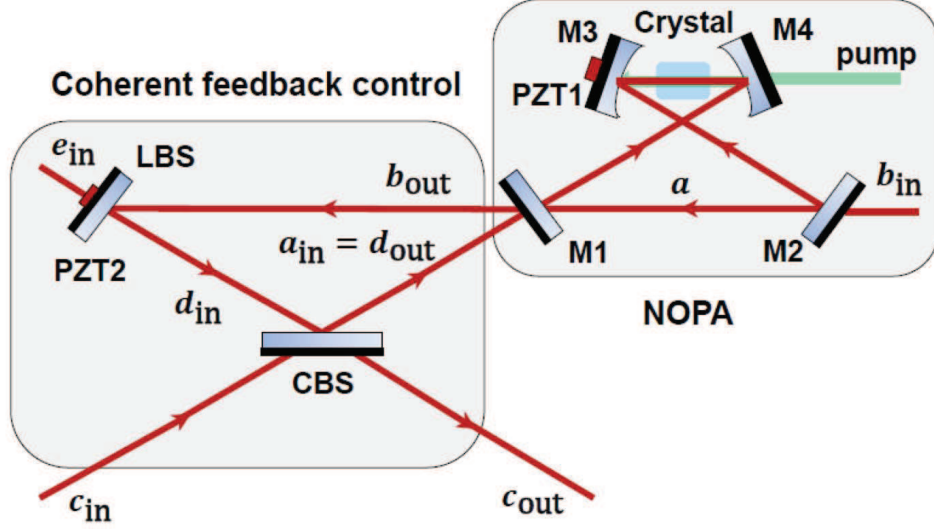


Figure 12: (Color online) Schematic diagram of a theoretical proposal [372] for continuous-variable multipartite entanglement control. The multipartite entangled states are generated by Nondegenerate Optical Parametric Amplifier (NOPA) and enhanced by a coherent feedback loop. The entanglement degree generated can be tuned by adjusting the transmissivity of the Control Beam Splitter (CBS).

3.3.6. Controlling entanglement

A proposal in Ref. [372] shows that coherent feedback can be used to generate and control continuous-variable multipartite optical entangled states. As shown in Fig. 12, in this scheme the multipartite entangled states generated by a non-degenerate optical parametric amplifier (NOPA), denoted by the output field a_i^{out} , are fed into a coherent feedback control loop. The optical beam d_i^{in} is split into two branches by a controlled beam splitter (CBS). One branch, denoted by $a_i^{\text{in}} = d_i^{\text{out}}$, is fed back to the NOPA and the other branch, c_i^{out} , provides the multipartite entangled output. The multipartite entanglement can be controlled by adjusting the transmissivity t of the CBS. The NOPA in Fig. 12 is composed of a nonlinear crystal and a bow-tie type ring cavity. The fields b_i^{in} and e_i^{in} are vacuum fields introduced to model the loss in the NOPA and the coherent feedback loop. The piezoelectric transducers (PZTs) are used to lock the cavity length for resonance. The authors evaluated the multipartite entanglement generated by this scheme using the nonseparable criterion developed in Ref. [373]. It was found that the coherent feedback loop can efficiently enhance the multipartite entanglement generated by the NOPA in particular parameter regimes which can be reached by tuning the transmissivity of the CBS.

4. Other Kinds of Quantum Feedback

4.1. Adaptive feedback

Adaptive feedback is a particular quantum feedback approach based on ensemble measurements and iteration corrections. Each iteration starts with a quantum system (the plant) prepared at particular quantum states (e.g., a thermal equilibrium). The system interacts with a trial control field, and then the yield (as an ensemble control) is measured and fed back to adjust the control. The updated control is applied in the next iteration to a system prepared at the same state. With proper updating strategies, the yield is expected to be improved after a sufficiently large number of iterations.

This idea was first proposed in 1992 by Judson and Rabitz for controlling molecular systems with femtosecond lasers. The motivation behind was that (1) the model of large molecule is almost impossible to be obtained with a satisfying precision; (2) shaping the laser pulse is impossible to be done in realtime. Such systems are ideal for iterative control because each duty cycle is so short that one can repeat the control process for thousands of times within one second.

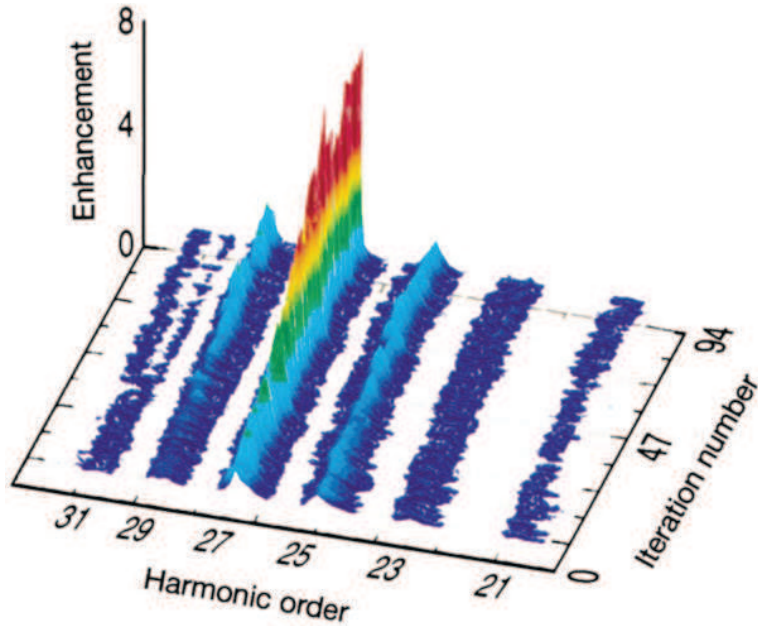


Figure 13: (Color online) The improved yield from a High-Harmonic Generation (HHG) experiment [374]. The Adaptive Feedback Control (AFC) guided search found a control that can selectively enhance the 27th-order harmonic mode. This figure is from Ref. [374].

Adaptive Feedback Control (AFC) can be automatically guided by any intelligent algorithm, such as genetic algorithm, evolutionary strategy and recently developed gradient algorithm, irrespective to the type of the systems to be controlled. In the laboratory, AFC has been successfully applied to over 10 different disciplines [4] including atomic/molecular excitation, selective isotope excitation, discrimination of very similar molecules, ionization, molecular isomerization, molecular alignment, nonlinear spectroscopy, ultrafast semiconductor optical switching, biomolecular energy, etc. For illustration, we select the example of High Harmonic Generation (HHG) for coherent manipulation of soft X-rays, which was first reported in 2000 [374]. Usually, second-order harmonics can be easily done in laboratory, but harmonics up to tens of order requires very high optical nonlinearity with intense lasers. In the experiment, shaped ultrafast and intense laser pulses (with 6-8 optical cycles) are shot into atomic gases. Guided by a learning control loop, their results show that the optimally-shaped laser pulses can improve the efficiency of X-ray generation by an order of magnitude. As shown in Fig. 13, specific high-order harmonics can be selectively generated by the optimal pulse. Up to now, over 150 successful AFC experiments have been reported in the literature [4], and this number is still increasing.

Due to the practical constraints on the control resource, the quality of control is different in these experiments, but all these experiments exhibit strong supports on the effectiveness of AFC. The high-duty cycle of automated laser control apparatus enables the experiments to repeat for many times in a minute, and thus the whole optimization process can be completed within an hour or even a few minutes. Considering the large amount of control variables to optimize in practice, the cost of such experiments to find the optimal solution is very high. Not only can the algorithm quickly find feasible controls that can dramatically enhance the yield, but also can the directed learning control often locate very robust control fields that can tolerate severe noises in the laser pulses, which implies a nice landscape topology that facilitates the location of a high-quality control [375].

4.2. Quantum self-feedback

Quantum self-feedback is also called autonomous feedback in the literature [376]. Different from the other feedback approaches presented, which can be seen as active feedback, self-feedback is a kind of passive feedback method. In self-feedback systems, the controlled system is coupled to an uncontrolled “bath” which works as the controller in the feedback loop. During the feedback control process, the state of the controlled system is to be changed by external control. The controlled system will then modulate the “bath” coupled to it, and the backaction effects from

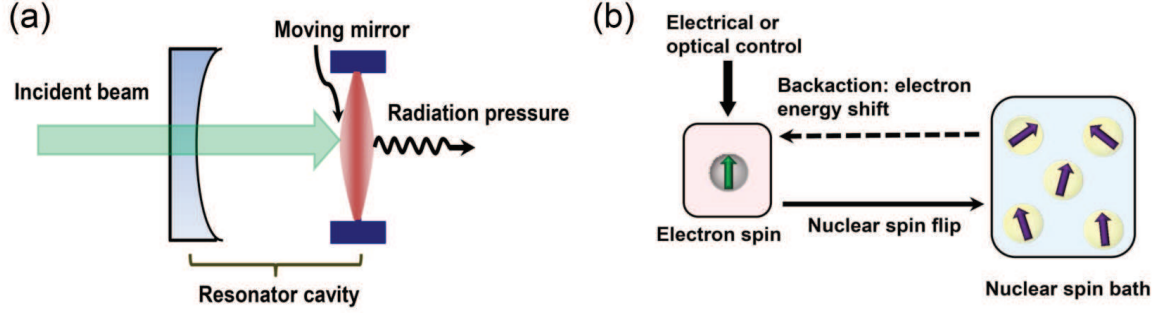


Figure 14: (Color online) Schematic diagram of self-feedback: (a) self-cooling in optomechanical systems and (b) electron-nuclear spin feedback in quantum dots.

the “bath” tune the state of the controlled system which finishes the whole feedback process [377]. Different from the active feedback, the “bath”, i.e., the “controller” in the feedback loop, is less controllable compared with the controlled system, and the active control is imposed directly on the controlled system which leads to the passive feedback backactions via the feedback loop.

Two main applications of the self-feedback mechanism presented above are self-cooling in nanomechanical systems [230–232, 378] and electron-nuclear spin feedback in quantum dots [379–389]. Other possible applications include qubit reset [390] and single-qubit state stabilization [391]. Quite recently, it is also experimentally demonstrated in solid-state superconducting circuits that quantum self-feedback can be used to manipulate two-qubit quantum states [376].

An example of self-cooling nanomechanical system is shown in Fig. 14(a). In such a system, the vibration of back mirror of a single-ended cavity leads to the change of the length of the cavity. When the cavity is driven in the blue detuning regime, the backaction effects from the cavity induce a negative linear force on the moving mirror and then suppress its thermal motion. In this case, the modified effective damping rate of the moving mirror can be given by [230]

$$\Gamma_{\text{eff}} = \Gamma_m \left(1 - 2Q \text{Im} \frac{\phi \phi_{\text{NL}}}{\Delta} \right), \quad (4.1)$$

where

$$\Delta = (1 - i\Omega_m/\Omega_c)^2 + \phi^2;$$

Ω_m and Γ_m are the resonance frequency and damping rate of the moving mirror; Q is the quality factor of the cavity mode; ϕ_{NL} is the nonlinear phase shift of the cavity induced by the static recoil effect of the resonator; and ϕ is the normalized detuning of the cavity mode. When $\phi < 0$, the optomechanical system is in the cooling regime such that $\Gamma_m < \Gamma_{\text{eff}}$, which leads to a lower effective temperature given by

$$\frac{T_{\text{eff}}}{T} \approx \frac{\Gamma_m}{\Gamma_{\text{eff}}}. \quad (4.2)$$

Another application of self-feedback mechanism is the electron-nuclear spin feedback in quantum dot systems [379–389]. As shown in Fig. 14(b). Optical pumping or microwave pumping is first imposed on the electron spin to flip the spin states. The electron spin then flips the nuclear spins through the contact hyperfine interaction to suppress the nuclear spin fluctuations. The backaction effects from the polarized nuclear spin bath with narrowed spectrum distribution protect the resonance and coherence of the electron spin and extend the dephasing time of the electron spin states.

Table 2: Characteristic scales of system parameters in different systems

	Linear optics	Optomechanics	Cavity QED	Superconducting circuits	Quantum dots
Time-scale of system dynamics	1-100 MHz	0.1-10 MHz	0.1-100 MHz	1-10 GHz	1-10 GHz
Measurement efficiency	0.9	< 0.1	0.8	0.4	–
Measurement rate	1 kHz - 10 MHz	–	0.1-10 MHz	0.15 MHz	kHz-MHz
Feedback delay	0.1-10 μ s	–	1 μ s-1 ms	250 ns	~ ms
Feedback bandwidth	1 MHz	1-10 kHz	–	10 MHz	–
Temperature	300 K	10 mK - 10 K	1 mK-1 K	30 mK	~ mK

5. Experiments Realizing Quantum Feedback

There have been considerable experiments in the existing literature to implement quantum feedback in various physical systems such as optical systems, cavity-QED systems, superconducting circuits, quantum dot systems, etc. The characteristic system parameters that are shown in the current experiments are also very important for the succeeding theoretical and experimental studies, and thus we summarize in table 2 the characteristic scales of system parameters in different systems that have been shown in the existing experiments.

5.1. Linear optics

The early-stage experimental demonstrations of quantum feedback show the power of feedback in quantum metrology. It is theoretically predicted in Ref. [292] that the adaptive homodyne measurement technique realized by quantum feedback can be used to estimate unknown optical phases of weak pulses of light for single-shot measurement. This method approaches closer to the intrinsic quantum uncertainty than any previous technique, such as heterodyne detection which is once believed [392] to be the best strategy for single-shot phase estimation without prior knowledge. This theoretical prediction is first experimentally confirmed in Ref. [308]. Figure 15 shows the schematic diagram of the experimental setup in Ref. [308]. Noisy weak coherent light from a single-mode cw Nd:YAG laser first passes through a high-finesse Fabry-Perot cavity (not shown in the figure) with ringdown time 16 μ s and shot noise limit 50 kHz to squeeze out the intensity noise in the signal light. The signal light is then fed into a Mach-Zehnder interferometer (MZI) to generate interference between the signal light and a local oscillator to fulfill the homodyne detection. The local oscillator (LO), i.e., a 230 μ W frequency-shifted light, is produced by an acousto-optic modulator (AOM), which is driven by an 84.6 MHz rf synthesizer (RF₁). The signal light is frequency-shifted by an electro-optic modulator (EOM), which is driven a rf synthesizer (RF₂). The two rf synthesizers RF₁ and RF₂ are phase-locked to each other to achieve synchronization between the local oscillator and the signal light. By changing the amplitude and switching RF₂ on and off, we can tune the power of the signal light from 5 fW to 5 pW and pulse length for about 50 μ s. The two output ports of MZI are detected by two photon detectors and the corresponding balanced photon current $I(t)$, i.e., the difference of the photocurrents from the two photon detectors, can be used to extract information for heterodyne measurements and adaptive homodyne measurements. In experiment, the shot noise in the difference photocurrent (from 1 kHz to 10 MHz) is about 6 dB. The adaptive homodyne measurement is realized by setting the relative phase between the signal light and the local oscillator via the feedback acting on RF₂. The local oscillator phase is adaptive in real time to the phase of the signal pulse. The feedback bandwidth is about 1.5 MHz which is mainly limited by the maximum slew rate of RF₂. The feedback signal acting on RF₂ is [294]

$$\Phi(t) = \frac{\pi}{2} + \int_0^T dv \frac{I(v)}{\sqrt{v}}, \quad (5.1)$$

which is generated by a Field Programmable Gate Array (FPGA) by integrating the photocurrent. The final output estimated phase is

$$\hat{\phi} = \int_0^T dv \frac{I(v)}{\sqrt{v}}. \quad (5.2)$$

Although the heterodyne measurement performs better than the adaptive approach for signals with large mean photon, the experimental data in Ref. [308] shows that the ‘‘Gaussian width’’, i.e, the variance, of the phase estimate is much smaller for adaptive homodyne measurement than heterodyne measurement for intermediate values of the average

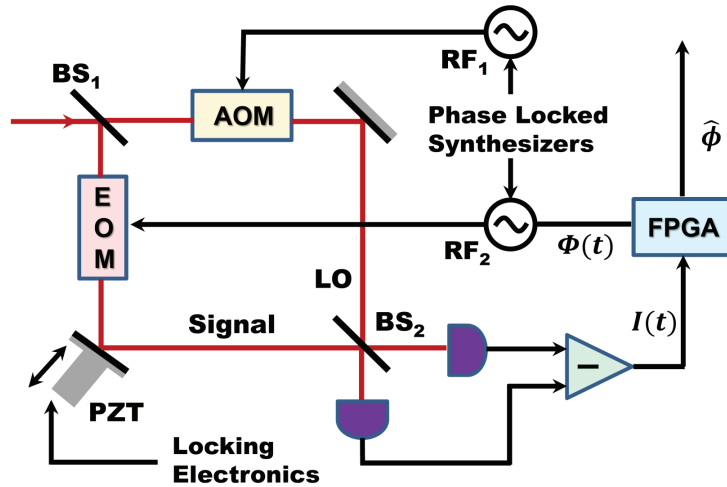


Figure 15: (Color online) Schematic diagram of the adaptive homodyne measurement of an optical phase in Ref. [308]. Optical beams are indicated by red lines and electronic beams by black lines. The AOM and EOM represent the acousto-optic modulator and electro-optic modulator. BS and RF are the beam splitter and the radio-frequency synthesizer. PZT is the piezoelectric transducer and FPGA is the field programmable gate array.

photon number in the signal, which means that the adaptive measurement is hopeful to perform better than the single-shot measurement and approaches closer to the uncertainty limit in particular parameter regime.

Although the experiment in Ref. [308] has shown that the adaptive estimation by quantum feedback can achieve more compared with the traditional measurement approaches. It is still not quite clear how close we can approach the quantum uncertainty limit. The measurement precision of any quantum measurement and estimation is strongly limited by the amount of the quantum resources needed such as the number of photons. For quantum resources with N photons, the standard quantum limit for a phase estimate scales as $1/\sqrt{N}$. However, a smaller uncertainty is still hopeful to be achieved, which is only limited by the Heisenberg principle that improves the scaling to $1/N$. Before introducing the adaptive approach, it is widely believed that possible improvement approaching such a small uncertainty limit requires introducing quantum entangled states, such as a NOON state $(|N\rangle|0\rangle + |0\rangle|N\rangle)/\sqrt{2}$ with large photon number N , which are extremely difficult to generate. Experiment in Ref. [309] shows that this problem can be avoided by replacing the highly entangled quantum states by repeatedly introducing phase shift on unentangled single-photon state and applying adaptive measurement by quantum feedback. The experimental setup in Ref. [309] is shown in Fig. 16. The basic component of the experimental setup is a common-spatial-mode polarization interferometer. The two arms of the interferometer correspond to the right-circular and left-circular polarization modes. A photon experiences a phase shift $p\theta$ ($p\phi$) for left-circular (right-circular) polarization mode induced by the feedback wave plate (unknown phase wave plate). To achieve the σ_x measurement on the single-photon qubit to extract the phase information, the photon is selected by moving mirrors and discriminated in horizontal and vertical basis by a Polarizing Beam Displacer (PBD). After transmitting through a 10 nm bandwidth interference filter, the signal is detected by Single Photon Counting Modules (SPCMs) to finish the σ_x measurement on the photon state. The processor compares the estimated phase θ and the unknown phase ϕ to update the control, i.e., the phase shift $p\theta$, imposed on the feedback half wave plate (HWP). For the largest number of resources $N = 378$ in experiments in Ref. [309], an uncertainty of the phase estimate, which is more than 10 dB below the standard quantum limit, is hopeful to be achieved. It is very close to the quantum Heisenberg limit. There are still other phase estimation experiments presented to avoid the difficulty for generating highly-entangled NOON state [310–312]. For example, in Ref. [310], Xiang *et al.* use n -photon dual Fock state as the inputs to replace the NOON state and introduce Bayesian analysis and optimal adaptive feedback to make full use of the multiphoton states. This is the first time to show sub standard-quantum-limit phase measurement using entangled states.

In the adaptive measurement experiments in Refs. [308] and [309], the filtering strategies introduced to design feedback control are to obtain time-asymmetric estimate, in which the information is only extracted from the past-

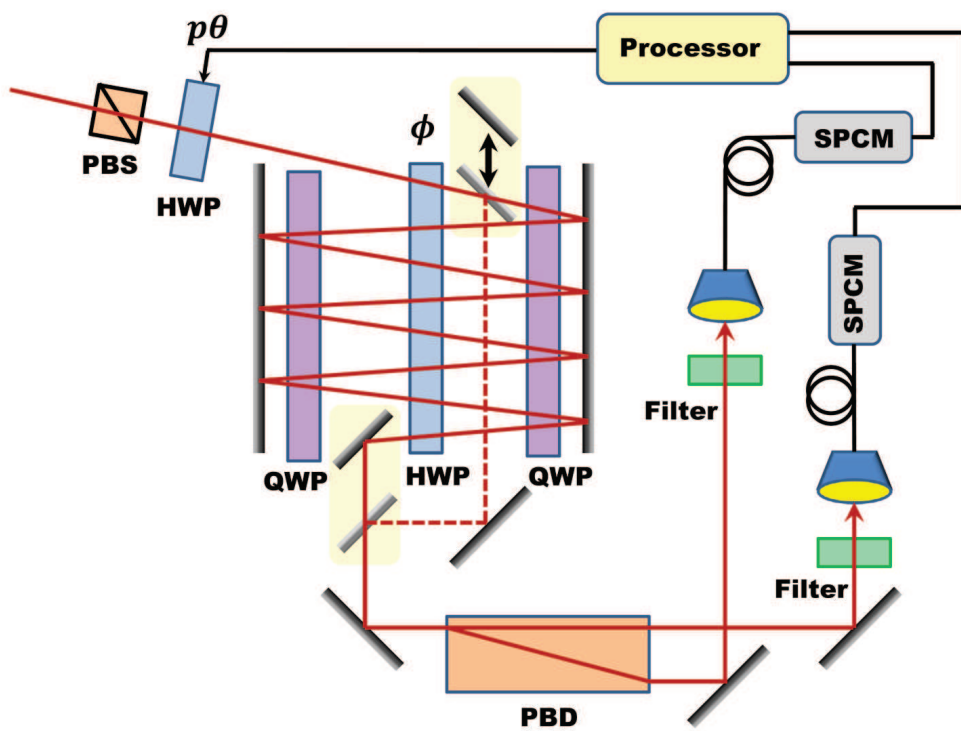


Figure 16: (Color online) Schematic diagram of the Heisenberg-limited phase estimation by adaptive measurement in Ref. [309]. PBD and PBS represent the polarizing beam displacer and the polarizing beam splitter. SPCM is the single-photon counting module. QWP and HWP are the quarter-wave plate and half-wave plate, respectively.

time observations. In order to make full use of the information extracted by the measurement and achieve higher precision of phase estimation, a time symmetric estimation technique called smoothing is introduced in Ref. [169] to experimentally estimate a classical phase noise process, in which the estimated phase is obtained at a time point based on information extracted both before and after that time point. Strictly, smoothing is an acausal estimation technique and thus cannot be used in real-time. But, we can solve this problem by designing the feedback control law after a time delay corresponding to the estimation time. Since more information is provided in smoothing compared with filtering, the estimate obtained by smoothing technique is hopeful to be more precise than that obtained by filtering, and the experimental results in Ref. [169] confirm this conclusion. The schematic diagram of experiment in Ref. [169] is shown in Fig. 17. A Ti:sapphire laser with 860 nm wavelength is used as the source. The two acousto-optic modulators (AOMs) in Fig. 17(a) are used to generate a pair of optical beams with ± 5 MHz frequency shifts and photon flux $\mathcal{N} = |\alpha|^2 \approx 10^6$ photons per second. An Ornstein-Uhlenbeck (OU) noise source $\phi(t)$ given by

$$d\phi(t) = -\lambda\phi(t)dt + \sqrt{\kappa}dV(t) \quad (5.3)$$

is used to drive an Electro-Optic Modular (EOM) to act as a classical phase noise process, where dV is a Wiener increment and λ and κ are exponential decay rate and inverse coherence time respectively. The signal $|\alpha|e^{i\phi}$ and the output of the local oscillator generated in Fig. 17(a) are both fed into the measurement circuits in Fig. 17(c). The two homodyne detection setups with output photocurrents $I_{\pm}(t)$ and detection efficiency 89% in Fig. 17(c) give symmetric phase estimates $\Theta_{-}(t)$ and $\Theta_{+}(t)$ obtained before and after time t , which can be calculated by

$$\Theta_{\pm}(t) = \pm 2\sqrt{\kappa}|\alpha| \int_t^{\pm\infty} \exp[\omega_0(s-t)]I_{\pm}(t)/2|\alpha|ds, \quad (5.4)$$

where $\omega_0 = 1.5 \times 10^5 \text{ s}^{-1}$ is the cutoff frequency of the linear Low-Pass Filter (LPF) and is far smaller than the feedback gain $2\sqrt{\kappa}|\alpha|$. The final optimal smoothed estimate $\Theta(t) = [\Theta_{+}(t) + \Theta_{-}(t)]/2$ of the unknown phase $\phi(t)$ is just the symmetric weighted average of the forwards and backwards estimates $\Theta_{\pm}(t)$. The experimental results in Ref. [169] predict that the adaptive smoothing approach can give an estimate with uncertainty $2\sqrt{2}$ times smaller than that of the best nonadaptive filtering approach. The latter is just the standard quantum limit.

The above presented experiments mainly use coherent light to estimate optical phase, and thus the precision of the phase estimation is greatly limited by the quantum fluctuation of coherent light. In order to improve the precision of estimation to surpass this coherent-state limit, an experiment in Ref. [313] introduces continuous-wave squeezed light to take place of coherent light for phase estimation. The experimental setup in Ref. [313] is shown in Fig. 18. In the experiment, a 860 nm titanium sapphire laser in the signal beam transmits through an Optical Parametric Oscillator (OPO), which is driven below threshold by a 430 nm pump beam. A squeezed light with squeezing ≈ -3 dB and antisqueezing ≈ 5 dB can be generated by a 80 mW pump field, which corresponds to an optical beam with $|\alpha|^2 = 1 \times 10^6$ photon per second. The squeezed light is modulated by a stochastic phase $\phi(t)$ given by the following equation

$$\phi(t) = \sqrt{\kappa} \int_{-\infty}^t \exp[-\lambda(t-s)]dV(s), \quad (5.5)$$

where $dV(s)$ is a classical Wiener process; λ^{-1} is the correlation time of $\phi(t)$; and κ is the magnitude of the phase variation. This stochastic phase $\phi(t)$ is just the unknown phase needed to be estimated, which is produced by a digital random generator and a low-pass filter with $\kappa \approx 2 \times 10^4 \text{ rad/s}$ and cutoff frequency $\lambda \approx 6 \times 10^4 \text{ rad/s}$. The signal beam interfered with a local oscillator (LO) is detected by a homodyne measurement with overall efficiency $\eta = 0.85$. The output photocurrent transmits through another low-pass filter (feedback filter) and generate a phase signal $\hat{\phi}(t)$, which is shifted by $\pi/2$ to obtain the control signal $\Phi(t) = \hat{\phi}(t) + \pi/2$. The control signal $\Phi(t)$ is applied to the phase of the LO beam by an electro-optic modulator. The estimated stochastic phase $\phi(t)$, the photon current $I(t)$, and the signal $\hat{\phi}(t)$ are all recorded by an oscilloscope with a sampling rate 100 MHz. Experimental results in Ref. [313] show that $15 \pm 4\%$ reduction of the estimated error below the coherent-state limit can be achieved by optimizing the squeezing rate of the signal beam.

The quantum feedback control based on continuous measurement can also be used to correct the qubit states against decoherence. This is experimentally demonstrated in Ref. [284] to verify the theoretical proposal presented in Ref. [283]. The schematic diagram of the experimental setup in Ref. [284] is shown in Fig. 19. The qubit states

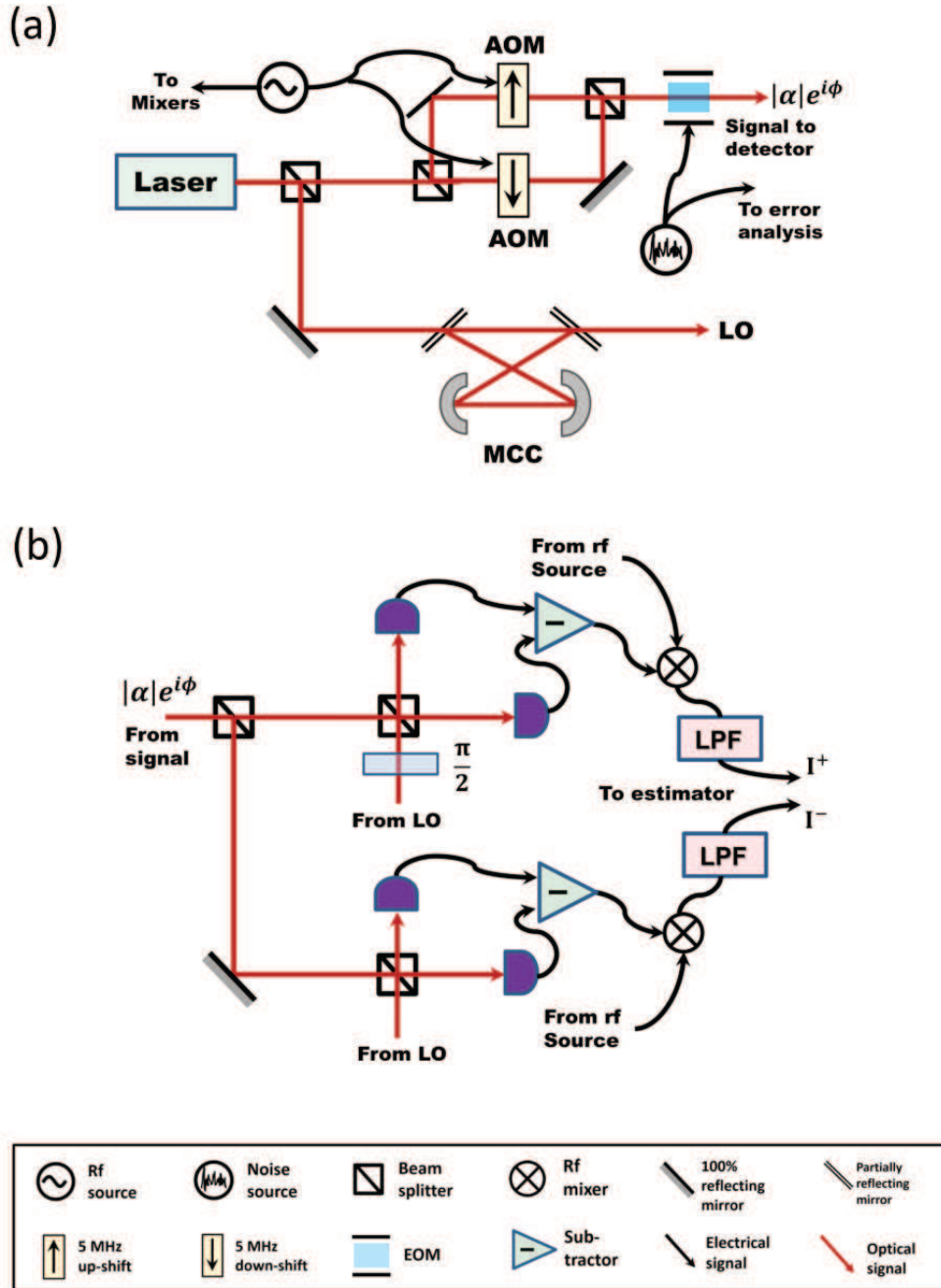


Figure 17: (Color online) Schematic diagrams of the experimental setups for (a) signal and local oscillator generation and (b) adaptive dual-homodyne phase estimation in Ref. [169]. AOM is the acousto-optic modulator. LPF and MCC are the low-pass filter and mode-cleaning cavity, respectively.

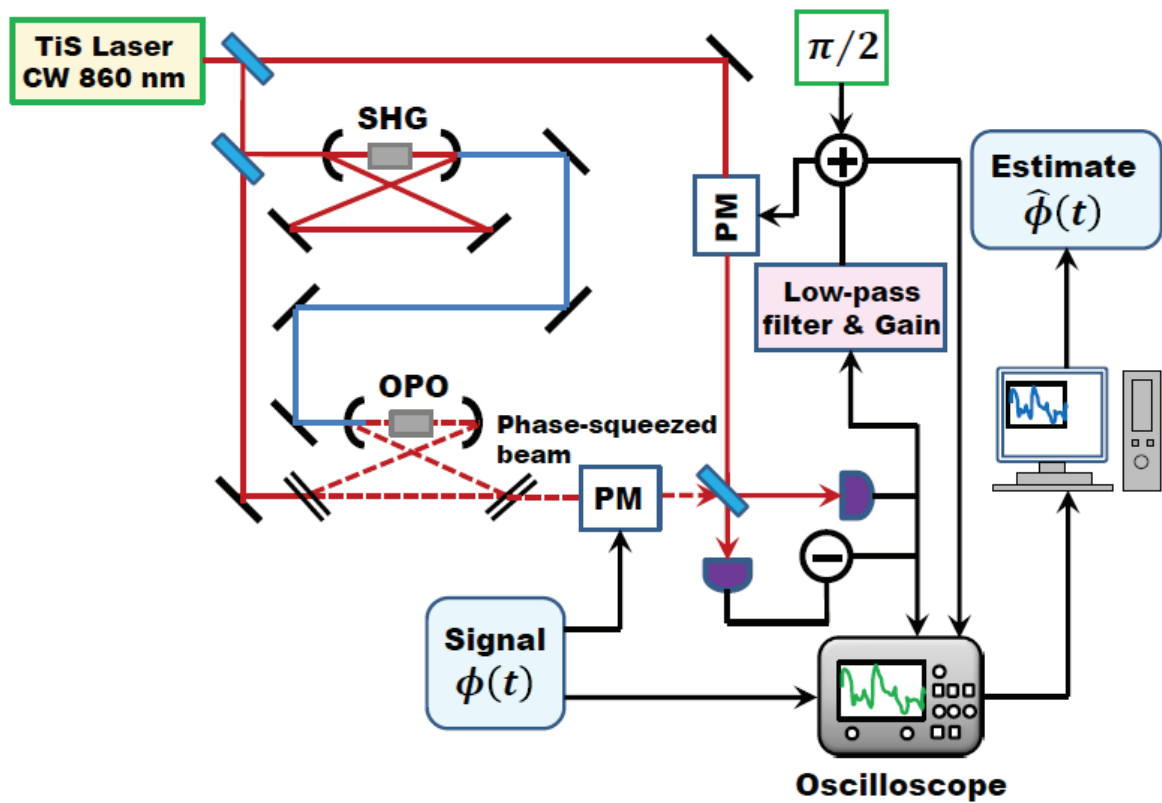


Figure 18: (Color online) Schematic diagram of the experimental setup used in Ref. [313]. TiS and CW refers to titanium sapphire and continuous wave. PM and SHG denote the phase modulator and the second-harmonic-generator. The squeezed signal light generated by the optical parametric oscillator (OPO) is modulated by a stochastic phase $\phi(t)$ and then interferes with a local oscillator. The output field is detected by a homodyne detection and then fed back to update the phase imposed on the local oscillator.

are encoded in the polarization of single photons with horizontal $|H\rangle = |1\rangle$ and vertical $|V\rangle = |0\rangle$. A degenerate 820 nm photon pair is first generated by the spontaneous parametric down-conversion process of a type I BiBO crystal pumped by a 100 mW beam at 410 nm obtained from the second harmonic generation of an 820 nm Ti:sapphire laser. The photon pair is then filtered by ± 1 nm Interference Filters (IFs) centered at 820 nm and fed into single-mode fibers. One photon in this photon pair works as the signal photon and is prepared in the qubit state

$$|\psi\rangle = \cos \frac{\theta}{2} |+\rangle \pm \sin \frac{\theta}{2} |-\rangle$$

by transmitting through a polarizing beam splitter with reflectivity $R_H = 0$ and $R_V = 1$ and a Half Wave Plate (HWP), where

$$|\pm\rangle = \frac{1}{\sqrt{2}} (|0\rangle \pm |1\rangle).$$

The other photon in the photon pair is the detection photon which is prepared in the qubit state

$$|\phi\rangle = \cos \frac{\chi}{2} |+\rangle + \sin \frac{\chi}{2} |-\rangle.$$

The signal photon and the detection photon are then interfered through a partially polarizing beam splitter with reflectivity $R_H = 1/3$ and $R_V = 1$. Conditional on there being only one photon in each mode, the partially polarizing beam splitter executes a control-Z gate operation $|0\rangle\langle 0| \otimes \mathbf{1} + |1\rangle\langle 1| \otimes Z$ on the signal photon and the detection photon [393–395]. If we average over the degrees of freedom of the detection photon, the qubit state of the signal photon will be in the mixed state

$$\rho' = (1 - p) |\psi\rangle\langle\psi| + p Z |\psi\rangle\langle\psi| Z,$$

which means that we just impose an equivalent phase-flip decoherence channel for the signal photon. The output detection photon is then fed into a measurement setup used to implement a projective measurement of the detection photon in the \pm -basis by rotating the polarizing basis via a wave plate set and transmitting through a polarizing beam splitter with $R_H = 0$ and $R_V = 1$. This leads to a continuous measurement with measurement operators

$$M_+ = \cos \frac{\chi}{2} |0\rangle\langle 0| + \sin \frac{\chi}{2} |1\rangle\langle 1|, \quad M_- = \sin \frac{\chi}{2} |0\rangle\langle 0| + \cos \frac{\chi}{2} |1\rangle\langle 1|$$

on the qubit state of the signal photon. The signal photon is then fed into a 50 m fiber delay to allow time for the quantum weak measurement and transmits through the wave plate set A to compensate the unwanted polarization rotations introduced by the fiber delay. After that, the signal photon is fed into a 3 mm Rubidium Titanyl Phosphate (RTP) Pockels cell with a half-wave voltage of 700 V at 820 nm. Depending on the continuous measurement output \pm , a correction rotation $Y_{\pm\eta} = \exp(\pm i\eta Y)$ around the y axis of the Bloch sphere is imposed on the signal photon by the Pockels cell. This is implemented by first using the fixed wave plates labelled by “signal analysis” in Fig. 19 to rotate the signal photon by $-\eta$ and then using the Pockels cell to rotate the signal photon by $+2\eta$ conditional on the measurement outcome of M_+ . The experimental results in Ref. [284] show that quantum continuous measurements and feedback control will lead to an improvement of the qubit state stabilization compared with strong projective measurements and methods without any measurement, and there is a tradeoff between information gain and measurement backaction.

Coherent quantum feedback has also been experimentally demonstrated in linear optical systems. Figure 20 shows the experimental setup of the first coherent feedback control experiment [350] designed to test the linear quantum stochastic control theory proposed in Ref. [81]. As shown in Fig. 20, two four-mirror ring resonators couple with each other by a 852 nm diode laser. These two ring resonators work as the plant (controlled system) and the controller respectively. As shown in Fig. 20, an external “noise” signal is injected into the plant cavity at the input w . The output component y reflected from the plant input coupler acts as the error signal, which is processed by a quantum controller, i.e., a four-mirror ring resonator, to generate a control signal u . This control signal is then fed back into the plant cavity again to change the dynamics of the plant. Finally, the optical power is detected at the system output z . The control goal of this experiment is to minimize the ratio of the optical power at the output z to that of the “noise” input w ,

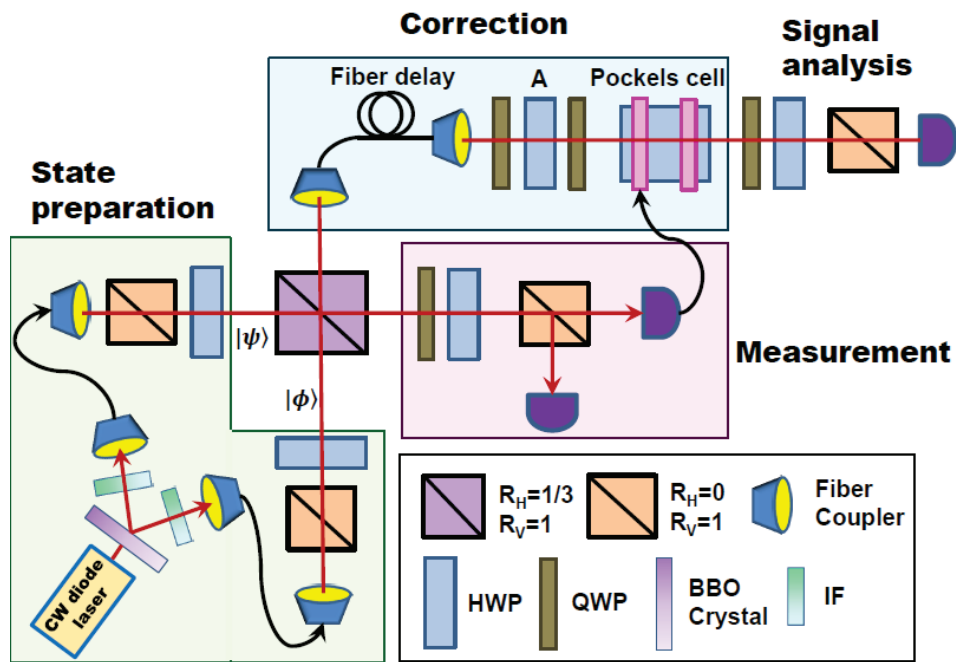


Figure 19: (Color online) Schematic diagram of the experimental setup in Ref. [284]. A photon pair composed of a signal photon and an auxiliary detection photon is prepared by the spontaneous parametric down-conversion of a BiBO crystal. The signal and detection photons are then prepared in the quantum states $|\psi\rangle$ and $|\phi\rangle$, respectively, by transmitting through the polarization beam splitters and half wave plates (HWP). The two branches of signals are combined by a partially-polarizing beam splitter which works as a phase-damping decoherence channel on the signal photon. A succeeding projective measurement in the $+/-$ basis is imposed on the detection photon which leads to a continuous measurement on the signal photon. The measurement output is then fed into a Pockels cell to rotate the signal photon conditional on the meter outcome. QWP is the quarter wave plate and IF is the interference filter.

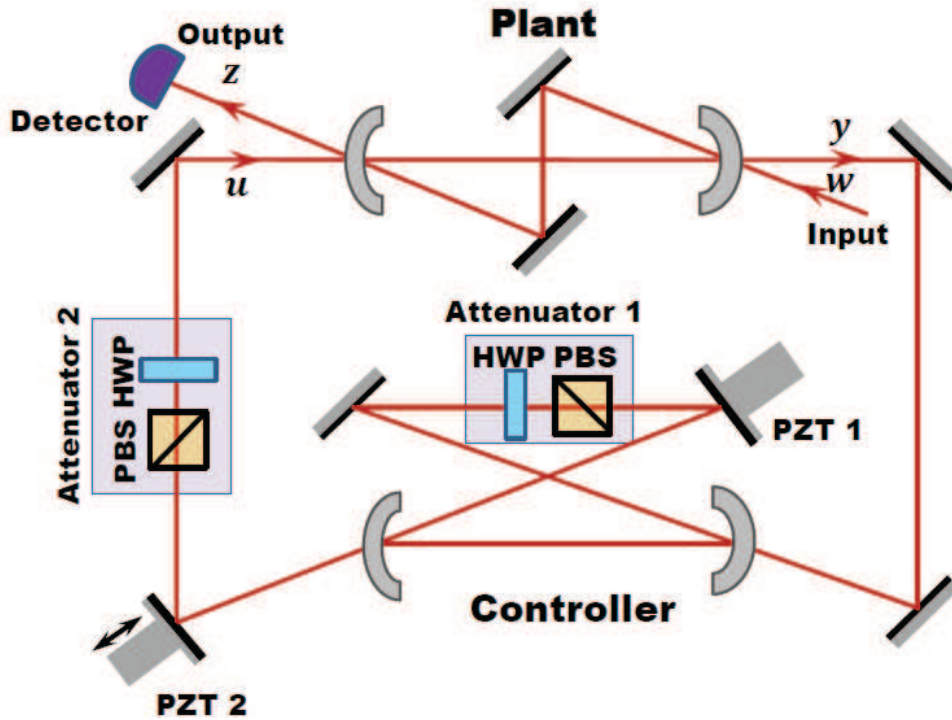


Figure 20: (Color online) Schematic diagram of the experimental setup in Ref. [350]. Two four-mirror ring resonators couple with each other by a transmitting optical field, which work as the plant cavity and controller, respectively. The control goal is to tailor the behaviors of the controller to minimize the power detected at the system output z , when a “noise” signal w is fed into the plant cavity. This can be achieved by tuning the parameters via the two variable attenuators, i.e., attenuator 1 and attenuator 2, and the two actuator piezoelectric transducers (PZTs), i.e., PZT 1 and PZT 2.

or, equivalently, the magnitude of the so-called system closed-loop transfer function by tuning the parameters of the controller. It is shown in Ref. [81] that a simple proportional controller does not work very well, and thus a dynamic compensator with a non-trivial frequency response, i.e., another four-mirror optical cavity, are introduced. There are mainly four possible ways to tune the parameters of the controller: (i) the resonance frequency of the controller cavity can be tuned by the actuator PZT 1; (ii) the phase of the transfer function of the controller is continuously adjusted via the actuator PZT 2; (iii) the decay rate of the controller cavity can be tuned by intracavity variable attenuator, i.e., the attenuator 1; and (iv) the magnitude of the transfer function of the controller can be adjusted by the variable attenuator at the output of the controller cavity, i.e., attenuator 2. By optimizing the parameters of the controller cavity, optimal noise suppression can be achieved such that the ratio of the optical power in z by negative coherent feedback to that achieved by open-loop control is approximately 7 dB.

Coherent quantum feedback is also demonstrated experimentally to be capable of enhancing optical squeezing effects [352], which has been predicted theoretically in the previous literature [351]. Different from Ref. [352] which mainly demonstrates classical noise reduction in the sense that the quantum state is restricted as a coherent state, the experiment in Ref. [352] shows that coherent feedback can lead to non-classical noise reduction and beat the quantum noise limit. The experimental setup of Ref. [352] is shown in Fig. 21. The central part of the experimental setup is the coherent feedback loop which is composed of an Optical Parametric Oscillator (OPO) as the plant and a Control Beam Splitter (CBS) acting both as a controller and as an input-output port. The final squeezing-enhancement effects are detected by interfering the output field of the coherent feedback loop with a Local Oscillator (LO) beam to achieve a homodyne measurement. The information flow over the control network can be described in more details as follows. A continuous-wave Ti:sapphire laser with 860 nm wavelength and horizontal polarization is first split into three branches. The first branch is fed into a frequency-doubler to generate a second-order harmonic beam of 430 nm, which is then used as a pumping beam for the OPO. The second branch works as the probe beam, which is injected

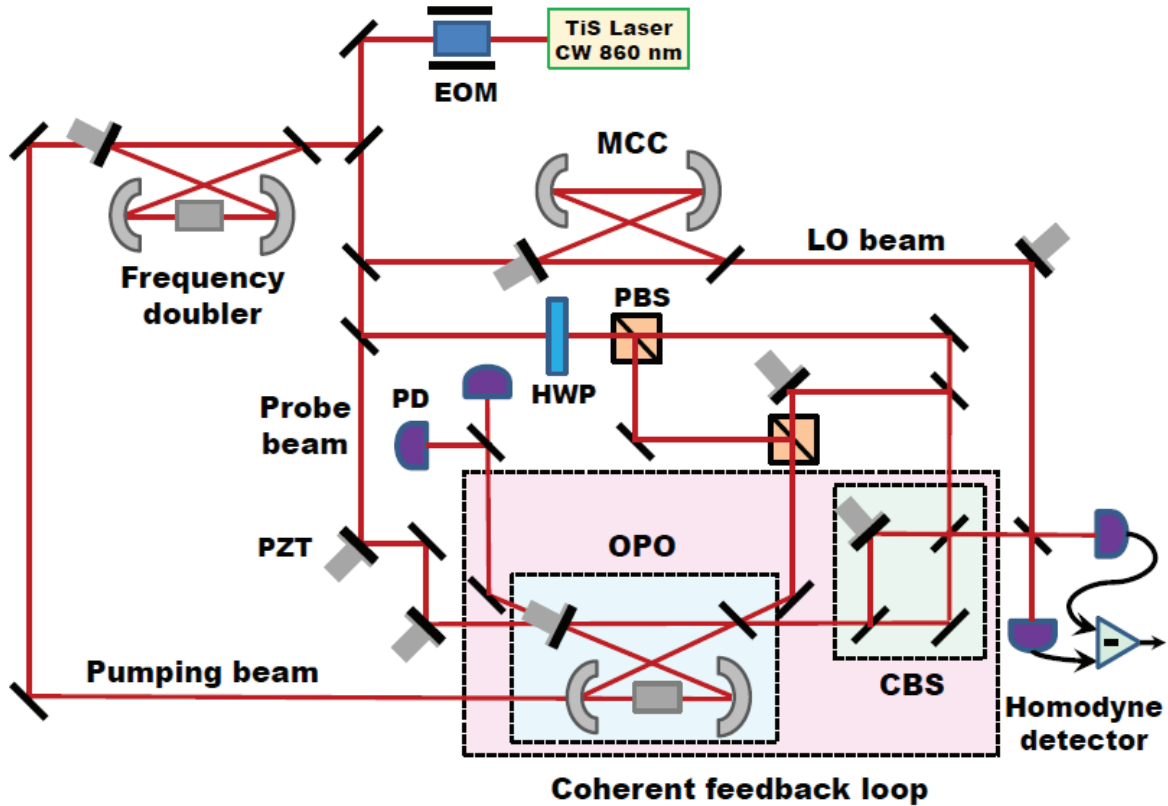


Figure 21: (Color online) Schematic diagram of the experimental setup [352] of squeezing enhancement by coherent feedback. The bottom right part (inside the large dashed rectangle) is the coherent feedback control loop which is composed of an optical parametric oscillator (OPO) and a control-BS (CBS). The squeezing enhancement effect by coherent feedback are detected by a homodyne measurement. The MCC and CW laser represent the mode cleaning cavity and the continuous-wave laser. Here, EOM, PD, PZT, HWP, PBS, and LO are the electro-optic modulator, the photon detector, the piezoelectric transducer, the half-wave plate, the polarized beam splitter, and the local oscillator.

into the OPO directly from the high-reflection-coated mirror. A classical feedback control is implemented by a set of actuator Piezoelectric Transducers (PZTs) and Photon Detectors (PDs) to lock the cavity and the relative phase between the probe beam and the pump beam. The CBS is achieved by a Mach-Zehnder (MZ) interferometer of which the transmissivity can be tuned by adjusting the phase difference between the two arms of the MZ interferometer. The third branch of laser is fed into a mode cleaning cavity to generate the signal for the LO beam used for homodyne measurement. For the homodyne measurement, the power of the probe beam is set to be $4 \mu\text{W}$ and that of the LO beam is 3 mW . The output of the homodyne detector is finally fed into a spectrum analyzer to study the squeezing-enhancement effects. The experimental data reported in Ref. [352] shows that the squeezing enhancement from $-1.64 \pm 0.15 \text{ dB}$ to $-2.20 \pm 0.15 \text{ dB}$ and the anti-squeezing enhancement from $1.52 \pm 0.15 \text{ dB}$ to $2.75 \pm 0.15 \text{ dB}$ can be achieved by coherent feedback. However, larger laser noises and modulation signals used for several locking lead to the deterioration of the control effects in the low-frequency regime.

5.2. Trapped particles and Cavity-QED

Quantum feedback control has also been demonstrated in cavity-QED system. In the early stage of studies [396–398], the feedback implementations in such systems are well understood in a classical way, because the magnitude of quantum fluctuations are too small to be compared with the mean fields and thus can be omitted. However, with the development of techniques, it is now possible to trap atoms in the cavity of which the average occupation can approach or even be less than one photon and the coupling strength between the atoms and cavity is strong enough to

be comparable with the damping rates of the atoms and cavity. In this regime, the quantum behaviors induced by the quantum fluctuations should be considered in the feedback control system. Figure 22 shows the experimental setup in Ref. [215] which is an early-stage experiment in this deep quantum regime. By changing the amplitude of the driving field injected into the cavity via feedback, the conditional state of the atom-cavity system induced by optical intensity measurement can be stabilized and then released. The central component of the feedback control system is an optical cavity composed of two high-reflectivity curved mirrors with separation $l = 880 \mu\text{m}$. A thermal beam of Rb^{85} atoms is produced from an effusive oven heated to 440 K, and then enters the cavity. The cavity field is driven by an Ar^+ -pumped titanium sapphire (Ti:sapphire) laser which leads to the transition of Rb^{85} from $5S_{1/2}, F = 3$ to $5P_{3/2}, F = 4$. The coupling strength between the atom and the cavity, the decay rate of the cavity, and the decay rate of the atom are $(g, \kappa, \gamma/2)/2\pi = (5.1, 3.7, 3.0)$ MHz. The output field from the cavity is splitted by a beam splitter and then detected by two (“start” and “stop”) Avalanche Photodiodes (APDs). The output signal from the start detector is splitted into two branches again. One branch enters the start channel and is fed into a Time to Digital Converter (TDC) used to measure the second-order correlation function $g^{(2)}(\tau)$ of the field, and the other is sent to a delay generator and then fed back to control the strength of the driving field of the cavity by an electro-optical modulator in front of a polarizer. The feedback delay in the experiment is 45 ns. For such a cavity-QED system, the state of the cavity and atom tends to a steady state

$$|\psi_{ss}\rangle \approx |0, g\rangle + \lambda \left(|1, g\rangle - \frac{2g\sqrt{N}}{\gamma} |0, e\rangle \right), \quad (5.6)$$

where N is the number of the atoms interacting with the cavity and λ is a control parameter determined by the strength of the input driving field. $|0\rangle$ and $|1\rangle$ are the photon number state of the cavity, and $|g\rangle$ and $|e\rangle$ are the two qubit states of the atom. After a photodetection, the system state evolves to the conditioned state

$$|\psi_c(\tau)\rangle = |0, g\rangle + \lambda \left[\xi(\tau) |1, g\rangle - \theta(\tau) \frac{2g\sqrt{N}}{\gamma} |0, e\rangle \right], \quad (5.7)$$

which oscillates coherently induced by the energy exchange between the atomic polarization and the cavity field. At the time $\tau = T$ such that $\xi(T) = \theta(T)$, the control parameter λ is changed to $\tilde{\lambda} = \xi(T)\lambda$ by tuning the driving intensity of the cavity via feedback and the conditioned state $|\psi_c(T)\rangle$ is captured accordingly. The capture of the conditioned state can be observed by measuring the normalized correlation function $g^{(2)}(\tau) = \xi_{fb}^2(\tau)$.

More delicate quantum feedback experiment can be realized in cavity-QED systems in recent years with the developments of the measurement and control techniques in the single-atom and single-photon level. An experiment in Ref. [399] shows that real-time quantum feedback can be used to prepare Fock states of a microwave field in a superconducting cavity. Different from the traditional approaches to prepare Fock state of the field by swapping energy between a periodically pumped qubit and the field initially in the vacuum state [400, 401] or by Quantum Nondemolition (QND) measurement imposed on the field initially in the coherent states, the quantum feedback method is more robust for counteracting decoherence and can deterministically prepare the desired Fock state. The experimental setup of Ref. [399] is shown in Fig. 23. The central component is a superconducting cavity C with damping time $T_c = 65$ ms cooled to 0.8 K. The cavity state is weakly measured by a QND measurement via an atomic beam transmitting through an atomic Ramsey interferometer (auxiliary cavities R_1 and R_2 resonant with the atom) controlled by source 1. The cavity C is with frequency of $\omega_c/2\pi = 51$ GHz and dispersively coupled to the atoms with atom-cavity detuning $\delta/2\pi = 245$ KHz, and finally measured by a field-ionization detector D with detection efficiency of 35%. This quantum continuous measurement can be described by the cavity-state mapping

$$\rho \rightarrow \tilde{\rho} = \frac{M_j \rho M_j^\dagger}{\text{tr}(\rho M_j^\dagger M_j)}, \quad j = e, g, \quad (5.8)$$

with two non-orthogonal Kraus operators

$$M_e = \cos \left[\frac{1}{2} \left(\phi_r + \phi_0 \left(\hat{N} + \frac{1}{2} \right) \right) \right], \quad M_g = \sin \left[\frac{1}{2} \left(\phi_r + \phi_0 \left(\hat{N} + \frac{1}{2} \right) \right) \right], \quad (5.9)$$

where the phase ϕ_r can be tuned by the Ramsey interferometer and $\hat{N} = a^\dagger a$ is the photon number operator. The measurement output is fed into an information processor (a CPU-based Adwin Pro-II system composed of fast signal

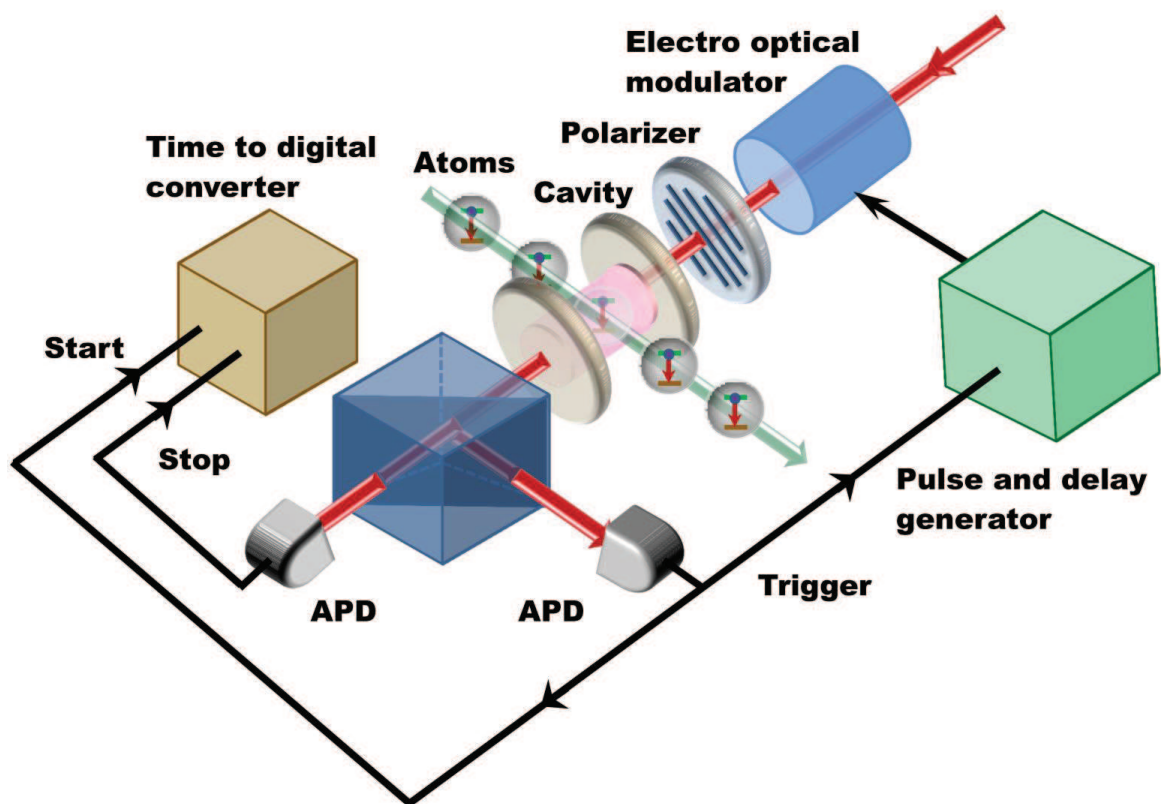


Figure 22: (Color online). Schematic diagram of the experimental setup in Ref. [215] to capture and release quantum state by feedback. Here, APD denotes an avalanche photodiode.

input-output and CPU capacity for feedback calculations) to estimate the system state $\tilde{\rho}$ which is further used to estimate the control parameter α by minimizing a proper distance $d(\rho_t, D(\alpha)\tilde{\rho}D(-\alpha))$ between the desired Fock state $\rho_t = |n_t\rangle\langle n_t|$ and the cavity state $D(\alpha)\tilde{\rho}D(-\alpha)$ under feedback control, where $D(\alpha) = \exp(\alpha a^\dagger - \alpha^* a)$ is the displacement operator of the cavity field. The optimization can be achieved by the Lyapunov-based state stabilization technique [402, 403] that is widely used in classical control. To reduce the data-processing time to decrease the feedback delay, a second-order approximation to expand $D(\alpha)$ is used. The estimated control parameter α is then fed back to control the amplitude and the phase of the driving field fed into the cavity C induced by source 2. The feedback delay in each round can be estimated to be 83 ns. It is shown in the experiment that the Fock states up to $n = 4$ can be very well stabilized by the feedback control approach and the convergence time for $n = 3$ is 50 ms which is 5 times shorter than that achieved by a traditional optimized trial-and-error project method by QND measurements.

A recent experiment by modified design in Ref. [404] from the same experimental group show that the feedback diagram can be realized in a simpler way to prepare the desired photon number state in the superconducting cavity C . A series of Rydberg atoms transmit through three cavities, i.e., R_1 , C , and R_2 , and finally measured by a field-ionization detector. The atom beam both works as quantum nondemolition sensor and single-photon emitter or absorber. The measurement output is fed into a ADwin Pro-II controller which controls the voltage V applied to the cavities C and the sources S_1 and S_2 driving the cavities R_1 and R_2 respectively. When the atom acts as a sensor to detect the cavity state in C , the voltage V is tuned to achieve a dispersive coupling between the cavity C and the atom. S_1 and S_2 send $\pi/2$ pulses and thus R_1 - R_2 combination is just a Ramsey interferometer. The whole system introduces a QND measurement of the photon number in cavity C . When the atom acts as an emitting actuator, S_1 sends a π pulse to excite the atom to the excited state in R_1 . The voltage V is set so that the atom interacts resonantly with C and thus the atom emits a photon into the cavity C . S_2 is switched off and thus does not change the state of the atom. When the atom acts as an absorber actuator, both S_1 and S_2 are switched off and the resonant interaction between the cavity C and the atom is controlled by the voltage V to let the atom absorb one photon from the cavity C . In this modified experiment, photon number state up to $n = 7$ are prepared by quantum feedback approach.

Quantum feedback control has also been used experimentally to manipulate the internal states of trapped particles [405, 406] or even many-body quantum states [272] in cavity-QED systems to protect and stabilize quantum superposition states against decoherence. For example, in Ref. [272], the authors introduce Bayes feedback control to stabilize two-atom joint states sharing a single excitation, which is hard to be prepared deterministically without feedback. Two Cs atoms are trapped inside a high finesse optical cavity, and the qubit state of each atom is encoded in the two long-lived hyperfine ground states. A probe laser transmits through the cavity and is on resonance with the cavity frequency. By optimizing the system parameters such as the cavity-atom detuning and the positions of atoms, the two-atom quantum states $\rho_{\alpha=0} = |\downarrow\downarrow\rangle\langle\downarrow\downarrow|$, $\rho_{\alpha=1} = 1/2(|\uparrow\downarrow\rangle\langle\uparrow\downarrow| + |\downarrow\uparrow\rangle\langle\downarrow\uparrow|)$, and $\rho_{\alpha=2} = |\uparrow\uparrow\rangle\langle\uparrow\uparrow|$ reduce the probe laser transmission by 0%, 30%, and 60%, and thus can be well distinguished with highest contrast. The cavity transmission is then measured by a single-photon detector. The output signal is fed into a Digital Signal Processor (DSP), i.e., a TMS6713 by Texas Instruments, to implement a real-time state estimation of the occupation probabilities and transition rates, which is further used to find the optimal intense pulses of repumping and depumping laser lights to minimize the Kolmogorov distance between the probability distribution under control and the target probability distribution. The repumping and depumping laser fields can control the state transition of each atom between the two qubit states and drive the two-atom state to approach the desired balanced mixed state $\rho_{\alpha=1}$. The feedback delay induced by the computation of the feedback algorithm is about $6 \mu\text{s}$ which is far smaller than the characteristic data-update time $\approx 1 \text{ ms}$ in the experiment. The time taken by the feedback iterations until the target state is reached is experimentally given by 1.12 ms. The final mean probability of the target state achieved in experiment is about 84% which is far larger than the highest passively achievable mean probability of the target state approximately estimated by 50%. Although the state estimation and feedback algorithms used in Ref. [272] are fully classical, we believe that the theory of Bayesian quantum feedback which encloses the estimates of the non-diagonal entries of the system density matrix is hopeful to give a better explanation of the experimental results.

Feedback control is also used to control the mechanical motions of electrode-trapped ions [246], electrode-trapped one-electron oscillators [247], laser-trapped nanoparticles [248], and optical-cavity [228, 229] and optical-lattice [249] trapped neutral atoms which are even harder to track compared with charged particles due to the weaker coupling strength between the detectors and particles. As shown in Fig. 24, in Ref. [228], ^{85}Rb atoms are trapped by a 775

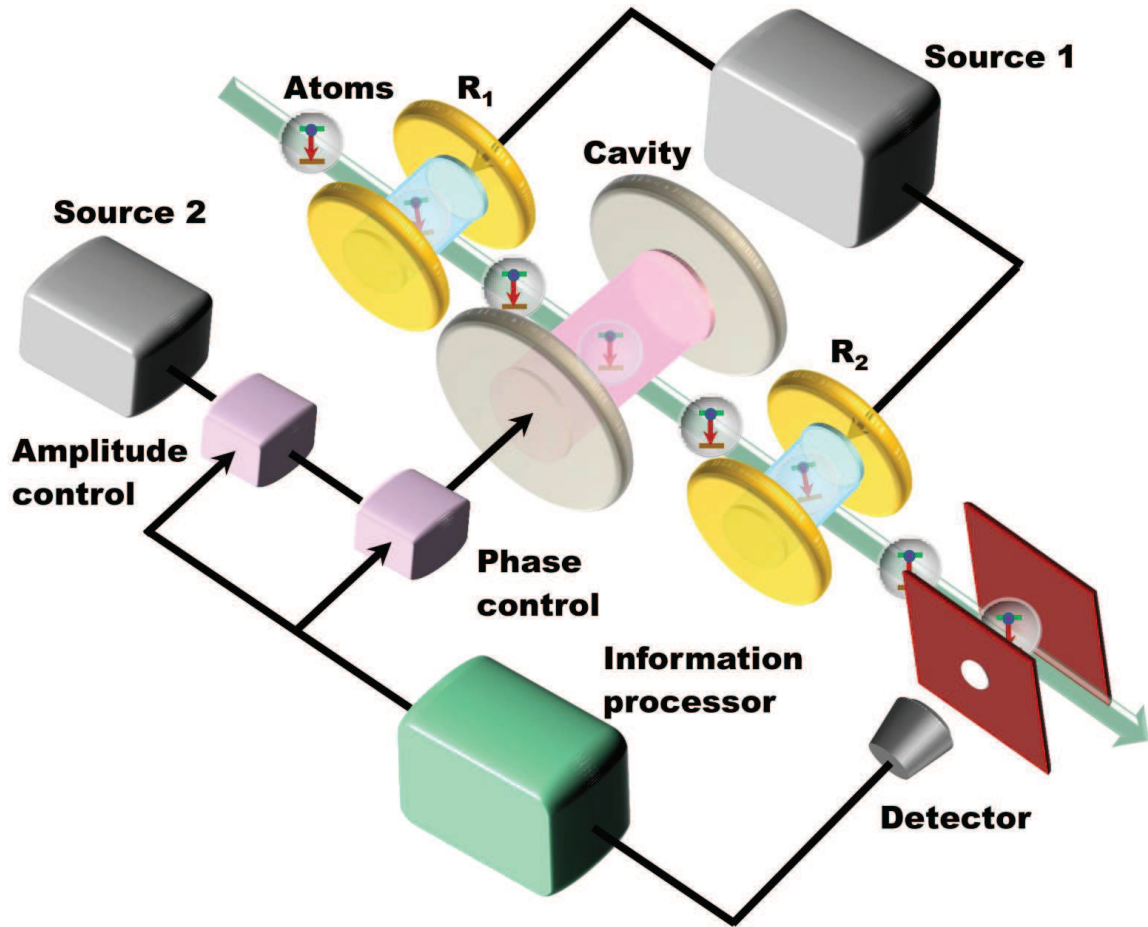


Figure 23: (Color online) Schematic diagram of the experimental set-up in Ref. [399]. The photon state of the cavity C is weakly measured by an atomic beam which is resonant with the two cavities R_1 and R_2 of an atomic Ramsey interferometer driven by source 1, dispersively coupled to the cavity C , and finally measured by a field-ionization detector. The measurement output is fed into the information processor to execute the state estimations and feedback calculations to obtain the control parameter α . This control parameter is further used to control the amplitude and phase of the field driving the cavity C implemented by the source 2.

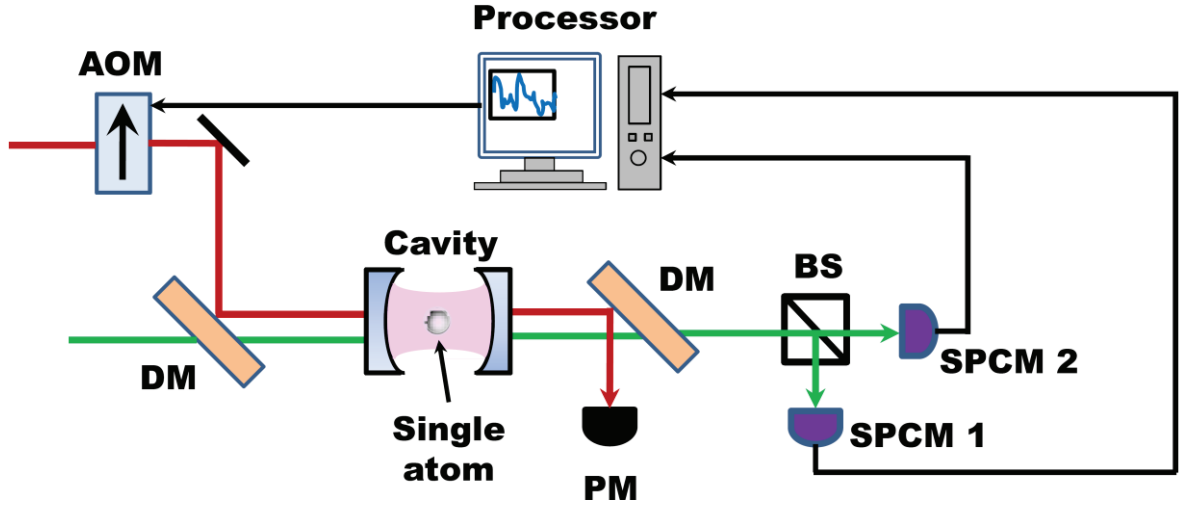


Figure 24: (Color online). Experimental setup in Ref. [228]. Both a blue-detuned dipole light, which acts as an actuator to trap the atom, and a weak probe light, used to detect the motion of the atom by light scattering, is fed into the cavity to interact with the ^{38}Rb atom in the cavity, and then superimposed with each other by a dichroic mirror (DM). The blue-detuned control light is then detected by a photomultiplier (PM), and the probe light is detected by two single-photon counting modules (SPCM 1 and SPCM 2). The output signals for the probe light are fed into a feedback processor to generate a control signal to switch the blue-detuned dipole light by an acousto-optical modulator (AOM). The control light pushes the atom towards the center of the cavity and thus reduces the atomic kinetic energy.

nm toroidal blue-detuned dipole light in a high-finesse cavity nearly resonant with the interior transitions of the ^{85}Rb atoms with atom-cavity coupling strength of $g_0/2\pi = 16$ MHz, atomic polarization damping rate of $\gamma/2\pi = 3$ MHz, and cavity damping rate of $\kappa/2\pi = 1.25$ MHz. A weak probe laser resonantly excites the mode of the cavity detuned by $2\pi \times 100$ kHz and then nearly resonant with the Stark-shifted atomic resonance by $2\pi \times 20$ MHz, which leads to the transmission of photons from 1 photon to 0.03 photons per microsecond. The photon flux of the probe light depends on the exact atomic position when the coupling strength is large and thus extracts the information of atomic motion. The information-bearing probe light is detected by two Single Photon Counting Modules (SPCM 1 and SPCM 2) and then fed into a feedback processor (ADwin-Pro II system). The feedback processor generates a bangbang control signal to switch the intensity of the blue-detuned torus light by an Acousto-Optical Modulator (AOM) between two extreme powers, i.e., 50 nW and 800 nW. The feedback delay which includes a decision-making time of $1.7 \mu\text{s}$ and a switching-process delay of $3 \mu\text{s}$ is much smaller than the atomic radial oscillation of $360 \mu\text{s}$. The exposure time is also used as a characteristic time for feedback which is tested from $10.2 \mu\text{s}$ to $85 \mu\text{s}$, for which longer exposure time leads to smoother switching but longer feedback delay time. The blue-detuned dipole light controlled by AOM is used to push the atom towards the center of the cavity, and then superimposed with the probe light by a Dichroic Mirror (DM) and detected by a Photomultiplier (PM). The feedback control can keep the atom two-times closer to the cavity axis compared with that without feedback and the average excursion is less than $4.5 \mu\text{m}$. It also increases the atomic average storage time to 24 ms, which is four times larger than that without feedback which is less than 6 ms, and a maximum trapping time exceeding 250 ms can be obtained.

Although there have been many experiments which show the cooling of the mechanical modes of various systems [230, 231, 235, 248, 407], most of these studies are in the classical regime. In Ref. [246], the authors introduce Markovian quantum feedback to cool the motion of a single trapped ion. As shown in Fig. 25, in this study, a single $^{138}\text{Ba}^+$ ion, which is driven by a laser near the atomic resonance, is trapped by miniature Paul trap electrodes and cooled to the Doppler limit. The light scattered by the ion and the light reflected from the mirror interfere with each other, and the interference light provides information of the instantaneous position of the ion. This information is contained in the photon counting signal and thus can be detected in the output spectrum. In experiment, the sideband at the frequency of 1 MHz with a width of 400 Hz is observed. The sideband spectrum information is continuously extracted, filtered, phase-shifted, and fed back to control the voltage on the trap electrode to introduce a linear damping

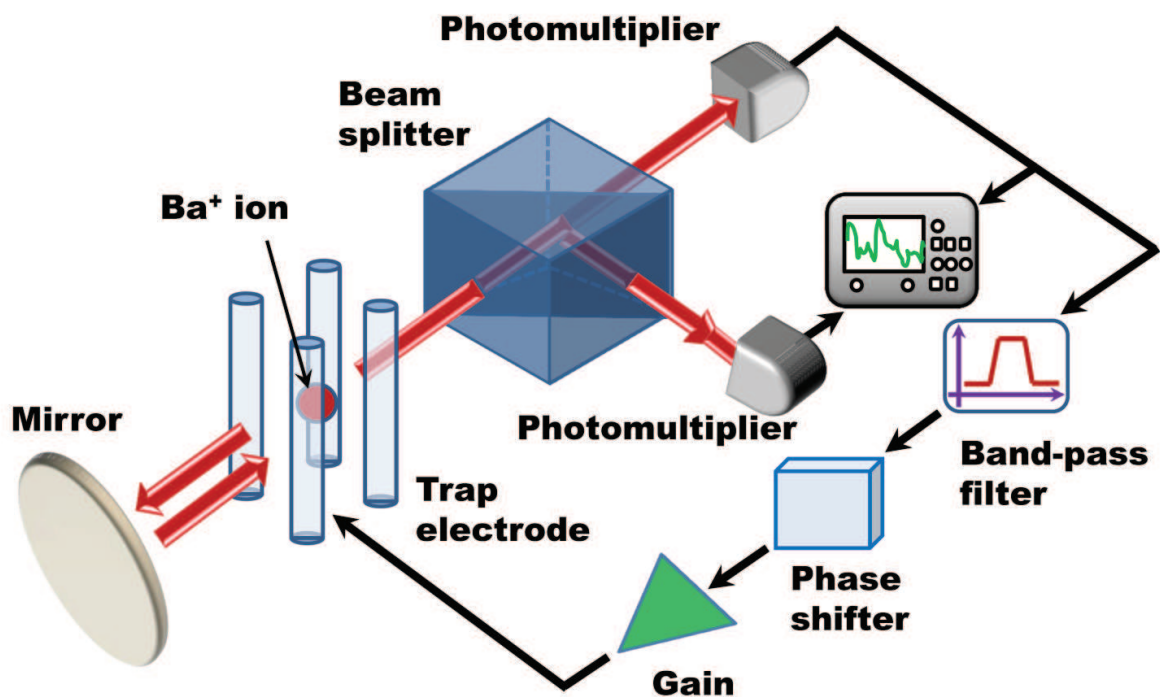


Figure 25: (Color online) Schematic diagram of the experimental setup in Ref. [246]. A $^{138}\text{Ba}^+$ ion is captured by a Paul trap and laser cooled to the Doppler limit. The light scattered by the ion and then reflected by a retro-reflecting mirror 25 cm away from the trap, interfere with each other, and the interference fringes with 73% contrast are detected by photomultipliers. The vibration mode of the ion leads to a sideband in the photomultiplier signal and then measured by a spectrum analyzer. The output sideband signal is then filtered, phase-shifted, and used to control the voltage on the trap electrodes to execute an active feedback cooling.

force proportional to the momentum of the ion to execute an active feedback cooling. The experiment is interpreted by the theory of Markovian quantum feedback presented in subsection 2.2, and the ion is cooled by more than 30% below the Doppler limit to yield a steady-state occupation number $N = 3$.

It should be pointed out that coherent feedback has also been introduced in cavity-QED system [371] quite recently to fulfill the optical “NOR” and “OR” gates by the four-wave mixing process in hot rubidium vapor for which the transition time of the logic gates exhibited is faster than the previous experiments demonstrated in rubidium vapor without feedback (see Fig. 26).

5.3. Superconducting circuits

Although quantum feedback control has been successfully experimentally demonstrated in optical systems more than ten years ago, it is just quite recently realized in solid-state systems (mostly in superconducting circuits). The first measurement-based quantum feedback experiment in solid-state system was implemented in 2012 by Siddiqi’s group and collaborators [205]. In this experiment, the authors introduce quantum continuous measurement and feedback to actively suppress the decay of Rabi oscillations of a superconducting charge qubit. The experimental setup is shown in Fig. 27. The controlled quantum system is a capacitively shunted Josephson junction which works as a superconducting qubit [408, 409] with a transition frequency of $\omega_q/2\pi = 5.4853$ GHz. This superconducting qubit is dispersively coupled to a three-dimensional microwave cavity with cavity resonant frequency of $\omega_c/2\pi = 7.2756$ GHz. The control and measurement pulses are fed into the cavity via the weakly-coupled input port and the measurement output leaves the cavity via the strongly-coupled port with decay rate of $\kappa/2\pi = 13.4$ MHz. The qubit-cavity dispersive coupling with strength of $\chi/2\pi = 0.687$ MHz leads to a state-dependent phase shift of the cavity mode, and thus

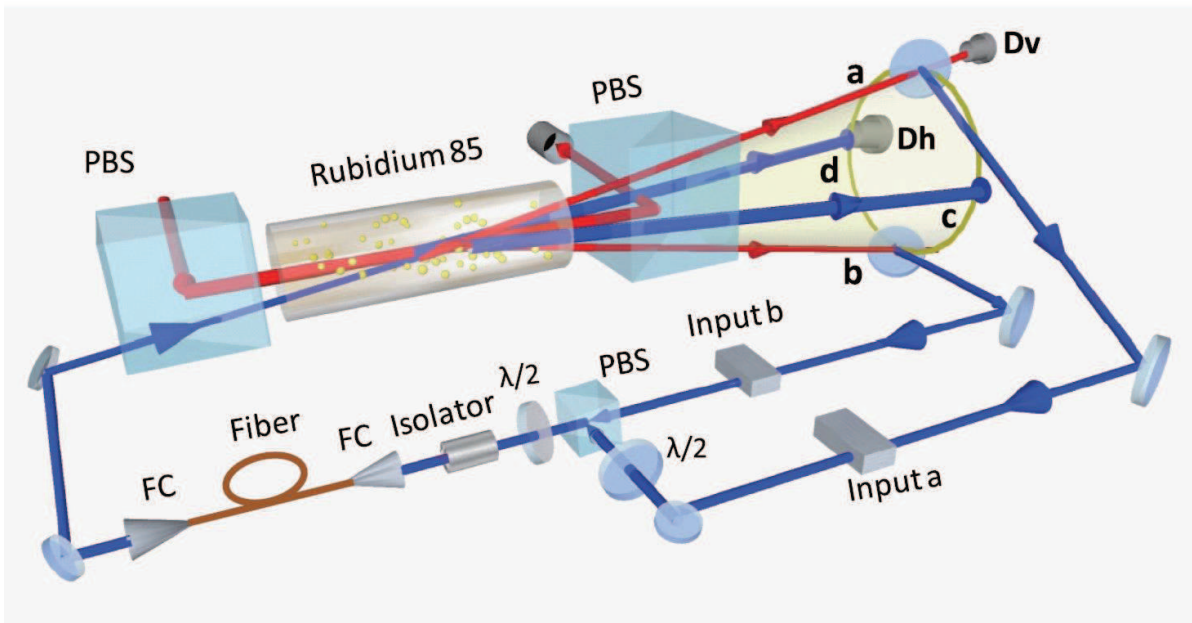


Figure 26: (Color online) Schematic diagram of the experimental setup [371] for achieving the optical logic “NOR” and “OR” gates by a Four-Wave Mixing (FWM) process in hot rubidium vapor via coherent feedback. The two inputs a and b are the spontaneous modes of the unseed FWM process used for encoding the feedback beams. Beams c and d denote the output beams of the FWM stimulated by feedback. The “NOR” gate and “OR” gate are fulfilled by feedback-suppressed state and feedback-boosted state, respectively. The feedback loop includes a polarized beam splitter (PBS), half-wave plates ($\lambda/2$), optical isolator, fiber, and fiber coupler (FC). Here, D_v and D_h are the optical detectors. The figure is from Ref. [371].

the information of the qubit state is contained in the quadratures of the cavity output field. The cavity mode is continuously excited at the frequency of $\omega_r/2\pi = 7.2749$ GHz ($\approx \omega_c - \chi$), i.e., readout drive in Fig. 27, to control the mean cavity photon occupation, \bar{n} , which additionally determines the measurement strength of the qubit state. The qubit is driven by the Rabi control pulse, i.e., the Rabi drive in Fig. 27, at the a.c. Stark-shifted frequency ($\omega_q - 2\chi\bar{n}$) which leads to a Rabi frequency of $\Omega_R/2\pi = 3$ MHz. At the output port of the cavity, the output quantum field transmits through two isolators to protect the qubit from the strong driving field imposed on the succeeding parametric amplifier. The output field is then fed into a parametric amplifier (paramp), i.e., a near-noiseless phase-sensitive quantum amplifier [410, 411], such that the amplified signal can be of the magnitude comparable with the classical circuitry. The output signal is further amplified by a High-Electron-Mobility Transistor (HEMT) amplifier, and then measured by a homodyne detection circuit. The best efficiency of the whole measurement process achieved in this experiment is $\eta = 0.40$. The feedback protocol used in the experiment is motivated by the classical phase-locked feedback design. As shown in Fig. 27, the output signal obtained from the homodyne detection is compared with a 3-MHz Rabi reference signal and low-pass-filtered to generate a signal proportional to the sine of the phase difference, θ_{err} , between the reference and the measurement output. This phase error signal is then fed back to modulate the amplitude of the Rabi drive, Ω_{fb} , by $\Omega_{\text{fb}}/\Omega_R = -F \sin(\theta_{\text{err}})$, where F is the dimensionless feedback gain. The feedback control method used here is just the Markovian quantum feedback which performs very well to stabilize the Rabi oscillations of the qubit. The efficiency of the feedback control is mainly limited by the signal attenuation and time delay in the feedback loop. There is a tradeoff between the feedback efficiency and the feedback loop bandwidth (the bandwidth of the feedback induced noises) by varying the measurement strength. With finite feedback bandwidth of 10 MHz and loop delay of 250 ns, an optimal measurement strength of $\Gamma_\phi/2\pi = 0.134$ MHz was found in experiment. The stabilization of non-equilibrium single-qubit states against decoherence induced by measurement-based feedback has also been demonstrated in superconducting circuits in other recent experiments [206]. Recent experiments also show that quantum feedback can be used to manipulate and stabilize two-qubit entanglement in circuit-QED systems [271, 376]. In Ref. [271], it is shown that quantum Bell state can be prepared with the fidelity of 88% by parity measurements. By introducing a feedback loop incorporating the parity measurements, the probabilistic entanglement generated can be transformed to deterministic one with the fidelity of 66%. Reference [376] shows that two-qubit entanglement can also be manipulated in superconducting circuits by autonomous feedback, which is believed to be essential tool for implementing quantum error correction.

Coherent feedback control is also experimentally realized in solid-state circuits quite recently [83] which can be seen as the experimental verification of the proposal in Ref. [84]. It is shown in Ref. [83] that two tunable Kerr circuits (TKCs) connecting coherently in the feedback loop may lead to bistable and astable phenomena for the microwave field in the superconducting circuit. This is the first coherent feedback experiment in solid-state systems and also the first experiment about nonlinear coherent feedback control. Compared with the measurement-based feedback system as shown in Ref. [205] which is fundamentally nonintergrable system requiring signal transfer between low-temperature quantum regime and room-temperature classical regime, the whole feedback loop in Ref. [83] resides in the full-quantum environment (< 50 mK). The experimental setup in Ref. [83] is shown in Fig. 28. The system considered is just a two-port input-output circuit with two input fields $b_{\text{in},0}$, $b_{\text{in},1}$ and two output fields $b_{\text{out},0}$, $b_{\text{out},1}$. The central components of the coherent feedback loop are two tunable Kerr circuits, TKC_0 and TKC_1 . Each TKC is composed of a quarter-wave transmission line resonator generated by a coplanar waveguide. In the center of the coplanar waveguide, a series array of 40 Josephson Junction Superconducting Quantum Interference Devices (JJ-SQUIDS) interrupt the waveguide and lead to nonlinear Kerr effects for the transmission line resonator [412]. One end of the transmission line resonator is capacitively coupled to an external circuit working as the signal input/output port for TKC. The two TKCs are connected by a 4-8 GHz commercial quadrature hybrid acting as a 50:50 microwave beam splitter. The two directional couplers are just two microwave isolators which separate signals reflected from TKCs and the input fields. The nonlinear coherent feedback network in Fig. 28 can be used to demonstrate nonlinear optical phenomena that cannot be observed without such a feedback connection. For example, as shown in Ref. [83], if we drive the two TKCs, with central frequencies both equal to $\omega_0/2\pi = 6.408$ GHz, by probe fields with frequency of $\omega_p/2\pi = 6.39$ GHz, the output fields of the coherent feedback network exhibit bistable phenomena. However, if the two TKCs in isolation are driven at the same detuning, both TKCs would be monostable. The authors also discussed about the possible applications of their nonlinear coherent feedback control circuit as a binary memory element called set-reset latch that can feed out power according to prior inputs. Since the TKCs and the feedback control circuits typically contain in average about 1000 photons, the experimental results fit very well with the mean-field model under

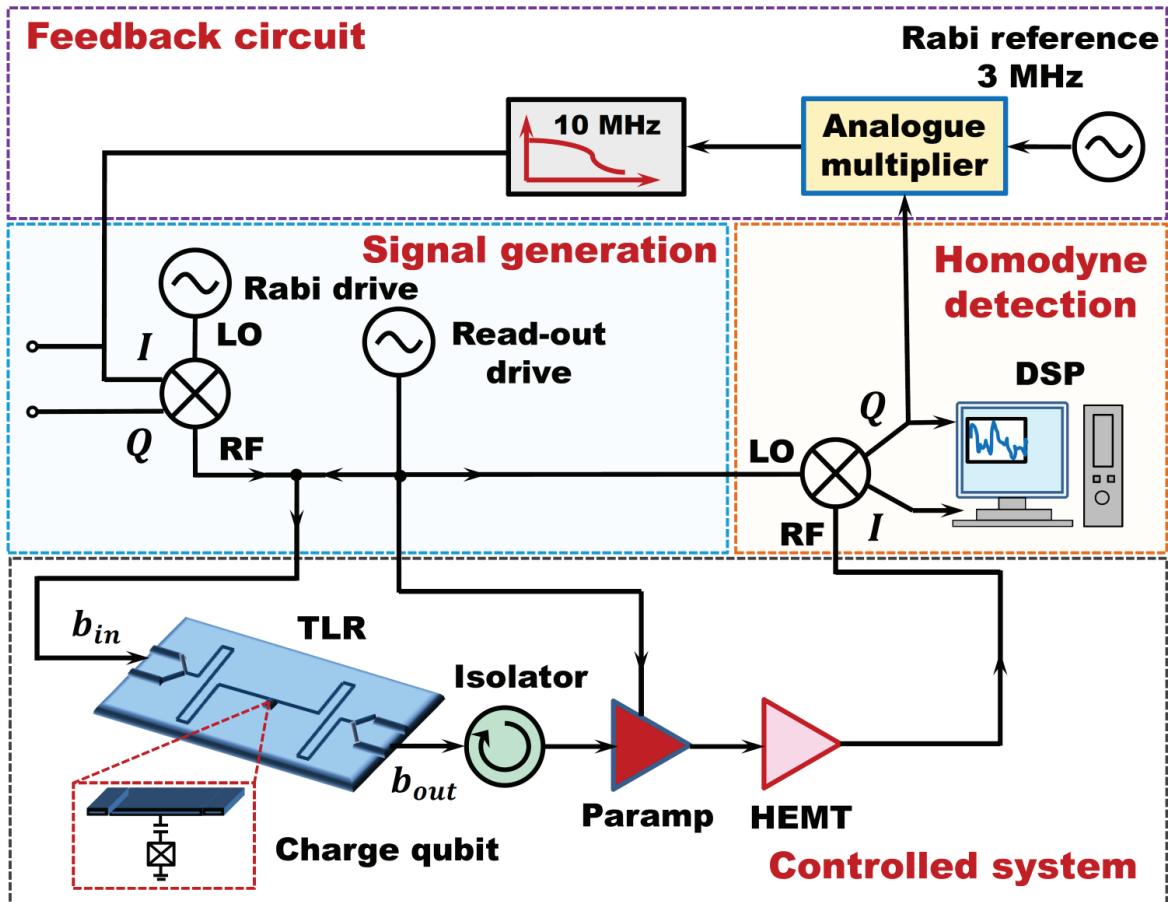


Figure 27: (Color online) Schematic diagram of the experimental setup in Ref. [205]. The Rabi drive at the ac stark-shifted qubit frequency and the read-out drive at frequency 7.2749 GHz are both fed into the weakly-coupled input port of a three-dimensional microwave cavity, which is dispersively coupled to a capacitively-shunted Josephson junction working as a superconducting qubit. The output signals leave from the strongly-coupled port of cavity and are then transmitted through two isolators. Afterwards, the output signals are amplified by a parametric amplifier (paramp) and a high-electron-mobility transistor (HEMT) amplifier, and then measured by a homodyne detection setup. The amplified quadrature Q is then sent to the feedback circuit to be compared to the 3 MHz Rabi reference signal and filtered by a 10 MHz low-pass-filter. The output signal is then fed back to correct the Rabi frequency imposed on the qubit by the Rabi drive. LO and RF represent the local oscillator and radio frequency. I and Q are the in-phase component and quadrature component, respectively.

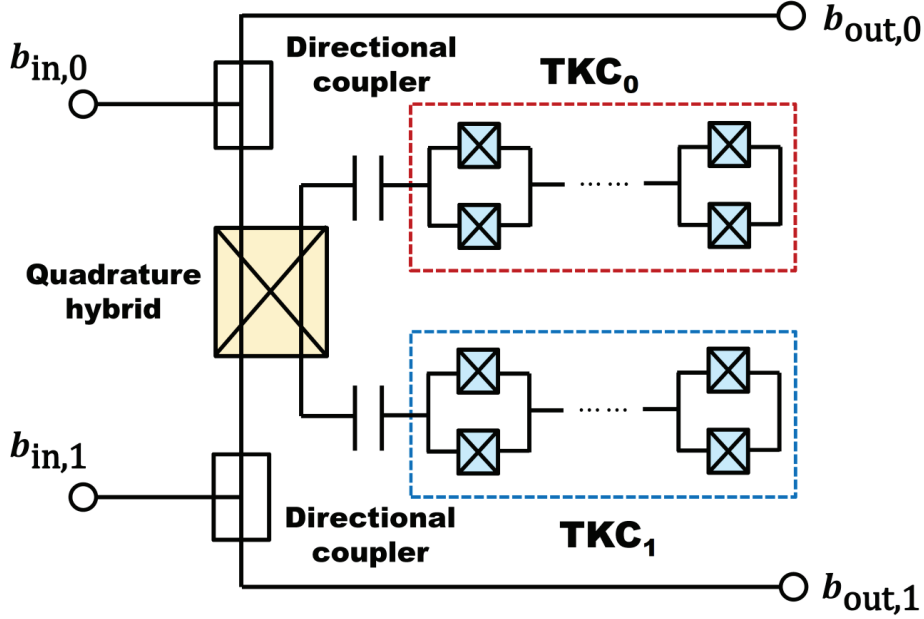


Figure 28: (Color online) Schematic diagram of the two-port coherent feedback control circuit used in Ref. [83] with input fields $b_{in,0}$, $b_{in,1}$ and output fields $b_{out,0}$, $b_{out,1}$. The two flux-biased tunable Kerr circuits (TKC₀, TKC₁) are connected in a feedback configuration. Each TKC is composed of a quarter-wave transmission line resonator interrupted by a series array of 40 Josephson junction SQUIDs, and one end of the transmission line resonator is capacitively coupled to the quadrature hybrid. The two couplers are introduced to separate the reflected fields from the TKCs and input fields. The entire system is housed in a dilution refrigerator (< 50 mK).

semiclassical approximation. The pure quantum effects such as quantum fluctuations and quantum optical phenomena such as sub-Poisson statistics and photon antibunching effects which violate the Cauchy-Schwartz inequality for the classical lights [85, 86] are expected to be observed in the future experiments.

5.4. Optomechanics and electromechanics

Feedback control has also been widely applied in nanomechanical systems especially those lasing-induced cooling systems. There are mainly two different feedback cooling approaches, i.e., passive [230–232, 378] and active feedback cooling [233–235].

Passive feedback cooling methods, which are also called self-cooling approaches presented in subsection 4.2, are introduced by the feedback backaction effects induced by the exchange of excitations between the optical modes and the mechanical modes. There are mainly two different self-cooling mechanisms, either by photothermal pressure [378] induced by the absorption of cavity photons by the mechanical resonators or the radiation pressure [230, 231] proportional to the intracavity intensity. A typical self-cooling setup is shown in Fig. 29 (see Ref. [230]). As shown in Fig. 29, the central component of the system is a single-ended Fabry-Perot cavity of which the back mirror coated on the surface of a silicon doubly-clamped beam ($1 \text{ mm} \times 1 \text{ mm} \times 60 \mu\text{m}$). The vibration mode of the beam with characteristic frequency of $\Omega_m/2\pi = 814 \text{ kHz}$, effective mass $m_{\text{eff}} = 190 \mu\text{g}$, spring constant $k = 5 \times 10^6 \text{ Nm}^{-1}$, and mechanical quality factor $Q = 10000$ is coupled to the Fabry-Perot cavity with optical finesse $\mathcal{F} = 30,000$, bandwidth $\Omega_c/2\pi = 1.05 \text{ MHz}$, and length $L = 2.4 \text{ mm}$. The whole optomechanical system is put into a vacuum room-temperature chamber with residual pressure below 10^{-2} mbar. The amplitude of the mechanical motion is of 10^{-13} m . The resonator cavity is driven by a 1064 nm Nd:YAG laser stabilized by a voltage-driven optical attenuator with feedback bandwidth of 1 kHz. The laser is locked by a triangular cavity with bandwidth of 200 kHz and optical finesse of 10000, which is introduced to control the shape of the beam and reduce the noises. The resonator cavity is locked by the Pound-Drever-Hall scheme and phase-modulated by an electro-optic modulator. The low-frequency demodulated signal is used to lock the laser at a negative detuning for cooling or a positive detuning for heating, and the

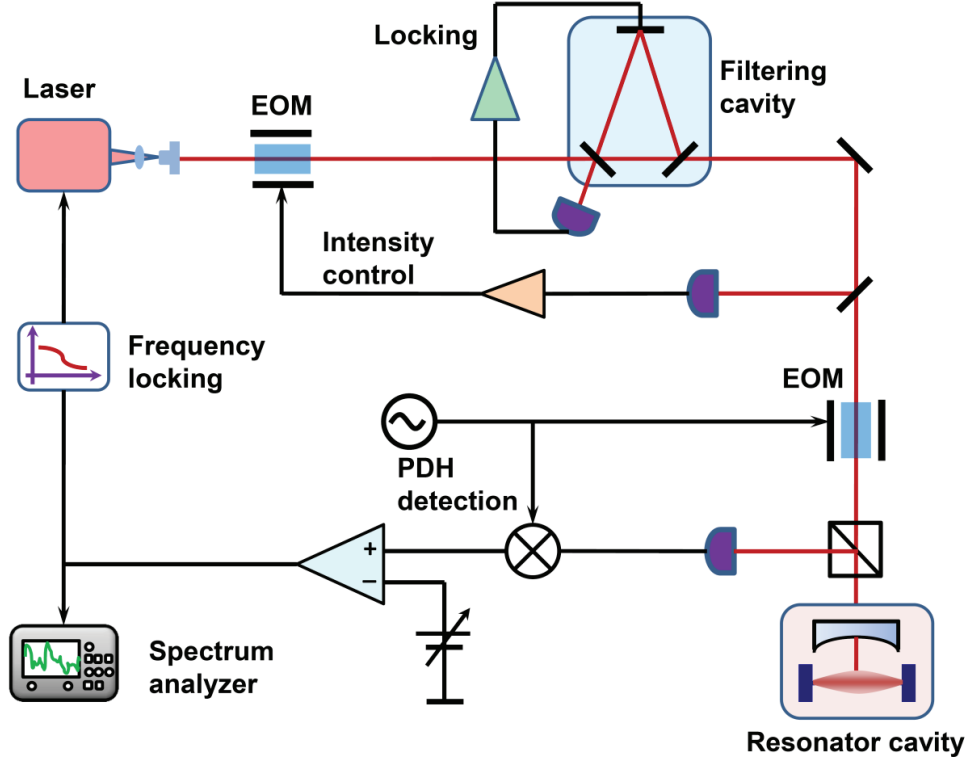


Figure 29: (Color online) Schematic diagram of the experimental setup of self-cooling used in Ref. [230]. The optomechanical resonator cavity is driven by a 1064 nm Nd:YAG laser and then intensity-stabilized by an electro-optic modulator and a triangle filtering cavity. The vibration mode of the resonator cavity is detected by a Pound-Drever-Hall scheme and phase modulated by an Electro-Optic Modulator (EOM). The low-frequency demodulated signal is used to lock the laser at a negative detuning for cooling and the high-frequency component is analyzed by a spectrum analyzer.

high-frequency component is analyzed by a spectrum analyzer. The whole system is with a displacement sensitivity of $4 \times 10^{-19} \text{ m}/\sqrt{\text{Hz}}$ in the MHz range. The mechanical resonator can be cooled from the room temperature 300 K to an effective temperature 10 K.

Different from the passive feedback cooling approaches, the motion of the mechanical resonator is controlled by an external feedback loop in active feedback cooling approaches. A typical active feedback cooling setup is shown in Fig. 30 (see Ref. [235]). As shown in Fig. 30, one end of the resonator cavity is formed by a moving mirror attached to an atomic force microscope cantilever ($450 \times 50 \times 2 \mu\text{m}$) with mechanical frequency of 12.5 kHz, effective mass of $(2.4 \pm 0.2) \times 10^{-11} \text{ kg}$, and mechanical quality factor of 137000. The spring constant of the cantilever is $0.15 \pm 0.01 \text{ Nm}^{-1}$ which corresponds to the thermal amplitude of the cantilever without feedback as $(1.2 \pm 0.1) \times 10^{-10} \text{ m}$. The cantilever is driven by a 780 nm probe laser which is locked to the optical cavity with optical finesse of 2100 by an external integrating circuit using the signal from a photo-multiplier tube. The output signal of the photo-multiplier tube is also fed into a 1.25 kHz bandpass filter at 12.5 kHz. The time derivative of the output signal generated by passing through a derivative circuit is proportional to the velocity of the cantilever tip and used to modulate the amplitude of another 980 nm tunable diode laser. The output of the 980 nm diode laser is fed back and injected into the optical cavity again to provide a radiation pressure on the cantilever to counteract the motion of the mirror and thus effectively cool the mechanical mode actively from the room temperature 300 K to an effective temperature 135 mK.

The active feedback has also been applied in on-chip optomechanical systems [413, 414] for cooling and sensitive measurements. In a recent experiment [413] as shown in Fig. 31, a doubly clamped Si_3N_4 nanomechanical beam with mechanical resonance frequency $\Omega_M/2\pi = 2.88 \text{ MHz}$, effective mass $m_{\text{eff}} = 9 \times 10^{-15} \text{ kg}$, and mechanical

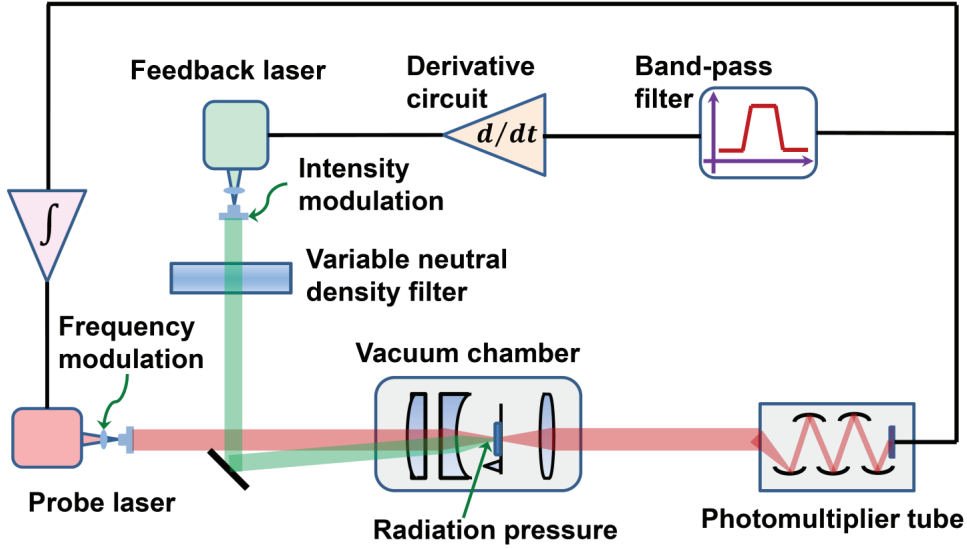


Figure 30: (Color online) Schematic diagram of the experimental setup for active feedback cooling in Ref. [230]. The 780 nm probe laser is frequency-locked to the optical cavity by the integrated signal emanating from the photo-multiplier tube. The output signal of the photo-multiplier is also sent through a bandpass filter, and then the time derivative of the output signal is used to modulate the amplitude of the 980 nm feedback laser, which is attenuated with a variable neutral density filter. The feedback laser provides a counteracting radiation pressure, which effectively cools the mechanical mode of the cantilever.

quality factor $Q_M = 4.8 \times 10^5$ is coupled via the near-field to a silica microdisk with damping rate $\gamma/2\pi = 3$ GHz and optical quality factor $Q = 65000$, which rest on silicon pedestals. The optomechanical coupling strength of the system is $G/2\pi = d\omega/dx = 2.9$ MHz nm⁻¹. The hybrid nanomechanical transducer system is then coupled to a tapered fibre, and the whole system is put into a vacuum chamber under a pressure of less than 1×10^{-4} mbar. A laser at the telecom wavelength of 1550 nm and a power of $400 \mu\text{W}$ is fed into the microdisk by the taper to observe the out-of plane mechanical mode of the beam and then fed back to induce radiation pressure by amplitude-modulating a second laser beam via dissipative feedback. Different from the previous active feedback approach limited to particular mechanical mode, the method used in Ref. [407] is based on the parametric-feedback demodulation-modulation technique, which enables control of any mechanical mode up to high frequencies. The dissipative feedback leads to an effective increasing of the mechanical damping rate for 57 times and thus cool the beam to 0.7 K. A third probe laser is then fed into the taper to detect an incoherent force with force spectral density of $15 \text{ aN Hz}^{-1/2}$. Although it is still arguable whether the linear dissipative feedback helps to improve the resolution of incoherent force detection [413], such an experiment shows that it is possible to introduce efficiently quantum feedback in on-chip optomechanical systems and a recent experiment reproduces the results for feedback-enhanced force sensing by straightforward filtering [414].

Coherent quantum feedback has also been used to feature an electromechanical device in superconducting circuits to coherently introduce continuous microwave signals to control mechanical oscillators in cryogenic environment [361]. Compared with the optomechanical systems, the electromechanical feedback control systems balance very well between the efficient control and the efficient readout of the mechanical modes, and provide tunable and faster control compared with the mechanical response time. As shown in Ref. [361], the microwave decay rates for superconducting control circuits can be modulated at a rate 10^4 times greater than the mechanical response rate. The controlled component in this feedback control system is an electromechanical circuit which is built from an over-coupled lumped-element resonator with center frequency of 4.672 GHz, coupling linewidth of $\kappa_c/2\pi = 2.7$ MHz, and internal loss rate of $\kappa_l/2\pi = 0.1$ MHz, and a mechanical membrane oscillator with an effective mass of 10 ng, center frequency of $\Omega_M/2\pi = 713.6$ kHz, and intrinsic linewidth of $\gamma_M/2\pi = 0.81$ Hz. The controller is a Josephson parametric amplifier composed of a 20-dB directional coupler and a single-port tunable Kerr circuit with coupling linewidth of $\gamma/2\pi = 50$ MHz and internal loss rate of $\gamma_l/2\pi = 5$ MHz. Such a feedback circuit is hopeful to generate

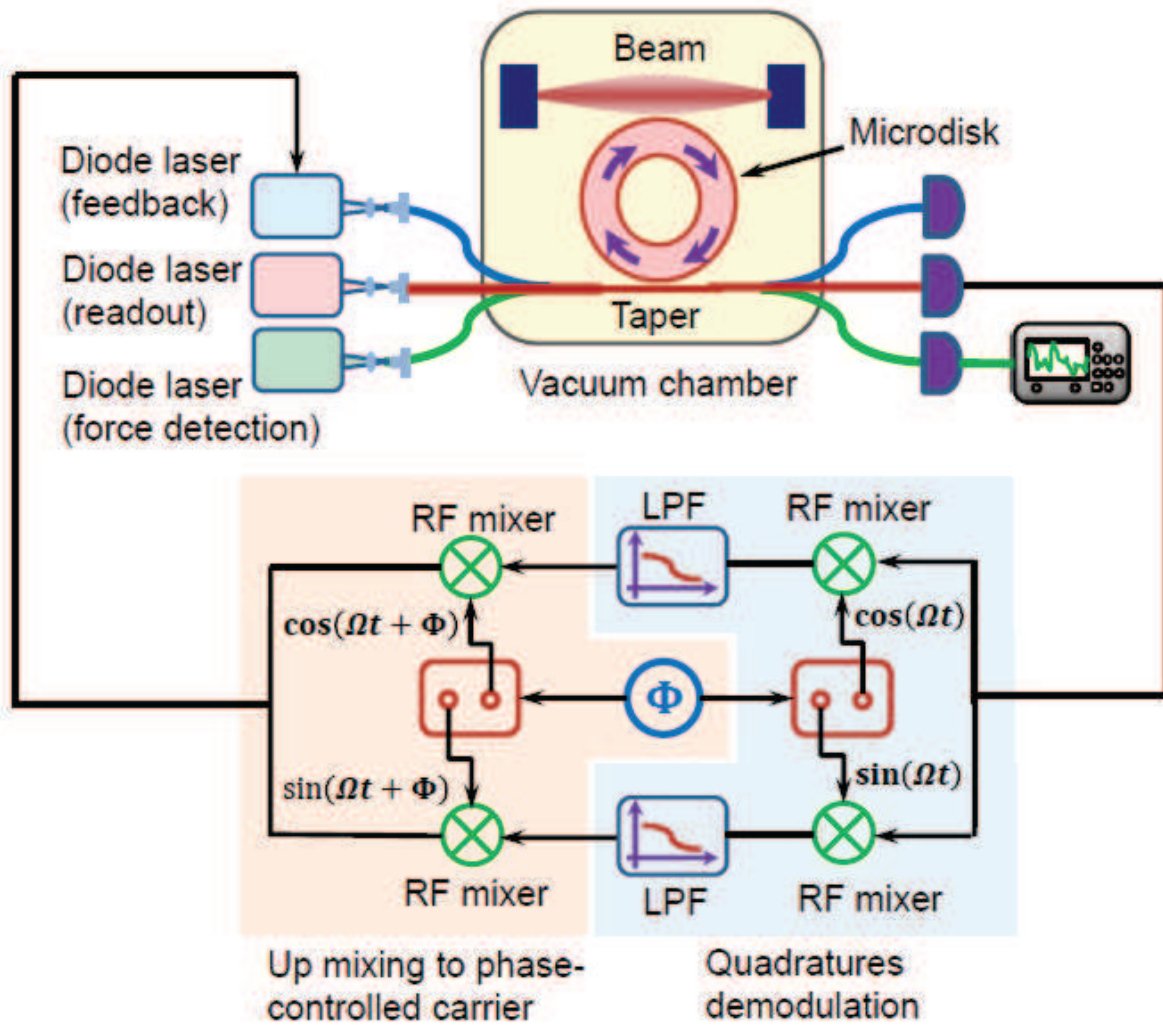


Figure 31: (Color online) Schematic diagram of the experimental setup of the on-chip optomechanical feedback system in Ref. [407]. A doubly-clamped nano-beam is coupled to a silica microdisk, which is then coupled to a tapered fiber. A readout laser is fed into the taper to observe the mechanical mode of the beam and fed back to modulate the radiation pressure of the beam by a second laser beam. The external feedback circuit realize a demodulation-modulation control, which enables control of any mechanical mode. A third probe laser is then introduced to an incoherent force.

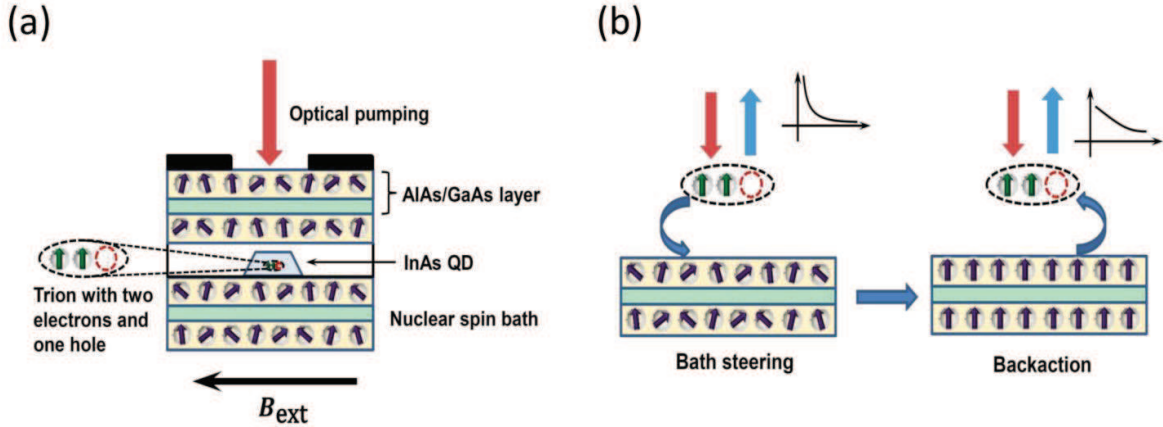


Figure 32: (Color online) Illustration of the experimental electron-nuclear spin feedback in optical-pumping single quantum dot systems (see Ref. [246]). The self-assembled InAs quantum dots are embedded in the planar GaAs microcavity with several AlAs/GaAs $\lambda/4$ layers as the bottom and top mirrors. The pump field flips the electron spin state, which then suppresses the nuclear fluctuations. The backaction from the nuclear spin bath protects the coherence of the electron spin by the hyperfine interaction.

scalable on-chip mechanical oscillator networks.

5.5. Quantum dots

In quantum dot systems, passive feedback control strategies, i.e., self-feedback mechanism shown in subsection 4.2, have been used to control the polarized nuclear spin baths of electron spins in optical pumping quantum dot ensembles [379, 380] or single quantum dots [381–384] via the electron-nuclear spin feedback mechanism. As an example, figure 32 shows the schematic diagram of the experiment in Ref. [383]. The sample with $2 \times 10^9 \text{ cm}^{-2}$ self-assembled InAs Quantum Dots (QDs) is grown by molecular beam epitaxy on a $4 \times 10^9 \text{ cm}^{-2}$ δ -doping layer of Si donor, and a single charged quantum dot is isolated for experiments. The QD is put at the center of a GaAs microcavity with several AlAs/GaAs $\lambda/4$ layers at the bottom and on the top as the reflecting mirrors. The quality factor of the GaAs microcavity is $Q = 200$. A QD electron, with two spin states split by a 4T external magnetic field B_{ext} and a Larmor frequency of 25.3 GHz, is optically coupled to a trion composed of three charged quasiparticles, i.e., two electrons and one hole. The external optical pumping flips the electron spin by the stimulated Raman transition process and the output light can be used to read out the spin states [415, 416]. During the feedback process, the pump field first flips the electron spin states, which then suppresses the nuclear fluctuations by the dynamic nuclear spin polarization process. After that, the backaction effects from the nuclear spin bath protect the resonance and coherence of the electron spin by the hyperfine interactions. The pulse sequence and the electron-spin dynamics are of the order of 143 ns. The nuclear dynamics is of millisecond time scale, and the measurement is on the order of several seconds which is long enough for the nuclear bath to reach quasiequilibrium. There is a competition between trion emission and nuclear spin diffusion.

Similar quantum self-feedback protocols have also been used to suppress decoherence of the electron spins induced by the background nuclear spin bath in microwave-driven double quantum dot systems [385–388]. Figure 33 shows the schematic diagram of the experiment in Ref. [387]. The double quantum dot which works as the qubit is generated by locally depleting the two-dimensional electron gas with electrostatic gates [417–420], and the qubit states are the linear combinations of the singlet and triplet of the double quantum dot. The qubit states are splitted by an external magnetic field $B_{\text{ext}} = 0.7 \text{ T}$ parallel to the two-dimensional electron gas, and the interdot tunnel coupling is controlled by an external gate with coupling strength $t_c = 20 \mu\text{eV}$. The nuclear polarization induces a hyperfine field for the electron spin, which can be detected by the standard spin-to-charge conversion technique and a quantum point contact to read out the charge signal. The measurement time is about 39 ms. Additionally, a software-based proportional-integral feedback is introduced to control the energy difference of the electron spin states by tuning the voltages V_L and V_R on the left and right gates. The time duration of a single feedback pumping pulse is 250 ns. The

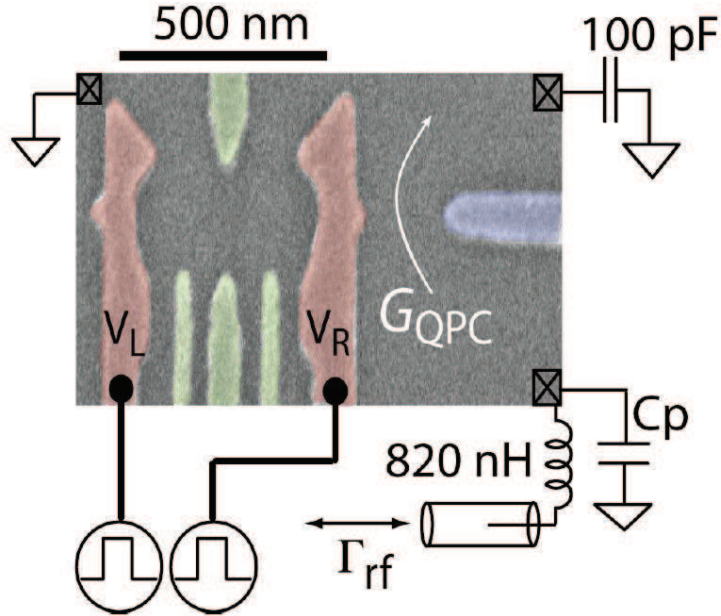


Figure 33: (Color online) Electron-nuclear spin feedback in a microwave-driven double quantum dot system [385]. The double quantum dot is obtained by depleting a two-dimensional electron gas with electrostatic gates. The electron spins couple to the background nuclear spins by hyperfine interaction. The hyperfine field gradient is detected by spin-charge conversion and charge measurement by a quantum point contact. The control voltage pulses V_L and V_R are applied to the gates to control the energy difference of electron spin states. This figure is from Ref. [385].

feedback control narrows the distribution of the nuclear-spin-induced hyperfine field acting on the electron spin and thus extends T_2 of the electron spin from 14 ns to 94 ns.

6. Summary and Outlook

We have seen in this review that continuous-time feedback can be implemented with or without measurements, and in the latter case can be implemented either with direct Hamiltonian coupling between the system and controller, or with couplings mediated by irreversible one-way quantum fields. We have also seen that the range of applications of feedback in quantum systems is rather broad, and further applications are yet to be discovered.

Measurement-based feedback control of quantum systems was first demonstrated in quantum optics, and for some time there was no other field in which this kind of feedback could be realized. It is only very recently, in 2012, that experimental technology has allowed measurement-based feedback to be achieved in superconducting circuits [205, 206]. This was possible because of recent breakthroughs in quantum-limited amplifiers [421–423]. We expect this development to open the door to many more implementations of measurement-based feedback in both electrical and electro-mechanical systems.

The situation regarding coherent feedback control is a little different. Experiments implementing coherent feedback had been realized for some time — for example those involving the laser cooling of atoms and ions — before the theoretical notion of coherent feedback was articulated. This notion provides a new way to think about interacting quantum systems, especially those coupled via irreversible fields. As pointed out in Ref. [83], coherent feedback provides not only a tool for controlling quantum systems, but also for changing the dynamics of a system and thus engineering new dynamics.

While measurement-based feedback control has been studied theoretically for a little over 20 years, coherent feedback has been much less studied, and there are still many basic questions that remain, particularly to do with the relationship between the various kinds of feedback. A basic question regarding any kind of control process is just how well it can perform, given a set of limitations on the physical control resources, such as the measurement

strength, coupling constant(s), and the speed and nature of the available control Hamiltonian. Since the dynamics of most measured quantum systems is nonlinear, and since the question of the limits to control is essentially one about optimality of control protocols, it may not be possible to obtain exact answers, or even numerical answers to these questions for measurement-based feedback. The connection between measurement-based feedback and coherent feedback however might provide a new way to analyze such questions.

There is one question regarding the limits to coherent feedback control that has been recently answered, at least with considerable confidence, and that is the limit to the fidelity of state-preparation given a bound on the rate of the coupling between the system and auxiliary components [424]. This was only solved, however, in the regime of good control, where the coupling is fast compared to the noise in the system, and in the regime of weak coupling in which the coupling rate is small compared to the energy scale of the system (the gaps between the energy levels of the system). The reason for the weak-coupling restriction is that without it, the master equation that describes the noise, even for Markovian weak-damping, is no longer independent of the control Hamiltonian. The reason that the noise depends on the control Hamiltonian for strong coupling is that in this case the energy levels of the system are altered by the coupling, and the noise that a system experiences usually depends on the energy levels of the system. As an example, thermal noise depends on a system's energy levels because the thermal steady-state depends on these levels. Since the control Hamiltonian is usually time-dependent, strong control Hamiltonians imply that the master equation will be time-dependent. Because of this, up until very recently, theoretical treatments of quantum control were restricted to the regime of weak coupling/weak control. Modelling strongly-controlled systems is an important challenge in quantum control, either by using methods for exact simulation of open-system dynamics (see e.g. [425–428]) or by obtaining approximate master equations that correctly model noise for time-dependent systems [429].

A key question regarding the relationship between various kinds of feedback is whether one kind is superior to the others for certain applications, or under certain kinds of constraints. Some results along these lines have already been obtained [79, 85–88]. It appears that under a constraint on the speed (equivalently the norm) of the interaction Hamiltonian between the system and controller, coherent feedback is fundamentally more powerful than measurement-based feedback, because it allows a larger class of joint evolutions [79]. It is not known whether the same is true under a bound on the measurement strength, equivalent to a bound on the input-output rate to a field or a damping rate into a Markovian bath. What is fairly clear is that a constraint on an irreversible Markovian damping rate is not equivalent to a constraint on the norm of an interaction Hamiltonian. This further suggests that while continuous-time measurement-based feedback can be compared directly with field-mediated coherent feedback, this may not be possible with coherent feedback implemented via direct coupling. Nevertheless the relationship between various forms of feedback raises questions that are both fundamental and relevant to potential applications.

Systems driven by white noise obey Markovian master equations, meaning that the time-derivative of the density matrix depends only on the density matrix at the current time. One way in which analyses of feedback control are being extended is to include systems coupled to baths that induce non-Markovian evolution, or feedback implemented via fields with a finite or tailored bandwidth. It turns out that the standard input-output formalism that we introduced in Section 3.2.1, and which is used to treat field-mediated feedback networks can be extended without difficulty to couplings with arbitrary bandwidths [348, 349]. Interestingly, with this extension the resulting formalism can handle strong damping and coupling, something that the standard formalism cannot. For nonlinear networks, the input-output equations must be converted to master equations to be solved, and these require considerable numerical resources. For linear systems, the input-output formalism provides an efficient means of solution, and thus appears to be a powerful method for analyzing non-Markovian feedback for linear systems. It can also be used to describe feedback in which there is a time-delay in the feedback control process. With the implementation of feedback in superconducting circuits, and beyond that to spins in, e.g., nitrogen-vacancy centers in diamond or quantum dots, the analysis of non-Markovian evolution will become increasingly important.

When feedback was introduced into quantum theory in the late 80's and early 90's, the number of physical systems in which feedback could be implemented were extremely limited, and such experiments were very difficult, especially for measurement-based feedback. With recent breakthroughs in the construction and measurement of mesoscopic circuits [430], the number of experimental applications for feedback control has greatly increased. We anticipate that the field of quantum feedback control will expand considerably due to these developments, and feedback will be realized in an increasing range of mesoscopic systems, including, e.g., superconducting circuits, quantum dots, and silicon-based on-chip optical devices [431–434].

Acknowledgements

We would like to thank Prof. T. J. Tarn and Dr. W. Cui for helpful discussions and Prof. G. Y. Xiang for providing related materials. J. Zhang and R. B. Wu are supported by the National Natural Science Foundation of China under Grant Nos. 61174084, 61134008, 60904034, and Y.-X. Liu is supported by this foundation under Grant Nos. 10975080, 61025022, 60836010. Y.-X. Liu and J. Zhang are supported by the National Basic Research Program of China (973 Program) under Grant No. 2014CB921401, the Tsinghua University Initiative Scientific Research Program, and the Tsinghua National Laboratory for Information Science and Technology (TNList) Cross-discipline Foundation. K. Jacobs is partially supported by the US National Science Foundation projects PHY-1005571 and PHY-1212413, and by the Army Research Office MURI project grant W911NF-11-1-0268. FN is partially supported by the RIKEN iTHES Project, MURI Center for Dynamic Magneto-Optics, and a Grant-in-Aid for Scientific Research (S).

References

- [1] D. D'Alessandro, *Introduction to Quantum Control and Dynamics*, Chapman and Hall, Boca Raton, LA, 2007.
- [2] H. Mabuchi, N. Khanuja, Principles and applications of control in quantum systems, *Int. J. Robust Nonlinear Control* 15 (2005) 647-667.
- [3] P. Rouchon, Quantum systems and control, *Arima* 9 (2008) 325-357.
- [4] C. Brif, R. Chakrabarti, H. Rabitz, Control of quantum phenomena: past, present and futures, *New J. Phys.* 12 (2010) 075008.
- [5] D. Y. Dong, I. R. Petersen, Quantum control theory and applications: a survey, *IET Control Theory and Applications* 4 (2010) 2651-2671.
- [6] C. Altafini, F. Ticozzi, Modeling and control of quantum systems: an introduction, *IEEE Trans. Automat. Contr.* 57 (2012) 1898-1917.
- [7] J. Bechhoefer, Feedback for physicists: A tutorial essay on control, *Rev. Mod. Phys.* 77 (2005) 783-836.
- [8] G. Huang, T. J. Tarn, J. W. Clark, On the controllability of quantum-mechanical systems, *J. Math. Phys.* 24 (1983) 2608-2618.
- [9] J. W. Clark, C. K. Ong, T. J. Tarn, G. M. Huang, Quantum nondemolition filters, *Math. Systems Theory* 18 (1985) 33-55.
- [10] D. Dong, I. R. Petersen, Sliding mode control of quantum systems, *New J. Phys.* 11 (2009) 105033.
- [11] F. Motzoi, J. M. Gambetta, S. T. Merkel, F. K. Wilhelm, Optimal control methods for rapidly time-varying Hamiltonians, *Phys. Rev. A* 84 (2011) 022307.
- [12] J. M. Gambetta, F. Motzoi, S. T. Merkel, F. K. Wilhelm, Analytic control methods for high-fidelity unitary operations in a weakly nonlinear oscillator, *Phys. Rev. A* 83 (2011) 012308.
- [13] P. Rebentrost, I. Serban, T. Schulte-Herbrueggen, F. K. Wilhelm, Optimal control of a qubit coupled to a non-Markovian environment, *Phys. Rev. Lett.* 102 (2009) 090401.
- [14] J. Q. You, F. Nori, Superconducting circuits and quantum information, *Physics Today* 58 (2005) 42-47.
- [15] J. Q. You, F. Nori, Atomic physics and quantum optics using superconducting circuits, *Nature* 474 (2011) 589-597.
- [16] P. D. Nation, J. R. Johansson, M. P. Blencowe, F. Nori, Stimulating uncertainty: amplifying the quantum vacuum with superconducting circuits, *Rev. Mod. Phys.* 84 (2012) 1-24.
- [17] S. N. Shevchenko, S. Ashhab, F. Nori, Landau-Zener-Stückelberg interferometry, *Physics Reports* 492 (2010) 1-30.
- [18] I. Buluta, F. Nori, Quantum Simulators, *Science* 326 (2009) 108-111.
- [19] I. Buluta, S. Ashhab, F. Nori, Natural and artificial atoms for quantum computation, *Reports on Progress in Physics* 74 (2011) 104401.
- [20] I. Georgescu, S. Ashhab, F. Nori, Quantum Simulation, *Rev. Mod. Phys.* 86 (2014) 153-185.
- [21] J. Ma, X. Wang, C. P. Sun, F. Nori, Quantum spin squeezing, *Physics Reports* 509 (2011) 89-165.
- [22] A. G. Kofman, S. Ashhab, F. Nori, Noperturbative theory of weak pre- and post-selected measurements, *Physics Reports* 520 (2012) 43-133.
- [23] I. Georgescu, F. Nori, Quantum technologies: an old new story, *Physics World* 25 (2012) 16-17.
- [24] C. Emary, N. Lambert, F. Nori, Leggett-Garg inequalities, *Reports on Progress in Physics* 77 (2014) 016001.
- [25] S. Cong, *Control of Quantum Systems: Theory and Methods*, John Wiley & Sons, Singapore Pte. Ltd. 2014.
- [26] S. S. Ge, T.-L. Vu, T. H. Lee, Quantum measurement-based feedback control: a nonsmooth time delay control approach, *SIAM J. Control and Optimization* 50 (2012) 845-863.
- [27] T. L. Vu, S. S. Ge, C. C. Hang, Real-time deterministic generation of maximally entangled two-qubit and three-qubit states via bang-bang control, *Phys. Rev. A* 85 (2012) 012332.
- [28] Z. G. Xue, H. Lin, T. H. Lee, Identification of unknown parameters for a class of two-level quantum systems, *IEEE Trans. Automat. Contr.* 58 (2013) 1805-1810.
- [29] F. Gao, R. Rey-de-Castro, A. M. Donovan, J. Xu, Y. Wang, H. Rabitz, F. Shuang, Pathway dynamics in the optimal quantum control of rubidium: Cooperation and competition, *Phys. Rev. A* 89 (2014) 023416.
- [30] T.-H. Zhang, M. Jiang, X. Huang, M. Wan, Deterministic teleportation of multi-qudit states in a network via various probabilistic channels, *International Journal of Theoretical Physics* 53 (2014) 1150-1158.
- [31] M. Jiang, S. Luo, Comparing quantum Markovianities: Distinguishability versus correlations, *Phys. Rev. A* 88 (2013) 034101.
- [32] C. Chen, L.-C. Wang, Y. Wang, Closed-loop and robust control of quantum systems, *The scientific world journal* 2013 (2013) 869285.
- [33] H. Z. Shen, M. Qin, X. X. Yi, Single-photon storing in coupled non-Markovian atom-cavity system, *Phys. Rev. A* 88 (2013) 033835.
- [34] X.-Y. Lü, Z.-L. Xiang, W. Cui, J. Q. You, F. Nori, Quantum memory using a hybrid circuit with flux qubits and nitrogen-vacancy centers, *Phys. Rev. A* 88 (2013) 012329.
- [35] X. Y. Lü, W. M. Zhang, S. Ashhab, Y. Wu, F. Nori Quantum-criticality-induced strong Kerr nonlinearities in optomechanical systems, *Sci. Rep.* 3 (2013) 2943.
- [36] J.-Q. Liao and F. Nori, Photon blockade in quadratically coupled optomechanical systems, *Phys. Rev. A* 88 (2013) 023853.

- [37] J.-Q. Liao, H. K. Cheung, C. K. Law, Spectrum of single-photon emission and scattering in cavity optomechanics, *Phys. Rev. A* 85 (2012) 025803.
- [38] S.-B. Xue, R.-B. Wu, W.-M. Zhang, J. Zhang, C.-W. Li, T.-J. Tarn, Decoherence suppression via non-Markovian coherent feedback control, *Phys. Rev. A* 86 (2012) 052304.
- [39] X.-W. Xu, H. Wang, J. Zhang, Y.-X. Liu, Engineering of nonclassical motional states in optomechanical systems, *Phys. Rev. A* 88 (2013) 063819.
- [40] N. Wiener, *Cybernetics: or Control and Communication in the Animal and the Machine*, Second Edition, The MIT Press, Cambridge, 1965.
- [41] R. E. Kalman, Y. C. Ho, K. S. Narendra, Controllability of linear dynamical systems, *Contributions to Differential Equations* 1 (1963) 189-213.
- [42] R. Bellman, *Introduction to Matrix Analysis*, McGraw-Hill Book Company, New York, 1960.
- [43] M. Athans, P. Falb, *Optimal Control: An Introduction to the Theory and Its Applications*, Dover Publications, New York, 2006.
- [44] A. Isidori, *Nonlinear Control Systems*, third ed., Springer, London, 1995.
- [45] M. A. Nielsen, I. L. Chuang, *Quantum Computation and Quantum Information*, Cambridge University Press, Cambridge, England, 2000.
- [46] H. Diels, *Antike Technik*, Teubner, Berlin, 1920.
- [47] O. Mayr, *The Origins of Feedback Control*, The M.I.T. Press, Cambridge, 1970.
- [48] A. M. Lepschy, Feedback control in ancient water and mechanical clocks, *IEEE Transactions on Education* 35 (1992) 3-10.
- [49] J. C. Maxwell, On Governors, *Proc. Roy. Soc. London* 16 (1868) 270-283.
- [50] H. M. Wiseman, G. J. Milburn, *Quantum Measurement and Control*, Cambridge University Press, Cambridge, United Kingdom, 2009.
- [51] M. R. James, *Control Theory: From Classical to Quantum Optimal, Stochastic, and Robust Control*, Australian National University, 2005.
- [52] H. Mabuchi, A. C. Doherty, Cavity Quantum Electrodynamics: Coherence in Context, *Science* 298 (2002) 1372-1377.
- [53] S. Habib, K. Jacobs, H. Mabuchi, Quantum feedback control: How can we control quantum systems without disturbing them? *Los Alamos Science* 27 (2002) 126-135.
- [54] G. Zhang, M. R. James, Quantum feedback networks and control: A brief survey, *Chinese Science Bulletin* 5 (2012) 2200-2214.
- [55] A. Serafini, Feedback control in quantum optics: an overview of experimental breakthroughs and areas of application, *ISRN Optics* 2012 (2012) 275016.
- [56] V. P. Belavkin, Quantum stochastic calculus and quantum nonlinear filtering, *J. Multivariate Anal.* 42 (1992) 171-202.
- [57] V. P. Belavkin, Quantum continual measurements and a posteriori collapse on CCR, *Commun. Math. Phys.* 146 (1992) 611-635.
- [58] P. S. Maybeck, *Stochastic Models, Estimation and Control (I and II)*, Academic Press, New York, 1982.
- [59] H. M. Wiseman, G. J. Milburn, Quantum theory of field-quadrature measurements, *Phys. Rev. A* 47 (1993) 642-662.
- [60] H. M. Wiseman, G. J. Milburn, Quantum theory of optical feedback via homodyne detection, *Phys. Rev. Lett.* 70 (1993) 548-551.
- [61] H. J. Carmichael, *An Open Quantum Systems Approach to Quantum Optics*, Springer verlag, Berlin, 1993.
- [62] H. J. Carmichael, S. Singh, R. Vyas, P. R. Rice, Photoelectron waiting times and atomic state reduction in resonance fluorescence, *Phys. Rev. A* 39 (1989) 1200-1218.
- [63] M. D. Srinivas, E. B. Davies, Photon counting probabilities in quantum optics, *J. Mod. Opt.* 28 (1981) 981-996.
- [64] N. Gisin, A model for the macroscopic description and continual observations in quantum mechanics, *Phys. Rev. Lett.* 52 (1984) 1657-1660.
- [65] L. Diosi, Stochastic pure state representation for open quantum systems, *Phys. Lett. A* 114 (1986) 451-454.
- [66] H. M. Wiseman, Quantum theory of continuous feedback, *Phys. Rev. A* 49 (1994) 2133-2150.
- [67] M. Yanagisawa, H. Kimura, A Control Problem for Gaussian States, in: Y. Yamamoto, S. Hara (Eds.), *Learning, Control and Hybrid Systems*, Lecture Notes in Control and Information Sciences, Springer-Verlag, New York, 1998, vol. 241, pp. 249-313.
- [68] A. C. Doherty, K. Jacobs, Feedback control of quantum systems using continuous state estimation, *Phys. Rev. A* 60 (1999) 2700-2711.
- [69] V. P. Belavkin, Non-demolition measurement and control in quantum dynamical systems, in: A. Blaquiere, S. Diner, G. Lochak (Eds.), *Information, Complexity and Control in Quantum Physics. Proceedings of the 4th International Seminar on Mathematical Theory of Dynamical Systems and Microphysics*, Springer-Verlag, New York, 1987, pp. 331-336.
- [70] V. P. Belavkin, Theory of the control of observable quantum systems, *Automatica and Remote Control* 44 (1983) 178-188.
- [71] H. M. Wiseman, G. J. Milburn, All-optical versus electro-optical quantum-limited feedback, *Phys. Rev. A* 49 (1994) 4110-4125.
- [72] I. Kenyon, *The Light Fantastic: A Modern Introduction to Classical and Quantum Optics*, Oxford University Press, Oxford, 2011.
- [73] C. W. Gardiner, M. J. Collett, Input and output in damped quantum systems: Quantum stochastic differential equations and the master equation, *Phys. Rev. A* 31 (1985) 3761-3774.
- [74] C. W. Gardiner, P. Zoller, *Quantum Noise*, Third edition, Springer-Verlag, Berlin, 2004.
- [75] C. W. Gardiner, Driving a quantum system with the output field from another driven quantum system, *Phys. Rev. Lett.* 70 (1993) 2269-2272.
- [76] H. J. Carmichael, Quantum trajectory theory for cascaded open systems, *Phys. Rev. Lett.* 70 (1993) 2273-2276.
- [77] S. Lloyd, Coherent quantum feedback, *Phys. Rev. A* 62 (2000) 022108.
- [78] R. J. Nelson, Y. Weinstein, D. Cory, S. Lloyd, Experimental demonstration of fully coherent quantum feedback, *Phys. Rev. Lett.* 85 (2000) 3045-3048.
- [79] K. Jacobs, X. Wang, H. M. Wiseman, Coherent feedback that beats all measurement-based feedback protocols, *New J. Phys.* (2014) in press.
- [80] B. Qi, L. Guo, Is measurement-based feedback still better for quantum control systems? *Sys. Contr. Lett.* 59 (2010) 333-339.
- [81] M. R. James, H. I. Nurdin, I. R. Petersen, H^∞ Control of Linear Quantum Stochastic Systems, *IEEE Trans. Automat. Contr.* 53 (2008) 1787-1803.
- [82] J. E. Gough, M. R. James, The series product and its application to quantum feedforward and feedback networks, *IEEE Trans. Automat. Contr.* 54 (2009) 2530-2544.
- [83] J. Kerckhoff, K. W. Lehnert, Superconducting microwave multivibrator produced by coherent feedback, *Phys. Rev. Lett.* 109 (2012) 153602.
- [84] H. Mabuchi, Nonlinear interferometry approach to photonic sequential logic, *Appl. Phys. Lett.* 99 (2011) 153103.
- [85] J. Zhang, R. B. Wu, Y.-X. Liu, C. W. Li, T. J. Tarn, Quantum coherent nonlinear feedbacks with applications to quantum optics on chip, *IEEE trans. Automat. Contr.* 57 (2012) 1997-2008.
- [86] Z.-P. Liu, H. Wang, J. Zhang, Y.-X. Liu, R.-B. Wu, C.-W Li, F. Nori, Feedback-induced nonlinearity and superconducting on-chip quantum

- optics, Phys. Rev. A 88 (2013) 063851.
- [87] H. I. Nurdin, M. R. James, I. R. Petersen, Coherent quantum LQG control, Automatica 45 (2009) 1837-1846.
 - [88] R. Hamerly, H. Mabuchi, Advantages of coherent feedback for cooling quantum oscillators, Phys. Rev. Lett. 109 (2012) 173602.
 - [89] K. Maruyama, F. Nori, V. Vedral, Colloquium: The physics of Maxwell's demon and information, Rev. Mod. Phys. 81 (2009) 1-23.
 - [90] T. Sagawa, M. Ueda, Second law of thermodynamics with discrete quantum feedback control, Phys. Rev. Lett. 100 (2008) 080403.
 - [91] T. Sagawa, M. Ueda, Nonequilibrium thermodynamics of feedback control, Phys. Rev. E 85 (2012) 021104.
 - [92] D. Abreu, U. Seifert, Thermodynamics of genuine nonequilibrium states under feedback control, Phys. Rev. Lett. 108 (2012) 030601.
 - [93] K. Jacobs, Second law of thermodynamics and quantum feedback control: Maxwell's demon with continuous measurements, Phys. Rev. A 80 (2009) 012322.
 - [94] P. W. Shor, Scheme for reducing decoherence in quantum computer memory, Phys. Rev. A 52 (1995) R2493-R2496.
 - [95] A. M. Steane, Multiple-particle interference and quantum error correction, Proc. R. Soc. London, Ser. A 452 (1996) 2551-2577.
 - [96] E. Knill, R. Laflamme, Theory of quantum error-correcting codes, Phys. Rev. A 55 (1997) 900-911.
 - [97] J. I. Cirac, T. Pellizzari, P. Zoller, Enforcing coherent evolution in dissipative quantum dynamics, Science 273 (1996) 1207-1210.
 - [98] W. H. Zurek, R. Laflamme, Quantum logical operations on encoded qubits, Phys. Rev. Lett. 77 (1996) 4683-4686.
 - [99] L. M. Duan, G. C. Guo, Preserving coherence in quantum computation by pairing quantum bits, Phys. Rev. Lett. 79 (1997) 1953-1956.
 - [100] S. Lloyd, J.J.E. Slotine, Analog quantum error correction, Phys. Rev. Lett. 80 (1998) 4088-4091.
 - [101] K. Jacobs, Twenty open problems in quantum control, arxiv: 1304.0819v2, 2013.
 - [102] M. J. Collett, C. W. Gardiner, Squeezing of intracavity and traveling-wave light fields produced in parametric amplification, Phys. Rev. A 30 (1984) 1386-1391.
 - [103] R. I. Hudson, K. R. Parthasarathy, Quantum Ito's formula and stochastic evolution, Commun. Math. Phys. 93 (1984) 301-323.
 - [104] K. Jacobs, Stochastic Processes for Physicists: Understanding Noisy Systems, Cambridge University Press, Cambridge, 2010.
 - [105] K. Jacobs, Quantum Measurement Theory and its Applications, Cambridge University Press, Cambridge, 2014.
 - [106] D. Wineland, H. Dehmelt, Proposed $10^{14} \Delta\nu < \nu$ laser fluorescence spectroscopy on Ti^+ mono-ion oscillator, Bull. Am. Phys. Soc. 20 (1975) 637.
 - [107] F. Diedrich, J. C. Bergquist, W. M. Itano, D. J. Wineland, Laser cooling to the zero-point energy of motion, Phys. Rev. Lett. 62 (1989) 403-406.
 - [108] F. Golnaraghi, B. C. Kuo, Automatic Control Systems, eighth ed., Wiley, New York, 2009.
 - [109] K. Zhou, J. Doyle, K. Glover, Robust and optimal control, Prentice Hall, Englewood Cliffs, New Jersey, 1995.
 - [110] C. Ahn, A. C. Doherty, A. J. Landahl, Continuous quantum error correction via quantum feedback control, Phys. Rev. A 65 (2002) 042301.
 - [111] C. Ahn, H. M. Wiseman, G. J. Milburn, Quantum error correction for continuously detected errors Phys. Rev. A 67 (2003) 052310.
 - [112] L. Bouten, R. van Handel, M. R. James, An introduction to quantum filtering, SIAM J. Control Optim. 46 (2007) 2199-2241.
 - [113] A. C. Doherty, S. Habib, K. Jacobs, H. Mabuchi, S. M. Tan, Quantum feedback control and classical control theory, Phys. Rev. A 62 (2000) 012105.
 - [114] K. Jacobs, D. A. Steck, A straightforward introduction to continuous quantum measurement, Contemporary Physics 47 (2006) 279-303.
 - [115] M. B. Plenio, P. L. Knight, The quantum-jump approach to dissipative dynamics in quantum optics, Rev. Mod. Phys. 70 (1998) 101-144.
 - [116] K. Mølmer, Y. Castin, J. Dalibard, Monte Carlo wave-function method in quantum optics, J. Opt. Soc. Am. B 10 (1993) 524.
 - [117] N. Gisin, I. C. Percival, The quantum-state diffusion model applied to open systems, J. Phys. A: Math. Gen. 25 (1992) 5677-5691.
 - [118] I. C. Percival, Quantum State Diffusion, Cambridge University Press, Cambridge, 1998.
 - [119] J. Dalibard, Y. Castin, K. Mølmer, Wave-function approach to dissipative processes in quantum optics, Phys. Rev. Lett. 68 (1992) 580-583.
 - [120] C. W. Gardiner, A. S. Paskins, P. Zoller, Wave-function quantum stochastic differential equations and quantum-jump simulation methods, Phys. Rev. A 46 (1992) 4363-4381.
 - [121] H. M. Wiseman, G. J. Milburn, Interpretation of quantum jump and diffusion processes illustrated on the Bloch sphere, Phys. Rev. A 47 (1993) 1652-1666.
 - [122] Y. Aharonov, D. Z. Albert, L. Vaidman, How the result of a measurement of a component of the spin of a spin-1/2 particle can turn out to be 100, Phys. Rev. Lett. 60 (1988) 1351-1354.
 - [123] Y. Aharonov, L. Vaidman, Properties of a quantum system during the time interval between two measurements, Phys. Rev. A 41 (1990) 11-20.
 - [124] A. J. Scott, G. J. Milburn, Quantum nonlinear dynamics of continuously measured systems, Phys. Rev. A 63 (2001) 042101.
 - [125] J. Gough, A. Sobolev, Continuous measurement of canonical observables and limit stochastic Schrodinger equations, Phys. Rev. A 69 (2004) 032107.
 - [126] U. Leonhardt, H. Paul, Phase measurement and Q function, Phys. Rev. A 47 (1993) 2460(R).
 - [127] K. Jacobs, J. Finn, S. Vinjanampathy, Real-time feedback control of a mesoscopic superposition, Phys. Rev. A 83 (2011) 041801.
 - [128] D. A. Steck, K. Jacobs, H. Mabuchi, T. Bhattacharya, S. Habib, Quantum feedback control of atomic motion in an optical cavity, Phys. Rev. Lett. 92 (2004) 223004.
 - [129] D. A. Steck, K. Jacobs, H. Mabuchi, S. Habib, T. Bhattacharya, Feedback cooling of atomic motion in cavity QED, Phys. Rev. A 74 (2006) 012322.
 - [130] J. Wang, H. M. Wiseman, Feedback-stabilization of an arbitrary pure state of a two-level atom, Phys. Rev. A 64 (2001) 063810.
 - [131] H. F. Hofmann, O. Hess, G. Mahler, Quantum control by compensation of quantum fluctuations, Opt. Exp. 2 (1998) 339-346.
 - [132] H. F. Hofmann, G. Mahler, O. Hess, Quantum control of atomic systems by homodyne detection and feedback, Phys. Rev. A 57 (1998) 4877-4888.
 - [133] J. Wang, H. M. Wiseman, G. J. Milburn, Dynamical creation of entanglement by homodyne-mediated feedback, Phys. Rev. A 71 (2005) 042309.
 - [134] J.-G. Li, J. Zou, B. Shao, J.-F. Cai, Steady atomic entanglement with different quantum feedbacks, Phys. Rev. A 77 (2008) 012339.
 - [135] N. Yamamoto, Parametrization of the feedback Hamiltonian realizing a pure steady state, Phys. Rev. A 72 (2005) 024104.
 - [136] S. Mancini, J. Wang, Towards feedback control of entanglement, Eur. Phys. J. D 32 (2005) 257-260.

- [137] Y. Li, B. Luo, H. Guo, Entanglement and quantum discord dynamics of two atoms under practical feedback control, *Phys. Rev. A* 84 (2011) 012316.
- [138] A.R.R. Carvalho, M. Busse, O. Brodier, C. Viviescas, A. Buchleitner, Optimal dynamical characterization of entanglement, *Phys. Rev. Lett.* 98 (2007) 190501.
- [139] C. Viviescas, I. Guevara, A.R.R. Carvalho, M. Busse, A. Buchleitner, Entanglement dynamics in open two-qubit systems via diffusive quantum trajectories, *Phys. Rev. Lett.* 105 (2010) 210502.
- [140] A.R.R. Carvalho, J. J. Hope, Stabilizing entanglement by quantum-jump-based feedback, *Phys. Rev. A* 76 (2007) 010301(R).
- [141] A.R.R. Carvalho, A.J.S. Reid, J. J. Hope, Controlling entanglement by direct quantum feedback, *Phys. Rev. A* 78 (2008) 012334.
- [142] S. C. Hou, X. L. Huang, X. X. Yi, Suppressing decoherence and improving entanglement by quantum-jump-based feedback control in two-level systems, *Phys. Rev. A* 82 (2010) 012336.
- [143] R. N. Stevenson, A.R.R. Carvalho, J. J. Hope, Production of entanglement in Raman three-level systems using feedback, *Eur. Phys. J. D* 61 (2011) 523-529.
- [144] L. C. Wang, J. Shen, X. X. Yi, Effect of feedback control on the entanglement evolution, *Eur. Phys. J. D* 56 (2010) 435-440.
- [145] D. Xue, J. Zou, J.-G. Li, W.-Y. Chen, B. Shao, Controlling entanglement between two separated atoms by quantum-jump-based feedback, *J. Phys. B: At. Mol. Opt. Phys.* 43 (2010) 045503.
- [146] J. Song, Y. Xia, X.-D. Sun, Noise-induced quantum correlation via quantum feedback control, *J. Opt. Soc. Am. B* 29 (2012) 268-273.
- [147] P. Tombesi, D. Vitali, Macroscopic coherence via quantum feedback, *Phys. Rev. A* 51 (1995) 4913-4917.
- [148] P. Goetsch, P. Tombesi, D. Vitali, Effect of feedback on the decoherence of a Schrodinger-cat state: A quantum trajectory description, *Phys. Rev. A* 54 (1996) 4519-4527.
- [149] D. Vitali, P. Tombesi, G. J. Milburn, Controlling the decoherence of a 'meter' via stroboscopic feedback, *Phys. Rev. Lett.* 79 (1997) 2442-2445.
- [150] D. Vitali, P. Tombesi, G. J. Milburn, Quantum-state protection in cavities, *Phys. Rev. A* 57 (1998) 4930-4944.
- [151] M. Fortunato, J. M. Raimond, P. Tombesi, D. Vitali, Autofeedback scheme for preservation of macroscopic coherence in microwave cavities, *Phys. Rev. A* 60 (1999) 1687-1697.
- [152] H. M. Wiseman and G. J. Milburn, Squeezing via feedback, *Phys. Rev. A* 49 (1994) 1350-1366.
- [153] H. M. Wiseman, G. J. Milburn, Reduction in laser-intensity fluctuations by a feedback-controlled output mirror, *Phys. Rev. A* 46 (1992) 2853-2858.
- [154] A. Liebman, G. J. Milburn, Quantum-noise reduction in a driven cavity with feedback, *Phys. Rev. A* 47 (1993) 634-638.
- [155] P. Tombesi, D. Vitali, Physical realization of an environment with squeezed quantum fluctuations via quantum-nondemolition-mediated feedback, *Phys. Rev. A* 50 (1994) 4253-4257.
- [156] H. M. Wiseman, M. S. Taubman, H.-A. Bachor, Feedback-enhanced squeezing in second-harmonic generation, *Phys. Rev. A* 51 (1995) 3227-3233.
- [157] H. M. Wiseman, In-loop squeezing is like real squeezing to an in-loop atom, *Phys. Rev. Lett.* 81 (1998) 3840-3843.
- [158] R. Ruskov, K. Schwab, A. N. Korotkov, Squeezing of a nanomechanical resonator by quantum nondemolition measurement and feedback, *Phys. Rev. B* 71 (2005) 235407.
- [159] A. Vinante, P. Falferi, Feedback-enhanced parametric squeezing of mechanical motion, *Phys. Rev. Lett.* 111 (2013) 207203.
- [160] L. K. Thomsen, S. Mancini, H. M. Wiseman, Spin squeezing via quantum feedback, *Phys. Rev. A* 65 (2002) 061801(R).
- [161] J. K. Stockton, R. van Handel, H. Mabuchi, Deterministic Dicke-state preparation with continuous measurement and control, *Phys. Rev. A* 70 (2004) 022106.
- [162] J. Zhang, Y. X. Liu, R. B. Wu, C. W. Li, T. J. Tarn, Transition from weak to strong measurements by nonlinear quantum feedback control, *Phys. Rev. A* 82 (2010) 022101.
- [163] V. Giovannetti, P. Tombesi, D. Vitali, Non-Markovian quantum feedback from homodyne measurements: The effect of a nonzero feedback delay time, *Phys. Rev. A* 60 (1999) 1549-1561.
- [164] K. Nishio, K. Kashima, J. Imura, Effects of time delay in feedback control of linear quantum systems, *Phys. Rev. A* 79 (2009) 062105.
- [165] C. Emary, Delayed feedback control in quantum transport, *Phil. Trans. R. Soc. A* 371 (2013) 1999.
- [166] M. Sarovar, H.-S. Goan, T. P. Spiller, G. J. Milburn, High-fidelity measurement and quantum feedback control in circuit QED, *Phys. Rev. A* 72 (2005) 062327.
- [167] Z. Liu, L. L. Kuang, K. Hu, L. T. Xu, S. H. Wei, L. Z. Guo, X. Q. Li, Deterministic creation and stabilization of entanglement in circuit QED by homodyne-mediated feedback control, *Phys. Rev. A* 82 (2010) 032335.
- [168] W. Feng, P. Y. Wang, X. M. Ding, L. T. Xu, X. Q. Li, Generating and stabilizing the Greenberger-Horne-Zeilinger state in circuit QED: Joint measurement, Zeno effect, and feedback, *Phys. Rev. A* 83 (2011) 042313.
- [169] T. A. Wheatley, D. W. Berry, H. Yonezawa, D. Nakane, H. Arai, D. T. Pope, T. C. Ralph, H. M. Wiseman, A. Furusawa, E. H. Huntington, Adaptive optical estimation using time-symmetric quantum smoothing, *Phys. Rev. Lett.* 104 (2010) 093601.
- [170] H. M. Wiseman, S. Mancini, J. Wang, Bayesian feedback versus Markovian feedback in a two-level atom, *Phys. Rev. A* 66, (2002) 013807.
- [171] H. M. Wiseman, A. C. Doherty, Optimal unravellings for feedback control in linear quantum systems, *Phys. Rev. Lett.* 94 (2005) 070405.
- [172] N. Yamamoto, Robust observer for uncertain linear quantum systems, *Phys. Rev. A* 74 (2006) 032107.
- [173] N. Yamamoto, Relation between fundamental estimation limit and stability in linear quantum systems with imperfect measurement, *Phys. Rev. A* 76 (2007) 034102.
- [174] A. Chia, H. M. Wiseman, Quantum theory of multiple-input-multiple-output Markovian feedback with diffusive measurements, *Phys. Rev. A* 84 (2011) 012120.
- [175] A. Chia, H. M. Wiseman, Complete parametrizations of diffusive quantum monitorings, *Phys. Rev. A* 84 (2011) 012119.
- [176] P. Goetsch, R. Graham, F. Haake, Schrödinger cat states and single runs for the damped harmonic oscillator, *Phys. Rev. A* 51 (1995) 136-142.
- [177] H. M. Wiseman, L. K. Thomsen, Reducing the linewidth of an atom laser by feedback, *Phys. Rev. Lett.* 86 (2001) 1143-1147.
- [178] L. K. Thomsen, H. M. Wiseman, Atom-laser coherence and its control via feedback, *Phys. Rev. A* 65 (2002) 063607.
- [179] M. Sarovar, C. Ahn, K. Jacobs, G. J. Milburn, Practical scheme for error control using feedback, *Phys. Rev. A* 69 (2004) 052324.

- [180] B. A. Chase, A. J. Landahl, J. M. Geremia, Efficient feedback controllers for continuous-time quantum error correction, *Phys. Rev. A* 77 (2008) 032304.
- [181] H. Mabuchi, Continuous quantum error correction as classical hybrid control, *New J. Phys.* 11 (2009) 105044.
- [182] K. Keane, A. N. Korotkov, Simplified quantum error detection and correlation for superconducting qubits, *Phys. Rev. A* 86 (2012) 012333.
- [183] M. J. Biercuk, H. Uys, A. P. VanDevender, N. Shiga, W. M. Itano, J. J. Bollinger, Optimized dynamical decoupling in a model quantum memory, *Nature* 458 (2009) 996-1000.
- [184] L. Viola, E. Knill, S. Lloyd, Dynamical decoupling of open quantum systems, *Phys. Rev. Lett.* 82 (1999) 2417-2421.
- [185] P. Zanardi, Symmetrizing evolutions, *Phys. Lett. A* 258 (1999) 77-82.
- [186] F. Ticozzi, L. Viola, Single-bit feedback and quantum-dynamical decoupling, *Phys. Rev. A* 74 (2006) 052328.
- [187] J. Zhang, R.-B. Wu, C.-W. Li, T.-J. Tarn, Protecting coherence and entanglement by quantum feedback controls, *IEEE Trans. Automat. Contr.* 55 (2010) 619-633.
- [188] N. Ganesan, T.-J. Tarn, Decoherence control in open quantum systems via classical feedback, *Phys. Rev. A* 75 (2007) 032323.
- [189] A. Hopkins, K. Jacobs, S. Habib, K. Schwab, Feedback cooling of a nanomechanical resonator, *Phys. Rev. B* 68 (2003) 235328.
- [190] J. Zhang, Y.-X. Liu, F. Nori, Cooling and squeezing the fluctuations of a nanomechanical beam by indirect quantum feedback control, *Phys. Rev. A* 79 (2009) 052102.
- [191] M. J. Woolley, A. C. Doherty, G. J. Milburn, Continuous quantum nondemolition measurement of Fock states of a nanoresonator using feedback-controlled circuit QED, *Phys. Rev. B* 82 (2010) 094511.
- [192] R. Ruskov, A. N. Korotkov, Quantum feedback control of a solid-state qubit, *Phys. Rev. B* 6 (2002) 041401(R).
- [193] A. N. Korotkov, Quantum feedback of a double-dot qubit, *Microelectronics Journal* 36 (2005) 253-255.
- [194] A. N. Korotkov, Simple quantum feedback of a solid-state qubit, *Phys. Rev. B* 71 (2005) 201305(R).
- [195] Q. Zhang, R. Ruskov, A. N. Korotkov, Continuous quantum feedback of coherent oscillations in a solid-state qubit, *Phys. Rev. B* 72 (2005) 245322.
- [196] A. N. Jordan, A. N. Korotkov, Qubit feedback and control with kicked quantum nondemolition measurements: a quantum Bayesian analysis, *Phys. Rev. B* 74 (2006) 085307.
- [197] A. N. Korotkov, Selective quantum evolution of a qubit state due to continuous measurement, *Phys. Rev. B* 63 (2001) 115403.
- [198] A. N. Korotkov, Continuous quantum measurement of a double dot, *Phys. Rev. B* 60 (1999) 5737-5742.
- [199] W. Cui, N. Lambert, Y. Ota, X.-Y. L., Z.-L. Xiang, J. Q. You, F. Nori, Confidence and backaction in the quantum filter equation, *Phys. Rev. A* 86 (2012) 052320.
- [200] H.-S. Goan, G. J. Milburn, H. M. Wiseman, H. B. Sun, Continuous quantum measurement of two coupled quantum dots using a point contact: a quantum trajectory approach, *Phys. Rev. B* 63 (2001) 125326.
- [201] N. P. Oxtoby, P. Warszawski, H. M. Wiseman, H.-B. Sun, R.E.S. Polkinghorne, Quantum trajectories for the realistic measurement of a solid-state charge qubit, *Phys. Rev. B* 71 (2005) 165317.
- [202] N. P. Oxtoby, H. M. Wiseman, H.-B. Sun, Sensitivity and back action in charge qubit measurements by a strongly coupled single-electron transistor, *Phys. Rev. B* 74 (2006) 045328.
- [203] J. S. Jin, X. Q. Li, Y. J. Yan, Quantum coherence control of solid-state charge qubit by means of a suboptimal feedback algorithm, *Phys. Rev. B* 73 (2006) 233302.
- [204] P. Campagne-Ibarcq, E. Flurin, N. Roch, D. Darson, P. Morfin, M. Mirrahimi, M. H. Devoret, F. Mallet, B. Huard, Persistent control of a superconducting qubit by stroboscopic measurement feedback, *Phys. Rev. X* 3 (2013) 021008.
- [205] R. Vijay, C. Mcklin, D. H. Slichter, S. J. Weber, K. W. Murch, R. Naik, A. N. Korotkov, I. Siddiqi, Stabilizing Rabi oscillations in a superconducting qubit using quantum feedback, *Nature* 490 (2012) 77-80.
- [206] D. Riste, C. C. Bultink, K. W. Lehnert, L. DiCarlo, Feedback control of a solid-state qubit using high-fidelity project measurement, *Phys. Rev. Lett.* 109 (2012) 240502.
- [207] W. Cui, F. Nori, Feedback control of Rabi oscillations in circuit QED, *Phys. Rev. A* 88 (2013) 063823.
- [208] R. van Handel, J. K. Stockton, H. Mabuchi, Feedback control of quantum state reduction, *IEEE Trans. Auto. Contr.* 50 (2005) 768-780.
- [209] M. Mirrahimi, R. van Handel, Stabilizing feedback controls for quantum systems, *SIAM J. Control Optim.* 46 (2007) 445-467.
- [210] C. Altafini, Feedback stabilization of isospectral control systems on complex flag manifolds: application to quantum ensembles, *IEEE Trans. Auto. Contr.* 52 (2007) 2019-2028.
- [211] R. van Handel, J. K. Stockton, H. Mabuchi, Modelling and feedback control design for quantum state preparation, *J. Opt. B: Quantum Semiclass. Opt.* 7 (2005) S179-S197.
- [212] B. Qi, H. Pan, L. Guo, Further results on stabilizing control of quantum systems, *IEEE Trans. Automat. Contr.* 58 (2013) 1349-1354.
- [213] J. E. Reiner, H. M. Wiseman, H. Mabuchi, Quantum jumps between dressed states: A Proposed cavity-QED test using feedback, *Phys. Rev. A* 67 (2003) 042106.
- [214] J. E. Reiner, W. P. Smith, L. A. Orozco, H. M. Wiseman, J. Gambetta, Quantum feedback in a weakly driven cavity QED system, *Phys. Rev. A* 70 (2004) 023819.
- [215] W. P. Smith, J. E. Reiner, L. A. Orozco, S. Kuhr, H. M. Wiseman, Capture and release of a conditional state of a cavity QED system by quantum feedback, *Phys. Rev. Lett.* 89 (2002) 133601.
- [216] R. I. Karasik, H. M. Wiseman, How many bits does it take to track an open quantum system, *Phys. Rev. Lett.* 106 (2011) 020406.
- [217] R. I. Karasik, H. M. Wiseman, Tracking an open quantum system using a finite state machine: stability analysis, *Phys. Rev. A* 84 (2011) 052120.
- [218] V. B. Braginsky, Y. I. Vorontsov, K. S. Thorne, Quantum nondemolition measurements, *Science* 209 (1980) 547-557.
- [219] A. A. Clerk, F. Marquardt, K. Jacobs, Back-action evasion and squeezing of a mechanical resonator using a cavity detector, *New J. Phys.* 10 (2008) 095010.
- [220] A. Szorkovszky, A. C. Doherty, G. I. Harris, W. P. Bowen, Mechanical squeezing via parametric amplification and weak measurement, *Phys. Rev. Lett.* 107 (2011) 213603.
- [221] A. Szorkovszky, A. A. Clerk, A. C. Doherty, W. P. Bowen, Detuned mechanical parametric amplification as a quantum non-demolition

- measurement, *New J. Phys.* 16 (2014) 043023.
- [222] A. Szorkovszky, G. A. Brawley, A. C. Doherty, W. P. Bowen, Strong thermomechanical squeezing via weak measurement, *Phys. Rev. Lett.* 110 (2013) 184301.
- [223] I. D. Leroux, M. H. Schleier-Smith, and V. Vuletić, Implementation of cavity squeezing of a collective atomic spin, *Phys. Rev. Lett.* 104 (2010) 073602.
- [224] M. H. Schleier-Smith, I. D. Leroux, V. Vuletić, States of an ensemble of two-Level atoms with reduced quantum uncertainty, *Phys. Rev. Lett.* 104 (2010) 073604.
- [225] H. Zhang, R. McConnell, S. Ćuk, Q. Lin, M. H. Schleier-Smith, I. D. Leroux, V. Vuletić, Collective state measurement of mesoscopic ensembles with single-atom resolution, *Phys. Rev. Lett.* 109 (2012) 133603.
- [226] K. Xia and J. Evers, Ground-state cooling of a nanomechanical resonator coupled to two interacting flux qubits, *Phys. Rev. B* 82 (2010) 184532.
- [227] K. Xia and J. Evers, Ground state cooling of a nanomechanical resonator in the nonresolved regime via quantum interference, *Phys. Rev. Lett.* 103 (2009) 227203.
- [228] A. Kubanek, M. Koch, C. Sames, A. Ourjoumtsev, P.W.H. Pinkse, K. Murr, G. Rempe, Photon-by-photon feedback control of a single-atom trajectory, *Nature* 462 (2009) 898-901.
- [229] T. Fischer, P. Maunz, P.W.H. Pinkse, T. Puppe, G. Rempe, Feedback on the motion of a single atom in an optical cavity, *Phys. Rev. Lett.* 88 (2002) 163002.
- [230] O. Arcizet, P. F. Cohadon, T. Briant, M. Pinard, A. Heidmann, Radiation-pressure cooling and optomechanical instability of a micromirror, *Nature* 444 (2006) 71-74.
- [231] S. Gigan, H. R. Bohm, M. Paternostro, F. Blaser, G. Langer, J. B. Hertzberg, K. C. Schwab, D. Bauerle, M. Aspelmeyer, A. Zeilinger, Self-cooling of a micromirror by radiation pressure, *Nature*, 444 (2006) 67-70.
- [232] T. Corbitt, C. Wipf, T. Bodiya, D. Ottaway, D. Sigg, N. Smith, S. Whitcomb, N. Mavalvala, Optical dilution and feedback cooling of a Gram-scale oscillator to 6.9 mK, *Phys. Rev. Lett.* 99 (2007) 160801.
- [233] P. F. Cohadon, A. Heidmann, M. Pinard, Cooling of a mirror by radiation pressure, *Phys. Rev. Lett.* 83 (1999) 3174-3177.
- [234] O. Arcizet, P. F. Cohadon, T. Briant, M. Pinard, A. Heidmann, J. M. Mackowski, C. Michel, L. Pinard, O. Francais, L. Rousseau, High-sensitivity optical monitoring of a micromechanical resonator with a quantum-limited optomechanical sensor, *Phys. Rev. Lett.* 97 (2006) 133601.
- [235] D. Kleckner, D. Bouwmeester, Sub-kelvin optical cooling of a micromechanical resonator, *Nature* 444 (2006) 75-78.
- [236] J. D. Thompson, B. M. Zwickl, A. M. Jayich, F. Marquardt, S. M. Girvin, J.G.E. Harris, Strong dispersive coupling of a high-finesse cavity to a micromechanical membrane, *Nature* 452 (2008) 72-75.
- [237] S. Gröblacher, J. B. Hertzberg, M. R. Vanner, G. D. Cole, S. Gigan, K. C. Schwab, M. Aspelmeyer, Demonstration of an ultracold micro-optomechanical oscillator in a cryogenic cavity, *Nature Phys.* 5 (2009) 485-488.
- [238] A. Schliesser, R. Rivière, G. Anetsberger, O. Arcizet, T. J. Kippenberg, Resolved-sideband cooling of a micromechanical oscillator, *Nature Phys.* 5 (2008) 415-419.
- [239] S. Gröblacher, K. Hammerer, M. R. Vanner, M. Aspelmeyer, Observation of strong coupling between a micromechanical resonator and an optical cavity field, *Nature* 460 (2009) 724-727.
- [240] A. Schliesser, O. Arcizet, R. Rivière, G. Anetsberger, T. J. Kippenberg, Resolved-sideband cooling and position measurement of a micromechanical oscillator close to the Heisenberg uncertainty limit, *Nature Phys.* 5 (2009) 509-514.
- [241] G. Anetsberger, O. Arcizet, Q. P. Unterreithmeier, R. Rivière, A. Schliesser, E. M. Weig, J. P. Kotthaus, T. J. Kippenberg, Near-field cavity optomechanics with nanomechanical oscillators, *Nature Phys.* 5 (2009) 909-914.
- [242] M. Eichenfield, R. Camacho, J. Chan, K. J. Vahala, O. Painter, A picogram- and nanometre-scale photonic-crystal optomechanical cavity, *Nature*, 459 (2009) 550-555.
- [243] M. Eichenfield, J. Chan, R. M. Camacho, K. J. Vahala, O. Painter, Optomechanical crystals, *Nature*, 462 (2009) 78-82.
- [244] J. D. Teufel, D. Li, M. S. Allman, K. Cicak, A. J. Sirois, J. D. Whittaker, R. W. Simmonds, Circuit cavity electromechanics in the strong-coupling regime, *Nature*, 471 (2011) 204-208.
- [245] J. D. Teufel, T. Donner, D. Li, J. W. Harlow, M. S. Allman, K. Cicak, A. J. Sirois, J. D. Whittaker, K. W. Lehnert, R. W. Simmonds, Sideband cooling of micromechanical motion to the quantum ground state, *Nature* 475 (2011) 359-363.
- [246] P. Bushev, D. Rotter, A. Wilson, F. Dubin, C. Becher, J. Eschner, R. Blatt, V. Steixner, P. Rabl, P. Zoller, Feedback cooling of a single trapped ion, *Phys. Rev. Lett.* 96 (2006) 043003.
- [247] B. D'Urso, B. Odom, G. Gabrielse, Feedback cooling of a one-electron oscillator, *Phys. Rev. Lett.* 90 (2003) 043001.
- [248] J. Gieseler, B. Deutsch, R. Quidant, L. Novotny, Subkelvin parametric feedback cooling of a laser-trapped nanoparticle, *Phys. Rev. Lett.* 109 (2012) 103603.
- [249] N. V. Morrow, S. K. Dutta, G. Raithel, Feedback control of atomic motion in an optical lattice, *Phys. Rev. Lett.* 88 (2002) 093003.
- [250] A. J. Berglund, H. Mabuchi, Feedback controller design for tracking a single fluorescent molecule, *Appl. Phys. B* 78 (2004) 653-659.
- [251] A. J. Berglund, K. McHale, H. Mabuchi, Feedback localization of freely diffusing fluorescent particles near the optical shot-noise limit, *Opt. Lett.* 32 (2007) 145-147.
- [252] A. J. Berglund, K. McHale, H. Mabuchi, Fluctuations in close-loop fluorescent particle tracking, *Opt. Exp.* 15 (2007) 7752-7773.
- [253] K. W. Murch, K. L. Moore, S. Gupta, D. M. Stamper-Kurn, Observation of quantum-measurement backaction with an ultracold atomic gas, *Nature Phys.* 4 (2008) 561-564.
- [254] T. P. Purdy, D.W.C. Brooks, T. Botter, N. Brahms, Z.-Y. Ma, D. M. Stamper-Kurn, Tunable Cavity Optomechanics with Ultracold Atoms, *Phys. Rev. Lett.* 105 (2010) 133602.
- [255] M. Y. Vilensky, I. Sh. Averbukh, Y. Prior, Laser cooling in a feedback-controlled optical shaker, *Phys. Rev. A* 73 (2006) 063402.
- [256] Y. Kishimoto, J. K. Koga, T. Tajima, D. L. Fisher, Phase space control and consequences for cooling by using a laser-undulator beat wave, *Phys. Rev. E* 55 (1997) 5948-5963.
- [257] G.-C. Zhang, J.-L. Shen, J.-H. Dai, Cooling charged particles in a Paul trap by feedback control, *Phys. Rev. A* 60 (1999) 704-707.

- [258] J. A. Dunningham, H. M. Wiseman, D. F. Walls, Manipulating the motion of a single atom in a standing wave via feedback, *Phys. Rev. A* 55 (1997) 1398-1411.
- [259] S. Mancini, P. Tombesi, Atomic localization in the presence of optical feedback, *Phys. Rev. A* 56 (1997) 2466-2469.
- [260] S. Mancini, D. Vitali, P. Tombesi, Stochastic phase-space localization for a single trapped particle, *Phys. Rev. A* 61 (2000) 053404.
- [261] S. D. Wilson, A.R.R. Carvalho, J. J. Hope, M. R. James, Effects of measurement backaction in the stabilization of a Bose-Einstein condensate through feedback, *Phys. Rev. A* 76 (2007) 013610.
- [262] G. Kiebllich, G. Schaller, C. Emary, T. Brandes, Charge qubit purification by an electronic feedback loop, *Phys. Rev. Lett.* 107 (2011) 050501.
- [263] G. Kiebllich, C. Emary, G. Schaller, T. Brandes, Reverse quantum state engineering using electronic feedback loops, *New J. Phys.* 14 (2012) 123036.
- [264] T. Brandes, Feedback control of quantum transport, *Phys. Rev. Lett.* 105 (2010) 060602.
- [265] C. Polt, C. Emary, T. Brandes, Feedback stabilization of pure states in quantum transport, *Phys. Rev. B* 84 (2011) 085302.
- [266] S. Schneider, G. J. Milburn, Entanglement in the steady state of a collective-angular-momentum (Dicke) model, *Phys. Rev. A* 65 (2002) 042107.
- [267] W. K. Wootters, Entanglement of formation of an arbitrary state of two qubits, *Phys. Rev. Lett.* 80 (1998) 2245-2248.
- [268] N. Yamamoto, K. Tsumura, S. Hara, Feedback control of quantum entanglement in a two-spin system, *Automatica* 43 (2007) 981-992.
- [269] R. N. Stevenson, J. J. Hope, A.R.R. Carvalho, Engineering steady states using jump-based feedback for multipartite entanglement generation, *Phys. Rev. A* 84 (2011) 022332.
- [270] J. Song, Y. Xia, X.-D. Sun, H.-S. Song, Dissipative preparation of many-body entanglement via quantum feedback control, *Phys. Rev. A* 86 (2012) 034303.
- [271] D. Riste, M. Dukalski, C. A. Watson, G. de Lange, M. J. Tiggelman, Ya. M. Blanter, K. W. Lehnert, R. N. Schouten, L. DiCarlo, Deterministic entanglement of superconducting qubits by parity measurement and feedback, *Nature* 502 (2013) 350-354.
- [272] S. Brakhane, W. Alt, T. Kampschulte, M. Martinez-Dorantes, R. Reima, Bayesian feedback control of a two-atom spin-state in an atom-cavity system, *Phys. Rev. Lett.* 109 (2012) 173601.
- [273] S. Mancini, Markovian feedback to control continuous-variable entanglement, *Phys. Rev. A* 73 (2006) 010304(R).
- [274] G.-X. Li, H.-T. Tan, S.-S. Ke, Quantum-feedback-induced enhancement of continuous-variable entanglement in a self-phase-locked type-II nondegenerate optical parameter oscillator, *Phys. Rev. A* 74 (2006) 012304.
- [275] S.-S. Ke, G.-P. Cheng, L.-H. Zhang, G.-X. Li, Enhancement of entanglement in the nonlinear optical coupler by homodyne-mediated feedback, *J. Phys. B: At. Mol. Opt. Phys.* 40 (2007) 2827-2839.
- [276] S. Mancini, H. M. Wiseman, Optimal control of entanglement via quantum feedback, *Phys. Rev. A* 75 (2007) 012330.
- [277] M. G. Genoni, S. Mancini, A. Serafini, Optimal feedback control of linear quantum systems in the presence of thermal noises, *Phys. Rev. A* 87 (2013) 042333.
- [278] L. Vandenberghe, S. Boyd, Semidefinite Programming, *SIAM Review* 38 (1996) 49C95.
- [279] A. Serafini, S. Mancini, Determination of maximal Gaussian entanglement achievable by feedback-controlled dynamics, *Phys. Rev. Lett.* 104 (2010) 220501.
- [280] M. Yanagisawa, Quantum feedback control for deterministic entangled photon generation, *Phys. Rev. Lett.* 97 (2006) 190201.
- [281] N. Yamamoto, H. I. Nurdin, M. R. James, I. R. Petersen, Avoiding entanglement sudden death via measurement feedback control in a quantum network, *Phys. Rev. A* 78 (2008) 042339.
- [282] H. I. Nurdin, N. Yamamoto, Distributed entanglement generation between continuous-mode Gaussian fields with measurement-feedback enhancement, *Phys. Rev. A* 86 (2012) 034303.
- [283] A. M. Brańczyk, P.E.M.F. Mendonca, A. Gilchrist, A. C. Doherty, S. D. Bartlett, Quantum control of a single qubit, *Phys. Rev. A* 75 (2007) 012329.
- [284] G. G. Gillett, R. B. Dalton, B. P. Lanyon, M. P. Almeida, M. Barbieri, G. J. Pryde, J. L. O'Brien, K. J. Resch, S. D. Bartlett, A. G. White, Experimental feedback control of quantum systems using weak measurements, *Phys. Rev. Lett.* 104 (2010) 080503.
- [285] B. L. Higgins, B. M. Booth, A. C. Doherty, S. D. Bartlett, H. M. Wiseman, G. J. Pryde, Mixed state discrimination using optimal control, *Phys. Rev. Lett.* 103 (2009) 220503.
- [286] V. Giovannetti, S. Guha, S. Lloyd, L. Maccone, J. H. Shapiro, H. P. Yuen, Classical capacity of the lossy bosonic channel: the exact solution, *Phys. Rev. Lett.* 92 (2004) 027902.
- [287] S. Guha, J. L. Habif, M. Takeoka, Approaching Helstrom limits to optical pulse-position demodulation using single photon detection and optical feedback, *J. Mod. Opt.* 58 (2011) 257-265.
- [288] K. Tsujino, D. Fukuda, G. Fujii, S. Inoue, M. Fujiwara, M. Takeoka, M. Sasaki, Quantum receiver beyond the standard quantum limit of coherent optical communication, *Phys. Rev. Lett.* 106 (2011) 250503.
- [289] J. Chen, J. L. Habif, Z. Dutton, R. Lazarus, S. Guha, Optical codeword demodulation with error rates below the standard quantum limit using a conditional nulling receive, *Nat. Photon.* 6 (2012) 374-379.
- [290] F. E. Becerra, J. Fan, G. Baumgartner, J. Goldhar, J. T. Kosloski, A. Migdall, Experimental demonstration of a receiver beating the standard quantum limit for multiple nonorthogonal state discrimination, *Nat. Photon.* 7 (2013) 147-152.
- [291] C. W. Helstrom, Quantum Detection and Estimation Theory, *Mathematics in Science and Engineering*, Academic Press, New York, 1976.
- [292] H. M. Wiseman, Adaptive phase measurement of optical modes: going beyond the marginal Q distribution, *Phys. Rev. Lett.* 75 (1995) 4587-4590.
- [293] H. M. Wiseman, R. B. Killip, Adaptive single-shot phase measurements: A semiclassical approach, *Phys. Rev. A* 56 (1997) 944-957.
- [294] H. M. Wiseman, R. B. Killip, Adaptive single-shot phase measurements: The full quantum theory, *Phys. Rev. A* 57 (1998) 2169-2185.
- [295] T. C. Ralph, A. P. Lund, H. M. Wiseman, Adaptive phase measurements in linear optical quantum computation, *J. Opt. B: Quantum Semiclass. Opt.* 7 (2005) S245-S249.
- [296] D. W. Berry, H. M. Wiseman, Phase measurements at the theoretical limit, *Phys. Rev. A* 63 (2000) 013813.
- [297] D. T. Pope, H. M. Wiseman, N. K. Lanford, Adaptive phase estimation is more accurate than nonadaptive phase estimation for continuous

- beams of light, *Phys. Rev. A* 70 (2004) 043812.
- [298] D. W. Berry, H. M. Wiseman, Optimal states and almost optimal adaptive measurements for quantum interferometry, *Phys. Rev. Lett.* 85 (2000) 5098-5101.
- [299] D. W. Berry, H. M. Wiseman, J. K. Breslin, Optimal input states and feedback for interferometric phase estimation, *Phys. Rev. A* 63 (2001) 053804.
- [300] D. W. Berry, H. M. Wiseman, Adaptive quantum measurements of a continuously varying phase, *Phys. Rev. A* 65 (2002) 043803.
- [301] D. T. Pegg, S. M. Barnett, Unitary phase operator in quantum mechanics, *Europhysics Lett.* 6 (1988) 483-487.
- [302] D. T. Pegg, S. M. Barnett, Phase properties of the quantized single-mode electromagnetic-field, *Phys. Rev. A* 39 (1989) 1665-1675.
- [303] B. C. Sanders, G. J. Milburn, Optimal quantum measurements for phase estimation, *Phys. Rev. Lett.* 75 (1995) 2944-2947.
- [304] B. C. Sanders, G. J. Milburn, Z. Zhang, Optimal quantum measurements for phase-shift estimation in optical interferometry, *J. Mod. Opt.* 44 (1997) 1309-1320.
- [305] M. Tsang, Time-symmetric quantum theory of smoothing, *Phys. Rev. Lett.* 102 (2009) 250403.
- [306] M. Tsang, Optimal waveform estimation for classical and quantum systems via time-symmetric smoothing, *Phys. Rev. A* 80 (2009) 033840.
- [307] M. Tsang, Optimal waveform estimation for classical and quantum systems via time-symmetric smoothing. II. Applications to atomic magnetometry and Hardy's paradox, *Phys. Rev. A* 81 (2010) 013824.
- [308] M. A. Armen, J. K. Au, J. K. Stockton, A. C. Doherty, H. Mabuchi, Adaptive homodyne measurement of optical phase, *Phys. Rev. Lett.* 89 (2002) 133602.
- [309] B. L. Higgins, D. W. Berry, S. D. Bartlett, H. M. Wiseman, G. J. Pryde, Entanglement-free Heisenberg-limited phase estimation, *Nature* 450 (2007) 393-396.
- [310] G. Y. Xiang, B. L. Higgins, D. W. Berry, H. M. Wiseman, G. J. Pryde, Entanglement-enhanced measurement of a completely unknown optical phase, *Nat. Photon.* 5 (2011) 43-47.
- [311] G. Y. Xiang, T. C. Ralph, A. P. Lund, N. Walk, G. J. Pryde, Heralded noiseless linear amplification and distillation of entanglement, *Nat. Photon.* 4 (2010) 316-319.
- [312] R. Okamoto, M. Iefuji, S. Oyama, K. Yamagata, H. Imai, A. Fujiwara, S. Takeuchi, Experimental demonstration of adaptive quantum state estimation, *Phys. Rev. Lett.* 109 (2012) 130404.
- [313] H. Yonezawa, D. Nakane, T. A. Wheatley, K. Iwasawa, S. Takeda, H. Arao, K. Ohki, K. Tsumura, D. W. Berry, T. C. Ralph, H. M. Wiseman, E. H. Huntington, A. Furusawa, Quantum-enhanced optical-phase tracking, *Science* 337 (2012) 1514-1517.
- [314] F. Verstraete, A. C. Doherty, H. Mabuchi, Sensitivity optimization in quantum parameter estimation, *Phys. Rev. A* 64 (2001) 032111.
- [315] J. Gambetta, H. M. Wiseman, State and dynamical parameter estimation for open quantum systems, *Phys. Rev. A* 64 (2001) 042105.
- [316] P. Warszawski, J. Gambetta, H. M. Wiseman, Dynamical parameter estimation using realistic photodetection, *Phys. Rev. A* 69 (2004) 042104.
- [317] B. A. Chase, J. M. Geremia, Single-shot parameter estimation via continuous quantum measurement, *Phys. Rev. A* 79 (2009) 022314.
- [318] J. F. Ralph, K. Jacobs, C. D. Hill, Frequency tracking and parameter estimation for robust quantum state estimation, *Phys. Rev. A* 84 (2011) 052119.
- [319] J. K. Stockton, J. M. Geremia, A. C. Doherty, H. Mabuchi, Robust quantum parameter estimation: Coherent magnetometry with feedback, *Phys. Rev. A* 69 (2004) 032109.
- [320] K. Jacobs, How to project qubits faster using quantum feedback, *Phys. Rev. A* 67 (2003) 030301(R).
- [321] J. Combes, K. Jacobs, Rapid state reduction of quantum systems using feedback control, *Phys. Rev. Lett.* 96 (2006) 010504.
- [322] H. M. Wiseman, J. F. Ralph, Reconsidering rapid qubit purification by feedback, *New J. Phys.* 8 (2006) 90.
- [323] C. Hill, J. Ralph, Weak measurement and rapid state reduction in entangled bipartite quantum systems, *New J. Phys.* 9 (2007) 151.
- [324] E. J. Griffith, C. D. Hill, J. F. Ralph, H. M. Wiseman, K. Jacobs, Rapid-state purification protocols for a cooper pair box, *Phys. Rev. B* 7 (2007) 014511.
- [325] C. Hill, J. F. Ralph, Weak measurement and control of entanglement generation, *Phys. Rev. A* 77 (2008) 014305.
- [326] H. M. Wiseman, L. Bouten, Optimality of feedback control strategies for qubit purification, *Quant. Info. Proc.* 7 (2008) 71-83.
- [327] J. Combes, H. M. Wiseman, K. Jacobs, Rapid measurement of quantum systems using feedback control, *Phys. Rev. Lett.* 100 (2008) 160503.
- [328] J. Combes, H. M. Wiseman, A. J. Scott, Replacing quantum feedback with open-loop control and quantum filtering, *Phys. Rev. A* 81 (2010) 020301(R).
- [329] J. Combes, H. M. Wiseman, K. Jacobs, A. J. O'Connor, Rapid purification of quantum systems by measuring in a feedback-controlled unbiased basis, *Phys. Rev. A* 82 (2010) 022307.
- [330] J. Combes, H. M. Wiseman, Maximum information gain in weak or continuous measurements of qudits: complementarity is not enough, *Phys. Rev. X* 1 (2011) 011012.
- [331] K. Maruyama, F. Nori, Entanglement purification without controlled-NOT gates by using the natural dynamics of spin chains *Phys. Rev. A* 78 (2008) 022312.
- [332] T. Tanamoto, K. Maruyama, Y. X. Liu, X. Hu, F. Nori, Efficient purification protocols using iSWAP gates in solid-state qubits *Phys. Rev. A* 78 (2008) 062313.
- [333] F. Shuang, M. Zhou, A. Pechen, R. Wu, O. M. Shir, H. Rabitz, Control of quantum dynamics by optimized measurements, *Phys. Rev. A* 78 (2008) 063422.
- [334] A. Pechen, N. Il'in, F. Shuang, H. Rabitz, Quantum control by von Neumann measurements, *Phys. Rev. A* 74 (2006) 052102.
- [335] S. Ashhab, J.Q. You, F. Nori, The information about the state of a qubit gained by a weakly coupled detector, *New J. Phys.* 11 (2009) 083017.
- [336] S. Ashhab, J.Q. You, F. Nori, The information about the state of a charge qubit gained by a weakly coupled quantum point contact, *Phys. Scr. T* 137 (2009) 014005.
- [337] S. Ashhab, J. Q. You, F. Nori, Weak and strong measurement of a qubit using a switching-based detector, *Phys. Rev. A* 79 (2009) 032317.
- [338] S. Ashhab, F. Nori, Control-free control: manipulating a quantum system using only a limited set of measurements, *Phys. Rev. A* 82 (2010) 062103.

- [339] H. M. Wiseman, Quantum control: Squinting at quantum systems, *Nature* 470 (2011) 178-179.
- [340] K. Jacobs, Feedback control using only quantum back-action, *New J. Phys.* 12 (2010) 043005.
- [341] M. S. Blok, C. Bonato, M. L. Markham, D. J. Twitchen, V. V. Dobrovitski, R. Hanson, Manipulating a qubit through the backaction of sequential partial measurements and real-time feedback, *Nature Phys.* 10 (2014) 189-193.
- [342] M. Yanagisawa, H. Kimura, Transfer function approach to quantum control-part I: dynamics of quantum feedback systems, *IEEE Trans. Automat. Contr.* 48 (2003) 2107-2112.
- [343] M. Yanagisawa, H. Kimura, Transfer function approach to quantum control-part II: control concepts and applications, *IEEE Trans. Automat. Contr.* 48 (2003) 2121-2132.
- [344] J. E. Gough, R. Gohm, M. Yanagisawa, Linear quantum feedback networks, *Phys. Rev. A* 78 (2008) 062104.
- [345] J. E. Gough, M. R. James, H. I. Nurdin, Squeezing components in linear quantum feedback networks, *Phys. Rev. A* 81 (2010) 023804.
- [346] G. Zhang, M. R. James, Direct and indirect couplings in coherent feedback control of linear quantum systems, *IEEE Trans. Automat. Contr.* 56 (2011) 1535-1550.
- [347] G. Zhang, H.W.J. Lee, B. Huang, H. Zhang, Coherent feedback control of linear quantum optical systems via squeezing and phase shift, *SIAM J. Contr. Optim.* 50 (2012) 2130-2150.
- [348] L. Diosi, Non-Markovian open quantum systems: Input-output fields, memory, and monitoring, *Phys. Rev. A* 85 (2012) 034101.
- [349] J. Zhang, Y.-X. Liu, R.-B. Wu, K. Jacobs, F. Nori, Non-Markovian quantum input-output networks, *Phys. Rev. A* 87 (2013) 032117.
- [350] H. Mabuchi, Coherent-feedback quantum control with a dynamical compensator, *Phys. Rev. A* 78 (2008) 032323.
- [351] J. E. Gough, S. Wildfeuer, Enhancement of field squeezing using coherent feedback, *Phys. Rev. A* 80 (2009) 042107.
- [352] S. Iida, M. Yukawa, H. Yonezawa, N. Yamamoto, A. Furusawa, Experimental demonstration of coherent feedback control on optical field squeezing, *IEEE Trans. Automat. Contr.* 57 (2012) 2045-2050.
- [353] J. Kerckhoff, H. I. Nurdin, D. S. Pavlichin, H. Mabuchi, Designing quantum memories with embedded control: photonic circuits for autonomous quantum error correction, *Phys. Rev. Lett.* 105 (2010) 040502.
- [354] J. Kerckhoff, D. S. Pavlichin, H. Chalabi, H. Mabuchi, Design of nanophotonic circuits for autonomous subsystem quantum error correction, *New J. Phys.* 13 (2011) 055022.
- [355] H. Mabuchi, Cavity-QED models of switches for attojoule-scale nanophotonic logic, *Phys. Rev. A* 80 (2009) 045802.
- [356] J. Kerckhoff, L. Bouten, A. Silverfarb, H. Mabuchi, Physical model of continuous two-qubit parity measurement in a cavity-QED network, *Phys. Rev. A* 79 (2009) 024305.
- [357] I. Wilson-Rae, N. Nooshi, W. Zwerger, T. J. Kippenberg, Theory of ground state cooling of a mechanical oscillator using dynamical backaction, *Phys. Rev. Lett.* 99 (2007) 093901.
- [358] F. Marquardt, J. P. Chen, A. A. Clerk, S. M. Girvin, Quantum theory of cavity-assisted sideband cooling of mechanical motion, *Phys. Rev. Lett.* 99 (2007) 093902.
- [359] L. Tian, Ground state cooling of a nanomechanical resonator via parametric linear coupling, *Phys. Rev. B* 79 (2009) 193407.
- [360] X. T. Wang, S. Vinjanampathy, F. W. Strauch, K. Jacobs, Ultraefficient cooling of resonators: beating sideband cooling with quantum control, *Phys. Rev. Lett.* 107 (2011) 177204.
- [361] J. Kerckhoff, R. W. Andrews, H. S. Ku, W. F. Kindel, K. Cicak, R. W. Simmonds, K. W. Lehnert, Tunable coupling to a mechanical oscillator circuit using a coherent feedback network, *Phys. Rev. X* 3 (2013) 021013.
- [362] K. Jacobs, H. Nurdin, F. W. Strauch, M. James, When does resolved-sideband cooling beat measurement-based feedback cooling? Analytical results in the regime of ground-state cooling, in submission, 2014.
- [363] M. Yanagisawa, Non-Gaussian state generation from linear elements via feedback, *Phys. Rev. Lett.* 103 (2009) 203601.
- [364] M. F. Yanik, S. Fan, M. Soljacic, High-contrast all-optical bistable switching in photonic crystal microcavities, *Appl. Phys. Lett.* 83 (2003) 2739-2741.
- [365] X. Yang, C. Husko, C. W. Wong, M. Yu, D. L. Kwong, Observation of femtojoule optical bistability involving Fano resonances in high-Q/Vm silicon photonic crystal nanocavities, *Appl. Phys. Lett.* 91 (2007) 051113.
- [366] K. Nozaki, T. Tanabe, A. Shinya, S. Matsuo, T. Sato, H. Taniyama, M. Notomi, Sub-femtojoule all-optical switching using a photonic-crystal nanocavity, *Nat. Photonics* 4 (2010) 477-483.
- [367] R. Kumar, L. Liu, G. Roelkens, E.-J. Geluk, T. de Vries, F. Karouta, P. Regreny, D. Van Thourhout, R. Baets, G. Morthier, 10-GHz all-optical gate based on a III-V/SOI microdisk, *IEEE Photon. Technol. Lett.* 22 (2010) 981-983.
- [368] M. Armen, H. Mabuchi, Low-lying bifurcations in cavity quantum electrodynamics, *Phys. Rev. A* 73 (2006) 063801.
- [369] M. Armen, A. E. Miller, H. Mabuchi, Spontaneous dressed-state polarization in the strong driving regime of cavity QED, *Phys. Rev. Lett.* 103 (2009) 173601.
- [370] H. Mabuchi, Coherent-feedback control strategy to suppress spontaneous switching in ultralow power optical bistability, *Appl. Phys. Lett.* 98 (2011) 193109.
- [371] Z. Zhou, C. J. Liu, Y. M. Fang, J. Zhou, R. T. Glasser, L. Q. Chen, J. T. Jing, W. P. Zhang, Optical logic gates using coherent feedback, *Appl. Phys. Lett.* 101 (2012) 191113.
- [372] Z. H. Yan, X. J. Jia, C. D. Xie, K. C. Peng, Coherent feedback control of multipartite quantum entanglement for optical fields, *Phys. Rev. A* 84 (2011) 062304.
- [373] P. van Loock, A. Furusawa, Detecting genuine multipartite continuous-variable entanglement, *Phys. Rev. A* 67 (2003) 052315.
- [374] R. Bartels, S. Backus, E. Zeek, L. Misoguti, G. Vdovin, I. P. Christov, M. M. Murnane, H. C. Kapteyn, Shaped-pulse optimization of coherent emission of high-harmonic soft X-rays, *Nature* 406 (2000) 164-166.
- [375] H. A. Rabitz, M. M. Hsieh, C. M. Rosenthal, Quantum optimally controlled transition landscapes, *Science* 303 (2004) 1998-2001.
- [376] S. Shankar, M. Hatridge, Z. Leghtas, K. M. Sliwa, A. Narla, U. Vool, S. M. Girvin, L. Frunzio, M. Mirrahimi, M. H. Devoret, Autonomously stabilized entanglement between two superconducting quantum bits, *Nature* 504 (2013) 419-422.
- [377] Ya. S. Greenberg, E. Il'ichev, F. Nori, Cooling a magnetic resonance force microscope via the dynamical back action of nuclear spins, *Phys. Rev. B* 80 (2009) 214423.
- [378] C. H. Metzger, K. Karrai, Cavity cooling of a microlever, *Nature* 432 (2004) 1002-1005.

- [379] A. Greilich, A. Shabaev, D. R. Yakovlev, Al. L. Efros, I. A. Yugova, D. Reuter, A. D. Wieck, M. Bayer, Nuclei-induced frequency focusing of electron-spin coherence, *Nature* 317 (2007) 1896-1899.
- [380] S. G. Carter, A. Shavaev, S. E. Economou, T. A. Kennedy, A. S. Bracker, T. L. Reinecke, Directing nuclear spin flips in InAs quantum dots using detuned optical pulse trains, *Phys. Rev. Lett.* 102 (2009) 167403.
- [381] X. D. Xu, W. Yao, B. Sun, D. G. Steel, A. S. Bracker, D. Gammon, L. J. Sham, Optically controlled locking of the nuclear field via coherent dark-state spectroscopy, *Nature* 459 (2009) 1105-1109.
- [382] C. Latta, A. Hoge, Y. Zhao, A. N. Vamivakas, P. Maletinsky, M. Kroner, J. Dreiser, I. Carusotto, A. Badolato, D. Schuh, W. Wegscheider, M. Atatüre, A. Imamoglu, Confluence of resonant laser excitation and bidirectional quantum-dot nuclear-spin polarization, *Nat. Phys.* 5 (2009) 758-763.
- [383] T. D. Ladd, D. Press, K. De Greve, P. L. McMahon, B. Friess, C. Schneider, M. Kamp, S. Hofling, A. Forchel, Y. Yamamoto, Pulsed nuclear pumping and spin diffusion in a single charged quantum dot, *Phys. Rev. Lett.* 105 (2010) 107401.
- [384] B. Sun, C.M.E. Chow, D. G. Steel, A. S. Bracker, D. Gammon, L. J. Sham, Persistent narrowing of nuclear-spin fluctuations in InAs quantum dots using laser excitation, *Phys. Rev. Lett.* 108 (2012) 187401.
- [385] D. J. Reilly, J. M. Taylor, J. R. Petta, C. M. Marcus, M. P. Hanson, A. C. Gossard, Suppressing spin qubit dephasing by nuclear state preparation, *Science* 321 (2008) 817-821.
- [386] I. T. Vink, K. C. Nowack, F.H.L. Koppens, J. Danon, Y. V. Nazarov, Locking electron spins into magnetic resonance by electron-nuclear feedback, *Nat. Phys.* 5 (2009) 764-768.
- [387] H. Bluhm, S. Foletti, D. Mahalu, V. Umansky, A. Yacoby, Enhancing the coherence of a spin qubit by operating it as a feedback loop that controls its nuclear spin bath, *Phys. Rev. Lett.* 105 (2010) 216803.
- [388] C. Barthel, J. Medford, H. Bluhm, A. Yacoby, C. M. Marcus, M. P. Hanson, A. C. Gossard, Relaxation and readout visibility of a singlet-triplet qubit in an Overhauser field gradient, *Phys. Rev. B* 85 (2012) 035306.
- [389] W. Yao, Y. Luo, Feedback control of nuclear hyperfine fields in a double quantum dot, *Europhysics Letters* 92 (2010) 17008.
- [390] K. Geerlings, Z. Leghtas, I. M. Pop, S. Shankar, L. Frunzio, R. J. Schoelkopf, M. Mirrahimi, M. H. Devoret, Demonstrating a driven reset protocol for a superconducting qubit, *Phys. Rev. Lett.* 110 (2013) 120501.
- [391] K. W. Murch, U. Vool, D. Zhou, S. J. Weber, S. M. Girvin, I. Siddiqi, Cavity-assisted quantum bath engineering, *Phys. Rev. Lett.* 109 (2012) 183602.
- [392] C. M. Caves, P. D. Drummond, Quantum limits on bosonic communication rates, *Rev. Mod. Phys.* 66 (1994) 481-537.
- [393] R. Okamoto, H. F. Hofmann, S. Takeuchi, K. Sasaki, Demonstration of an optical quantum controlled-NOT gate without path interference, *Phys. Rev. Lett.* 95 (2005) 210506.
- [394] N. Kiesel, C. Schmid, U. Weber, R. Ursin, H. Weinfurter, Linear optics controlled-phase gate made simple, *Phys. Rev. Lett.* 95 (2005) 210505.
- [395] N. K. Langford, T. J. Weinhold, R. Prevedel, K. J. Resch, A. Gilchrist, J. L. O'Brien, G. J. Pryde, A. G. White, Demonstration of a simple entangling optical gate and its use in Bell-state analysis, *Phys. Rev. Lett.* 95 (2005) 210504.
- [396] Y. Yamamoto, N. Imoto, S. Machida, Amplitude squeezing in a semiconductor laser using quantum nondemolition measurement and negative feedback, *Phys. Rev. A* 33 (1986) 3243-3261.
- [397] H. A. Haus, Y. Yamamoto, Theory of feedback-generated squeezed states, *Phys. Rev. A* 34 (1986) 270-292.
- [398] J. H. Shapiro, G. Saplakoglu, S.-T. Ho, P. Kumar, B.E.A. Saleh, M. C. Teich, Theory of light detection in the presence of feedback, *J. Opt. Soc. Am. B* 4 (1987) 1604-1620.
- [399] C. Sayrin, I. Dotsenko, X. X. Zhou, B. Peaudecerf, T. Rybarczyk, S. Gleyzes, P. Rouchon, M. Mirrahimi, H. Amini, M. Brune, J.-M. Raimond, S. Haroche, Real-time quantum feedback prepares and stabilizes photon number states, *Nature* 477 (2011) 73-77.
- [400] M. Hofheinz, E. M. Weig, M. Ansmann, R. C. Bialczak, E. Lucero, M. Neeley, A. D. O'Connell, H. Wang, J. M. Martinis, A. N. Cleland, Generation of Fock states in a superconducting quantum circuit, *Nature* 454 (2008) 310-314.
- [401] M. Hofheinz, H. Wang, M. Ansmann, R. C. Bialczak, E. Lucero, M. Neeley, A. D. O'Connell, D. Sank, J. Wenner, J. M. Martinis, A. N. Cleland, Synthesizing arbitrary quantum states in a superconducting resonator, *Nature* 459 (2009) 546-549.
- [402] I. Dotsenko, M. Mirrahimi, M. Brune, S. Haroche, J.-M. Raimond, P. Rouchon, Quantum feedback by discrete quantum nondemolition measurements: towards on-demand generation of photon-number states, *Phys. Rev. A* 80 (2009) 013805.
- [403] H. Amini, M. Mirrahimi, P. Rouchon, Stabilization of a delayed quantum system: the photon box case-study, *IEEE Trans. Automat. Contr.* 57 (2012) 1918-1930.
- [404] X. Zhou, I. Dotsenko, B. Peaudecerf, T. Rybarczyk, C. Sayrin, S. Gleyzes, Field locked to a Fock state by quantum feedback with single photon corrections, *Phys. Rev. Lett.* 108 (2012) 243602.
- [405] T. Vanderbruggen, R. Kohlhass, A. Bertoldi, S. Bernon, A. Aspect, A. Landragin, P. Bouyer, Feedback control of trapped coherent atomic ensembles, *Phys. Rev. Lett.* 110 (2013) 210503.
- [406] R. Inoue, S.I.R. Tanada, R. Namiki, T. Sagawa, Y. Takahashi, Unconditional quantum-noise suppression via measurement-based quantum feedback, *Phys. Rev. Lett.* 110 (2013) 163602.
- [407] E. Gavartin, P. Verlot and T. J. Kippenberg, A hybrid on-chip optomechanical transducer for ultrasensitive force measurements, *Nat. Nano.* 7 (2012) 509-514.
- [408] J. Q. You, X. D. Hu, S. Ashhab, F. Nori, Low-decoherence flux qubit, *Phys. Rev. B* 75 (2007) 140515.
- [409] J. Koch, T. M. Yu, J. Gambetta, A. A. Houck, D. I. Schuster, J. Majer, A. Blais, M. H. Devoret, S. M. Girvin, R. J. Schoelkopf, Charge-insensitive qubit design derived from the Cooper pair box, *Phys. Rev. A* 76 (2007) 042319.
- [410] C. M. Caves, Quantum limits on noise in linear amplifiers, *Phys. Rev. D* 26 (1982) 1817-1839.
- [411] A. A. Clerk, M. H. Devoret, S. M. Girvin, F. Marquardt, R. J. Schoelkopf, Introduction to quantum noise, measurement, and amplification, *Rev. Mod. Phys.* 82 (2010) 1155-1208.
- [412] M. A. Castellanos-Beltran, K. D. Irwin, G. C. Hilton, L. R. Vale, K. W. Lehnert, Amplification and squeezing of quantum noise with a tunable Josephson metamaterial, *Nat. Phys.* 4 (2008) 928-931.
- [413] A. Vinante, M. Bonaldi, F. Marin, J.-P. Zendri, Dissipative feedback does not improve the optimal resolution of incoherent force detection,

- Nat. Nano. 8 (2013) 470.
- [414] G. I. Harris, D. L. McAuslan, T. M. Stace, A. C. Doherty, W. P. Bowen, Minimum requirements for feedback enhanced force sensing, *Phys. Rev. Lett.* 111 (2013) 103603.
 - [415] D. Press, T. D. Ladd, B. Y. Zhang, Y. Yamamoto, Complete quantum control of a single quantum dot spin using ultrafast optical pulses, *Nature* 456 (2008) 218-221.
 - [416] D. Press, K. De Greve, P. L. McMahon, T. D. Ladd, B. Friess, C. Schneider, M. Kamp, S. Hofling, A. Forchel, Y. Yamamoto, Ultrafast optical spin echo in a single quantum dot, *Nat. Photon.* 4 (2010) 367-370.
 - [417] J. R. Petta, A. C. Johnson, J. M. Taylor, E. A. Laird, A. Yacoby, M. D. Lukin, C. M. Marcus, M. P. Hanson, A. C. Gossard, Coherent manipulation of coupled electron spins in semiconductor quantum dots, *Science*, 309 (2005) 2180-2184.
 - [418] S. Foletti, H. Bluhm, D. Mahalu, V. Umansky, A. Yacoby, Universal quantum control of two-electron spin quantum bits using dynamic nuclear polarization, *Nat. Phys.* 5 (2009) 903-908.
 - [419] J. R. Petta, J. M. Taylor, A. C. Johnson, A. Yacoby, M. D. Lukin, C. M. Marcus, M. P. Hanson, A. C. Gossard, Dynamic nuclear polarization with single electron spins, *Phys. Rev. Lett.* 100 (2008) 067601.
 - [420] C. Barthel, D. J. Reilly, C. M. Marcus, M. P. Hanson, A. C. Gossard, Rapid single-shot measurement of a singlet-triplet qubit, *Phys. Rev. Lett.* 103 (2009) 160503.
 - [421] M. A. Castellanos-Beltran, K. W. Lehnert, Widely tunable parametric amplifier based on a superconducting quantum interference device array resonator, *Appl. Phys. Lett.* 91 (2007) 083509.
 - [422] T. Yamamoto, K. Inomata, M. Watanabe, K. Matsuba, T. Miyazaki, W. D. Oliver, Y. Nakamura, J. S. Tsai, Flux-driven Josephson parametric amplifier, *Appl. Phys. Lett.* 93 (2008) 042510.
 - [423] N. Bergeal, R. Vijay, V. E. Manucharyan, I. Siddiqi, R. J. Schoelkopf, S. M. Girvin, M. H. Devoret, Analog information processing at the quantum limit with a Josephson ring modulator, *Nat. Phys.* 6 (2010) 296-302.
 - [424] X. T. Wang, S. Vinjanampathy, F. W. Strauch, K. Jacobs, Absolute dynamical limit to cooling weakly coupled quantum systems, *Phys. Rev. Lett.* 110 (2013) 157207.
 - [425] R. Bulla, N.-H. Tong, M. Vojta, Numerical renormalization group for bosonic systems and application to the subohmic spin-boson model, *Phys. Rev. Lett.* 91 (2003) 170601.
 - [426] M. Thorwart, P. Reimann, P. Jung, R. F. Fox, Quantum hysteresis and resonant tunneling in bistable systems, *Chemical Physics* 235 (1998) 61-80.
 - [427] J. Prior, A. W. Chin, S. F. Huelga, M. B. Plenio, Efficient simulation of strong system-environment interactions, *Phys. Rev. Lett.* 105 (2010) 050404.
 - [428] A. Ishizaki, Y. Tanimura, Quantum dynamics of system strongly coupled to low-temperature colored noise bath: reduced hierarchy equations approach, *J. Phys. Soc. Jpn.* 74 (2005) 3131-3134.
 - [429] T. Albash, S. Boixo, D. A. Lidar, P. Zanardi, Quantum adiabatic Markovian master equations, *New J. Phys.* 14 (2012) 123016.
 - [430] Z.-L. Xiang, S. Ashhab, J. Q. You, F. Nori, Hybrid quantum circuits: Superconducting circuits interacting with other quantum systems, *Rev. Mod. Phys.* 85 (2013) 623-653.
 - [431] K. J. Vahala, Optical microcavities, *Nature* 424 (2003) 839-846.
 - [432] T. J. Kippenberg, K. J. Vahala, Cavity optomechanics: back-action at the mesoscale, *Science* 321 (2008) 1172-1176.
 - [433] L. He, S. K. Ozdemir, L. Yang, Whispering gallery microcavity lasers, *Laser Photonics Rev.* 7 (2013) 60-82.
 - [434] B. Peng, S. K. Ozdemir, F. C. Lei, F. Monifi, M. Gianfreda, G. L. Long, S. H. Fan, F. Nori, C. M. Bender, L. Yang, Parity-time-symmetric whispering-gallery microcavities, *Nat. Phys.* 10 (2014) 394-398.